HYDROTHERMAL SYNTHESIS AND CHARACTERIZATION OF TRANSITION METAL (Mn and V) OXIDES CONTAINING PHOSPHATES

A Thesis Submitted to
the Graduate School of Engineering and Sciences of
İzmir Institute of Technology
in Partial Fulfillment of the Requirements for the Degree of

MASTER OF SCIENCE

in Chemistry

by
Leyla ERAL

July 2006
İZMİR

We approve the thesis of **Leyla ERAL**

Date of Signature

……. **13 July 2006**
Assist. Prof. Dr. Mehtap EANES
Supervisor
Department of Chemistry
İzmir Institute of Technology

…… **13 July 2006**
Prof. Dr. Işıl TOPALOĞLU SÖZÜER
Department of Chemistry
İzmir Institute of Technology

…… **13 July 2006**
Assist. Prof. Dr. Funda DEMİRHAN
Department of Chemistry
Celal Bayar University

……..... **13 July 2006**
Assoc. Prof. Dr. Ahmet E. EROĞLU
Head of Department
İzmir Institute of Technology

……..
Assoc. Prof. Dr. Semahat ÖZDEMİR
Head of the Graduate School

ACKNOWLEDGEMENTS

I am grateful to my advisor Asst.Prof. Mehtap Emirdağ Eanes for her guidance, encouragement and support through my master program.

I would also thank to İYTE Research Foundation and L'oreal for their financial support to our Solid State Chemistry Laboratory. I would also thank to IYTE MAM Researchers for their help in analysis. My sincere gratitude also goes to my special friends who have helped me through the years.

I would also like to give special thank to my family, especially my mother, for their unconditional love, patience, support and encouragement through the years and all my life.

I would also need to thank the one person in my life to put up with me for the last eight years, my friend Fatih Doğan who has been supportive emotionally and also special thank to him for his amazing way of expression of my feeling with his short essay which is given below.

"If I were a photon roaming freely in the universe, possibly I would desire for my way to be through a crystal. That place could be my paradise: a perfect symmetry that would not permit me to get confused my path, a dazzling brilliance which would allow me to put my very existence in a definitive manner; in spite of the solidity of the medium, the opacity that would tolerate free-roaming; all would grant me a portion of the joy while making me a part of a visual celebration presented to man. That might be the place in which I could be observed as the most beautiful.

Something happens within the structure called crystal and then comes out a wonder of nature. It was such a wonderful place that we use its name as the symbol of brightness. It was a measure of purity. Crystal was the highest point that the structure of a substance could reach at. The word "crystal" had become the synonym of "beautiful". So, for a photon coming from a distant point in the universe and in the way of gaining a meaning within the human eye, the surest path would be the corridors of a crystal.

I might not be that lucky photon, but as being the owner of the eyes that joyfully hosts the photons passing through the crystal, I am a chemist who has an intention to solve this structure and give pleasure to not only her eyes but also to her mind."

ABSTRACT

HYDROTHERMAL SYNTHESIS AND CHARACTERIZATION OF TRANSITION METAL (Mn AND V) OXIDES CONTAINING PHOSPHATES

The synthesis of new manganese phosphate compound, $Sr_2MnP_3O_{11}$, by hydrothermal reaction of Mn_2O_3, $SrCO_3$ and H_3PO_4 in presence of water at 230ºC for 5 days is reported. The compound crystallizes in the space group P 21/c of the monoclinic system with three formula units in a cell of dimensions a=6.6410(13)Å, b=6.8341(14)Å, c=19.055(14)Å, β=99.22(3)Å, V=853.6(3)$Å^3$. The structure is composed of MnO_6, PO_4 and P_2O_7 groups and Sr^{+2} cations. It has three dimensional structure including channels in which the Sr cations are placed.

The pale pink single crystals of the Hureaulite mineral, $Mn_5(H_20)_4[PO_3(OH)]_2[PO_4]_2$, were synthesized hydrothermally via the reaction of $SrCO_3$, $MnCl_2$, H_3PO_4 and H_2O at 180ºC for 3 days. The compound is in the crystal system of monoclinic with unitcell parameters a=17.600(4)Å, b=9.1214(18)Å, c=9.4786(19)Å and β=96.52(3)Å and in the space group C2/c. The structure possesses a three-dimensional architecture containing channels and is made up of MnO_6 and PO_4, which are joined with others by sharing corners.

All detailed structural information of the synthesized materials was done via commercial software programs SHELX and Crystal Structure.

ÖZET

FOSFAT İÇEREN GEÇİŞ METAL (Mn ve V) OKSİTLERİNİN HİDROTERMAL SENTEZİ VE KARAKTERİZASYONU

Laboratuvarımızda hidrotermal metod kullanılarak Mn_2O_3, $SrCO_3$ ve H_3PO_4'ün 230ºC sıcaklıkta 5 günlük tepkimesiyle yeni bir mangan fosfat bileşiği sentezlenmiştir. Bileşik, monoklinik sistem de, P $2_{1/c}$ boşluk gurubunda, a=6.6410(13)Å, b=6.8341(14)Å, c=19.055(14)Å, β=99.22(3)Å, V=853.6(3)$Å^3$ hücre boyutlarında, üç formül birimindedir. Bileşiğinin yapısı ; MnO_6, PO_4 ve P_2O_7 gruplarıyla Sr^{+2} katyonlarından oluşmaktadır. Yapı üç boyutlu ve Sr katyonlarının yerleştiği kanallar ihtiva etmektedir.

Hureaulite mineralinin ($Mn_5(H_2O)_4[PO_3(OH)]_2[PO_4]_2$) soluk pembe renkli tek kristalleri, $SrCO_3$, $MnCl_2$, H_3PO_4 ve H_2O'nun hidrotermal metodla 180ºC'deki 3 günlük tepkimesiyle sentezlenmiştir. ($Mn_5(H_2O)_4[PO_3(OH)_2[PO_4]_2$) bileşiği monoklinik kristal sisteminde ve $C_{2/c}$ boşluk gurubundadır. Birim hücre parametreleri a=17.600(4) Å, b=9.1214(18) Å, c=9.4786(19), β=96.52(3)^o dir. Köşe paylaşımı ile birbirlerine bağlanmış MnO_6 ile PO_4 çokyüzlülerinden oluşan yapı üç boyutludur ve boş kanallı bir yapıya sahiptir.

Sentezlenen malzemelerin yapılarıyla ilgili tüm ayrıntılı bilgiler ticari yazılım programları olan SHELX ve Crystal Structure kullanılarak aydınlatılmıştır.

TABLE OF CONTENTS

LIST OF FIGURES viii

LIST OF TABLES xii

CHAPTER 1. INTRODUCTON 1

1.1. The Ceramic Method 2

1.2. Vapor Phase Transport Methods 5

1.3. Combustion Methods 6

1.4. Hydrothermal Synthesis 6

CHAPTER 2. EXPERIMENTAL METHOD 20

2.1. Synthesis 20

2.1.1. Reagents and Solvents 20

2.1.2. Reaction Containers: Autoclaves 21

2.2. Characterization Techniques 24

2.2.1. Diffraction Techniques 25

2.2.2. Microscopic Techniques 30

2.2.2.1. Scanning Electron Microscopy 31

CHAPTER 3. TRANSITION METAL OXIDES CONTAINING PHOSPHATES 32

3.1. Mn-O and Mn-P-O Systems 38

3.2. V-O and V- P-O Systems 42

CHAPTER 4. CRYSTALLOGRAPHY 47

4.1. Hydrothermal Synthesis and Structural Characterization of Strontium Manganese Phosphate ($Sr_2MnP_3O_{11}$) 55

4.1.1 Experimental 55

4.1.2 Single X-ray Crystallographic Analysis 56

4.1.3. Results and Discussion 60

CHAPTER 5. HYDROTHERMAL SYNTHESIS OF METAL OXIDES INCLUDING PHOSPHATES 65
5.1. Hydrothermal Synthesis and Structural Characterization Of Hureaulite $Mn_5(H_2O)_4[PO_3(OH)]_2[PO_4]_2$ 65
5.1.1. Experimental 65
5.1.2. Single X-ray Crystallographic Analysis 68
5.1.3. Results and Discussion 72
5.2.Hydrothermal Synthesis of Blue Platelike Crystals 79
5.3 Hydrothermal Synthesis of Green Rectangular Crystals 81

CHAPTER 6. CONCLUSION 84

REFERENCES 86

LIST OF FIGURES

Figure **Page**

Figure 1.1. Reaction pattern in a solid state reaction 3
Figure 1.2. Simple vapor phase transport reaction in a closed tube 6
Figure 1.3. Number of papers on hydrothermal research in materials 10
Figure 1.4. Phase Diagram of Water 12
Figure 1.5. Volume (density) / temperature dependence of water 14
Figure 1.6 Presentation of the P-T behavior of water at various degrees of filling 15
Figure 1.7. Schematic of hydrothermal bombs 17
Figure 2.1 Schematic representation of an autoclave. 21
Figure 2.2. An acid digestion bomb, PTFE cup with its cover and pieces of the bomb. 22
Figure 2.3. Carbolite CWF 1100 oven 24
Figure 2.4. Systematic X-ray powder diffraction pattern 26
Figure 2.5. Diagram of an X-ray Diffractometer. 27
Figure 2.6. Comparative X-ray scattering by crystalline solids and amorphous solid or liquids. The two vertical axes are not equal 28
Figure 2.7. Systematic single crystal X-ray precession photograph through a section of the reciprocal lattice.Relative intensities are indicated by the size of spots 29
Figure 2.7. A mounted single crystal to a capillary with epoxy 30
Figure 3.1. Polyhedral view of $Cs_2Co_3(HPO_4)(PO_4)_2.H_2O$ showing the 6-ring tunnels along the [100] direction: CoO_4, dark tetrahedral; PO_4, light tetrahedral; cesium, large circle; water, small circle 36
Figure 3.2. Polyhedral representation of the $NaFe_{3.67}(PO_4)_3$ unit cell showing the open-framework channel structure propagating along [0, 0, 1]. The FeO_6 and PO_4 polyhedra are filled by lined and dotted patterns, respectively. The sodium ions occupy the cavities at the face center 36

Figure 3.3. Polyhedral view of $[N_2C_3H_{12}]_2[Zn_4(PO_4)_4]$, along [001] axis. Note that the connectivity creates eight-membered channels.The amine molecule occupies these channels 36

Figure 3.4. Ball and stick representation of MnO_5 (a) triangular bipyramid and MnO_6 (b) octahedra. 39

Figure 3.5. (a) Ball and stick view of $[NH_4][Mn_4(PO_4)_3]$, showing one-dimensional channels containing ammonium ions along the *a*-axis. (b) Polyhedral view of the channels. The Mn–O polyhedras are shaded light grey whereas the phosphate tetrahedras are dark grey in color 40

Figure 3.6.(a) Stick-and-ball representation of $CH_3NH_2CH_3][Mn_2(OH_2)(HPO_4)(C_2O_4)_{1.5}]$ showing the framework structure formed by the one-dimensional chains made of the $[Mn_2O_{10}]$ dimers and the PO_4 tetrahedra along the a axis together with theC_2O_4 groups. 10-membered-ring channels running along the c axis with organic template lying inside the channels are seen. (b) Stick-and-ball representation of the same structure with the 10-membered-ring seen in the bc plane 41

Figure.3.7. Different arrangements of the PO tetrahedra different from mono and diphosphate found in the vanadium phosphates 43

Figure 3.8. Different environments of vanadium encountered in the vanadium phosphates with metallic cations. The V–O distances are given in Å. 44

Figure 3.9. The inorganic sheet with 3-, 6- and 7-membered rings built up by the alternate linkages of two kinds of 1-D chains in $(C_6H_{16}N_2)_3(VO)(V_2O_4)_2(PO_4)_4.2H_2O$ 45

Figure 3.10. Some of the most common mixed units composed of one VO polyhedra and examples of AVPO structures where they appear. The VO_6 and VO_5 polyhedras are represented in light and middle gray and the PO_4 tetrahedra in dark grey. The A cations are in dark gray circles from two VO polyhedra and examples of AVPO structures where they appear. (c) Most common mixed chains and examplesof AVPO structures where they appear. 46

Figure 4.1. Screens of SHELX. 48

Figure 4.2. Schematic diagram of SHELX program. 48
Figure 4.3. Schematic representation of the main areas of Crystal Structure information program. 49
Figure 4.4. The atoms positions of a compound in its unit cell. 50
Figure 4.5. SOLVE command in the crystal structure program. 51
Figure 4.6. Scheme of a crystal with the relative peak heights. 51
Figure 4.7. Scheme of peak heights and peak coordinates. 52
Figure 4.8. Scheme of Name Item dialog. 53
Figure 4.9. The report of the Fourier calculations. 53
Figure 4.10. Replacement of Hydrogen atoms. 54
Figure 4.11. The packing diagram of a crystal. 54
Figure 4.12. The powder X-ray diffraction pattern of $Sr_2MnP_3O_{11}$ 56
Figure 4.13. (a) Unique atom coordination (b) ORTEP plot of the asymmetric unit of $Sr_2MnP_3O_{11}$ Thermal ellipsoids are given at 70% probability 60
Figure 4.14. Unit cell view of $Sr_2MnP_3O_{11}$ running along a (a) and b (b) axis. The shaded circles represent the Mn atom, the crosshatched circles belong to Sr, the circles shaded bottom right to top left represent the P atoms and the dotted circles show the oxygen atoms. 63
Figure 4.15. View of the Mn/P/O layers of $Sr_2MnP_3O_{11}$ along the c axis. 62
Figure 5.1. Photos of pale pink colored $Mn_5(H_2O)_4[PO_3(OH)]_2$ crystals. 66
Figure 5.2. SEM EDX spectrum of the $Mn_5(H_2O)_4[PO_3(OH)]_2$ 67
Figure 5.3. X ray powder diffraction pattern of $Mn_5(H_20)_4[PO_3(OH)]_2$ 67
Figure 5.4. Unique atom coordination of $Mn_5(H_20)_4[PO_3(OH)]_2[PO_4]_2$ without hydrogens 72
Figure 5.5. ORTEP plot of the asymmetric unit in $Mn_5(H_20)_4[PO_3(OH)]_2[PO_4]_2$. 73
Figure 5.6. A photograph of Hureaulite mineral 73
Figure 5.7. The unit cell structure of title compound as viewed from both c and b direction. The shaded circle from the bottom left to the top right represents a Mn atom; the shaded circle from bottom right to the top left represents a P atom; the circles with dot patterns and

highlight represent a O atom and the smallest circle with a point belongs to hydrogen. 74
Figure 5.8. Polyhedral structure of the $Mn_5(H_20)_4[PO_3(OH)]_2[PO_4]_2$ as view from c direction. Hydrogen atoms are omitted for clarity. 76
Figure 5.9. The polyhedral view of the $Mn_5(H_20)_4[PO_3(OH)]_2[PO_4]_2$ from [100] direction showing linkanages of the slabs with phosphorous tetrahedras. 76
Figure 5.10. Pictures of the yellow crystals 78
Figure 5.11. SEM /EDX spectrum of the yellow bulk crystals. 78
Figure 5.12. The X-ray powder peaks of the yellow crystals. 79
Figure 5.13. Photos of unidentified blue plate like shaped crystals including C, N, O, P, V elements. 80
Figure 5.14. SEM/ EDX specturum of unidentified blue plate like crystals. 80
Figure 5.15. The X-ray powder peaks of unidentified blue plate like crystals. 81
Figure 5.16. Photos of green colored unidentified crystals containing B, C, N, O, V,Cu element. 82
Figure 5.17. SEM /EDX spectrum of the green rectangular crystals 82
Figure 5.18. The X-ray powder pattern of the green colored unidentified plate like crystals 83

LIST OF TABLES

Table **Page**

Table 1.1. Summary of high performance material applications of hydrothermal synthesis 11
Table 1.2. Action of Hydrothermal Fluid on Solid State Materials..... 13
Table 1.3. Critical Temperatures and Boiling Points for Selected Solvents..... 16
Table 4.1. Crystal Data and Structure Refinements for $Sr_2MnP_3O_{11}$ 57
Table 4.2. Atomic Coordinates and Equivalent Isotropic Thermal Parameters of $Sr_2MnP_3O_{11.}$ 57
Table 4.3. Anisotropic Displacement Coefficients ($Å^2$) of of $Sr_2MnP_3O_{11.}$ 58
Table 4.4. Selected Bond Angles (degrees) in $Sr_2MnP_3O_{11}$ 58
Table 4.5. Bond Length (Å) in $Sr_2MnP_3O_{11}$ 59
Table 5.1. Crystal Data and Structure Refinements for $Mn_5(H_2O)_4[PO_3(OH)]_2[PO_4]_2$ 68
Table 5.2. Atomic Coordinates and Equivalent Isotropic Thermal Parameters of $Mn_5(H_2O)_4[PO_3(OH)]_2[PO_4]_2$ 69
Table 5.3. Anisotropic Displacement Coefficients ($Å^2$) of $Mn_5(H_2O)_4[PO_3(OH)]_2[PO_4]_2$ 70
Table 5.4. Selected Bond Angles (degrees) in $Mn_5(H_2O)_4[PO_3(OH)]_2[PO_4]_{2.}$ 70
Table 5.5. Bond Length (Å) for $Mn_5(H_2O)_4[PO_3(OH)]_2[PO_4]_2$ 71
Table 5.6. Oxygen Valence in $Mn_5(H_2O)_4[PO_3(OH)]_2[PO_4]_2$ 72

CHAPTER 1

INTRODUCTION

Humans have been enamored with the dazzling brilliance of crystals for centuries. Crystals, natural or synthetic, have existed in historical accounts from symbolizing royalty and wealth to recent applications in lasing and optical fields. Ancient kings and queens adorned themselves with diamonds, sapphires, and other crystals. At the beginning of the seventeenth century, scientist were fascinated by naturally occurring crystals and attempted to duplicate mineral paragenesis (Inkster 1991).

In the laboratory, in 1960 the Hughes Aircraft Company placed a synthetic ruby crystal rod inside a powerful flash lamp that was similar to those used for flash photography in 1960. In this simple experiment that changed the scientific world, it was observed that after a triggered flash a coherent beam of deep red light emerged from the end of the crystal rod. Through this experiment, light amplification by the emission of radiation was successfully observed for the first time, in what it is known now as Light Amplification by Stimulated Emission of Radiation (LASER). Within a very short time laser action was demonstrated in solids, gasses liquids, and semiconductor crystals (Maiman 1960).

Solid state chemistry is one branch of science concerned with synthesis, structure, properties and applications of solid materials which are usually inorganic solids, but not exclusively so. All compounds are solids under suitable conditions of temperature and pressure. Many exist only as solids at room temperature. The materials of interest are usually in the crystalline form (Schubert and Hüsing 2000). Crystalline form is necessary for structural studies consisting of bonding of atoms in a formed structure, bond angle and bond length between the atoms, and so on. Crystal chemistry deals with the structures of crystals. Many inorganic solids can be prepared by direct or indirect reaction of a solid with another solid, liquid or gas at high temperatures,. Actually under such a condition, it can be said that many solid-solid reactions are solid-liquid reactions since high temperature causes the solid to melt to the liquid phase (Schubert and Hüsing 2000).

There are number of ways in order to prepare new kinetically stable solid state compounds. Up to now many methods have been applied to synthesize solids. Some of the important chemical methods for the preparation of metal oxides are coprecipitation, ion exchange, alkali flux methods, electrochemical methods, ceramic methods, the vapor phase transport method, the combustion method and solvo- /hydrothermal synthesis (Rao and Raveau 1998). The formed solid materials may be in different forms as follows (West 1996):

- a pure single crystal which is free from defects
- a single crystal which contains modified structures via the creation of defects (usually as a result of introduced impurities)
- a powder that of microcrystalline piece form
- a polycrystalline solid such as a ceramic tube
- a thin film
- a non-crystalline or glassy

1.1. The Ceramic Method

The oldest and most common method of synthesizing solid materials is the direct reaction of solid components at high temperatures that is known as the *ceramic method*. As it is not easy for solids to react with each other at room temperature, high temperature is needed to obtain a suitable reaction medium and to reach proper reaction rates to initiate the product formation. Under the high reaction temperature of traditional solid state synthesis, which is above 550°C, most of the inorganic phases are unstable (Liao and Kanatzidis 1992). The instability of reactants under high temperature makes the solids react with each other easily. High temperature is especially necessary for reactions in which large differences between the structure of the starting material and the product are present. During the formation of product, all bonds in the reactants must be broken, and atoms must migrate before forming new bonds (West 1996).

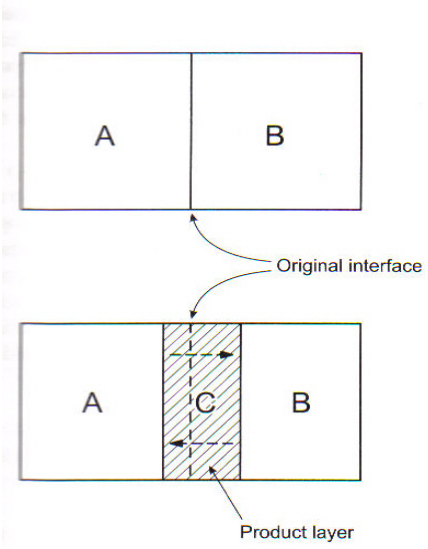

Figure 1.1. Reaction pattern in a solid state reaction
(Source: Schubert and Hüsing 2000).

If high temperatures are not used, the entire reaction has to occur in the solid state without melting. That is to say the reaction has to take place by direct contact of reactant solids A and B shown in Figure 1.1, then solids A and B start to go through some degree of reorganizations to form the product phase C. After this, a product layer is formed in which there is no direct interaction between the A and B. For further reaction there should be ion diffusion to obtain high yield product. As a result the path of atom migration becomes increasingly longer and longer and the reaction rate becomes slower (Rao 1994). As a rule, two-thirds of the melting temperature of one component is enough to activate the diffusion necessary to complete the solid state reaction (Schubert and Hüsing 2000).

Most compounds synthesized at high temperature are very stable thermodynamically. Because thermodynamically stable known phases cannot be avoided, the synthesis of new materials becomes difficult at high temperatures (Kanatzidis 1990). Synthesis of new kinetically stable or meta-stable compounds may be possible under the proper reaction conditions. Preparation of kinetically stabilized compounds requires relatively lower temperatures because the desired compounds are not thermodynamically stable. Sometimes it is impossible that the reaction between the solids takes place although the thermodynamic considerations favor the formation of product. So it shows that both thermodynamic and kinetic factors are important in solid state reactions. Thermodynamic considerations tell us whether or not a particular

reaction may occur by considering the free energy changes that are involved; kinetic considerations determine the rate at which the reaction takes place (Rao 1994). The ceramic method incorporates proper and long enough grinding process in order to maximize surface areas and hence reaction rates. The obtained powder is then pressed into a pellet form to provide intimate contact between grains, the single crystals in a polycrystalline aggregate (Liao and Kanatzidis 1992).

The area of contact between the reactants and hence their surface areas, the rate of nucleation of the product phase and the rates of diffusion of ions through the various phases and especially through the product phase are the important factors that effect the rate of solid-solid reactions. These factors should be considered in the case of direct solid-solid reactions.

Many oxides, carbonates, oxalates or the compounds (including the related metals) are ground to powder form and then heated at a desired temperature to synthesize new solids. The heating program depends on the structure and the reactivity of the reactants. Also sulfides, phosphides, and other solids have been prepared by the Ceramic Method.

For solid state reactions the choice of container requires attention. The container should be chemically inert to the reactants under elevated temperature. Platinum, alumina, stabilized zirconia, and silica containers are generally used for metal oxide synthesis while graphite containers are preferred for synthesizing sulphides and other compounds of the heavier chalcogens (particularly the sulfides, selenides, and tellurides). Containers, made from tungsten and tantalum, have been used in many preparations especially for the synthesis of halides. The containers may be reusable crucibles or boats which are made from foil and thus have limited lifetimes. In the case of volatile or very air sensitive constituents, the sealed evacuates capsules have been used to carry out reactions (West 1996 and Rao 1994).

For solid state reactions the starting materials precursors are available, making powder production on the industrial scale cost effective. Beside its advantages, the ceramic method suffers from several disadvantages: e.g. undesirable phases may be formed, such as $BaTi_2O_5$ during the synthesis of $BaTiO_3$; the homogeneous distribution of dopants is sometimes difficult to achieve; and there are only limited possibilities for in-situ monitoring of the progress of the reaction. Due to this difficulty, mixtures including both reactants and products are frequently obtained instead of homogeneous products. Separation of the desired product from these mixtures is generally difficult, if

not impossible. In many systems the reaction temperature cannot be raised enough for reasonable reaction rates. Furthermore at high temperatures one or more components of the reacting mixture may volatilize. In order to minimize reaction times and increase diffusion rates, optimizations of critical parameters must be investigated such as decreasing of particle sizes and increasing of surface area by grinding, performing the solid-state reactions in molten fluxes or performing the reactions in high temperature solvents (Schubert and Hüsing 2000).

1.2. Vapor Phase Transport Methods

Vapor phase transport methods were developed in 1970's, notably by Schafer (West 1996). It is used not only to synthesize new compounds, mostly binary compounds, but also both for the growth of single crystals and for the purification of the resulting compound. The method is suitable for the preparation of new kinetically stable solid state compounds at low temperatures (West 1996).

Under laboratory conditions, transport reactions are carried out in a closed tube, which has a length of 10-20cm and diameter of 1-2cm. The most important applications of the reactions are in silica and halogen lamps. The tube is evacuated at different pressures and then placed into a furnace to which a temperature gradient is applied. The temperature gradient inside the tube results in a combination of gaseous transporting agent and reactant to form gaseous AB. The volatility of the product AB causes eventual deposition of itself at the other end of the tube to yield the crystalline deposits. A non-volatile solid reactant, A, is placed at one end of the tube and the gaseous agent, B, is added (Figure 1.2). The gaseous agent acts as a carrier to transport the solid reactant and the new compound AB in vapor phase. Transport of two substances in opposite directions is possible in the case of the reactions with the opposite valves for change in enthalpy, ΔH. If $AB_{(g)}$ formation is an endothermic process, the formation occurs at T_2 and solid A deposits at the cooler end at which of the temperature is T_1. If the formation of $AB_{(g)}$ is exothermic, solid formation occurs at the hot end of the tube "(West 1996, Schubert and Hüsing 2000, and Rao 1994)".

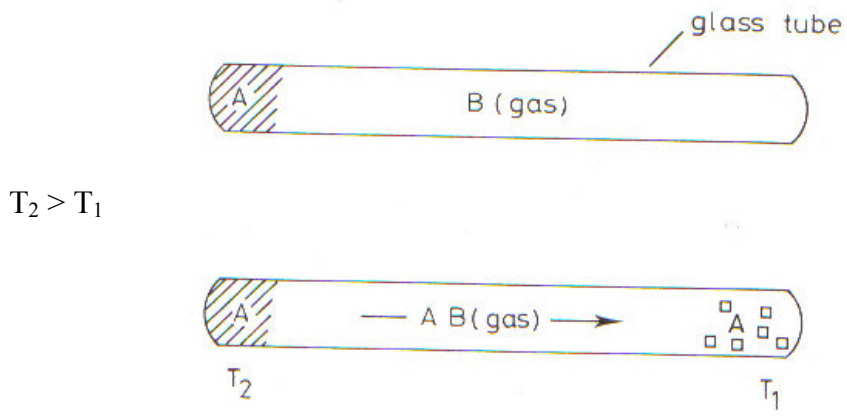

Figure 1.2. Simple vapor phase transport reaction in a closed tube
(Source: West 1996)

1.3. Combustion Methods

The combustion synthesis or the self-propagating high-temperature method is a versatile means by which to synthesize a variety of solids and involves highly exothermic reactions having high enough activation energies to produce a flame. The reactants are initiated by an external source (Rao 1994).

Solids which are of technological importance have been synthesized by combustion methods. Powdered reactants with sizes on the order of 0.1-100μ are placed for a short time in a medium under air or oxygen to favor an exothermic reaction. Binary and ternary metal borides (TiB_2, MoB_2, FeB), oxides ($BaTiO_3$, $LiNbO_2$), hyrides (NdH_2) and carbides (NbC, TiC) are a few examples of the solids formed using combustion methods (Rao and Merkanzow 1992).

1.4. Hydrothermal Synthesis

In the last few years a variety of oxides have been synthesized by the ceramic method which involves grinding of the reactants powder and heating at high temperature with occasional grinding during the intermediate stages, depending upon its necessity. Although a wide range of conditions including high temperatures or

pressures have been used in materials synthesis, the low temperature routes are of greatest interest. The trend throughout the world is to avoid the brute force methods to achieve the control of structure, stoichiometry and purity compound. The brute-force routes are actually desirable for synthesizing novel products, often meta-stable, whose preparations are difficult. Solvo- / hydrothermal synthesis is one of the more important chemical methods for the preparation of new metastable oxides (Rao and Raveau 1998).

Hydrothermal reactions, which as the name implies, use aqueous solutions, were developed more than one century ago during the development of geochemistry. Solvothermal reactions, using non-aqueous solvents, have been applied recently. Such reactions are characterized by mild temperature conditions using either sub- or supercritical conditions. These reactions are mainly divided into three different domains of materials science: the design of novel materials, the development of new processes (due, in particular, to the improvement of reactivity), and the shaping of materials (nanocrystallites, large single crystals, dense ceramics, thin films).

There is also a lot of confusion associated with the term hydrothermal. Instead of the word “hydrothermal” chemists prefer the term solvothermal meaning any chemical reaction. Most of the solvothermal processes are carried out in water, thus the processes are termed hydrothermal. According to most publications including works performed under mild hydrothermal conditions, it is stated that hydrothermal reaction is “any heterogeneous chemical reaction in the presence of a solvent above room temperature and at pressure greater than 1atm in a system”.

In literature many different definitions have been used for hydrothermal synthesis. According to Laudise (1970), hydrothermal growth means growth from aqueous solution at ambient or near-ambient conditions (Byrappa 1992). On the other hand according to Lobachev (1973) the hydrothermal method is defined as a group of methods in which crystallization is carried out in superheated aqueous solutions at high pressures (Lobachev 1973).

Rabenau (1985) defined hydrothermal reactions as heterogeneous reactions in aqueous media above 100°C and 1bar pressure (Rabenau 1985). According to Byrappa’s definition (1992) hydrothermal synthesis is a heterogeneous reaction in an aqueous media which is carried out above room temperature and at pressure greater than 1atm (Byrappa 1992). Yoshimura (1994) defines it as reactions occurring under the conditions of high temperature-high pressure (>100°C, >1atm) in aqueous solutions in a closed system (Yoshimura and Suda 1994). All definitions include lower limit for the

temperature and pressure but there is no exact value for this conditions. The majority of scientists apply the hydrothermal synthesis, for example, at above 100°C temperature and above 1atm.

The British Geologist, Sir Roderick Murchison (1792-1871) was the first to be interested in understanding the main action of water at elevated temperatures and pressures during the natural formation of various rocks and minerals in the earth's crust. A majority of the minerals formed in the different stages under elevated pressure and temperature conditions in the presence of water are said to be "of hydrothermal origin" (Byrappa and Yoshimura 2001).

It has been quite common to use high pressures for the synthesis of solids over the last few decades. Beketoff (1859) showed that metallic silver could be precipitated from a silver nitrate solution heated under hydrogen pressure. His work was the first attempt to study a chemical reaction under pressure (Mambote et al. 2000).

The German chemist Robert Wilhelm Bunsen achieved the first purposeful man-made hydrothermal chemical reaction in the 1830s and it was the first application of hydrothermal aqueous (water) or other solvents as a reaction medium. In the reaction, aqueous solutions were placed in thick walled glass tubes at temperatures above 200°C and at pressures above 100bar to form crystals of barium carbonate and strontium carbonate (Bunsen 1848).

Following the work of Robert Wilhelm Bunsen, deSenarmont investigated the synthesis of various crystalline solids in superheated water sealed in glass ampoules and counter-pressured in welded gun barrels (deSenarmont 1851). It was quite productive, and a majority of known minerals were prepared from various recipes in water above its boiling point. Most of these early works resulted in the synthesis various known minerals, including oxides, silicates, phosphates and sulfides under hydrothermal conditions (Roy and Tuttle 1956).

The natural beryl crystal (beryllium aluminum silicate) and some of the largest quantities of quartz crystals "(silicon oxide)" ever made by human also are of hydrothermal origin. Quartz crystals were obtained by Schafthaul in 1845 after transformation freshly precipitated silicic acid in a Papin's digestor (Schafthaul 1845). Later hydrothermal synthese found many other applications in the 19^{th} century. Hydrothermal technology was used commercially to leach bauxite ore (aluminum ore) with sodium hydroxide by Karl Josef Bayer in 1892 to obtain pure Al_2O_3 necessary for processing to metal (Goranson 1931). In the Bayer process alumina is extracted by

leaching with a sodium hydroxide solution in steam-heated autoclaves. The operation temperature depends upon the degree of hydration of bauxite ore. If the aluminum in bauxite is present as gibbsite, $Al(OH)_3$ or trihydrate, then it can be successfully leached by sodium hydroxide yielding a concentration of 130 to 200grams per liter, at temperatures between 120 and 140°C. Even today, the process is still used to treat bauxite ore. The below process is very simple and it is carried out at about 330°C and 25,000kPa (Habashi 1993).

$$Al(OH)_3 + OH^- \longrightarrow [AlO(OH)_2]^- + H_2O \qquad (1\text{-}1)$$

$$AlOOH + OH^- \longrightarrow . [AlO(OH)_2] \qquad (1\text{-}2)$$

After Al extraction, many other minerals and ores such as gold ore, ilmenite (iron titanium oxide), casterite (tin), uranium ores, copper, and nickel and so on also have been processed in similar fashion.

During World War II there were increasing demands for large amounts of pure materials, but natural sources were not being enough to supply. Quartz was in great demands thanks to its very low dielectric loss in microwave applications (Jessop and Leitner 1998). Large single crystals of α-quartz which is stable below 580°C were grown in the laboratory under controlled conditions (Laudise et al 1969). After the war single crystals up to 1kg in mass were grown successfully in the Bell labs (Beuhler and Walker 1950). Now, many companies throughout the world produce ά-quartz commercially at rates more than 500,000kg each year (Jessop and Leitner 1998).

The hydrothermal technique was used to also to synthesize inorganic compounds after the synthesis of large single crystals of quartz by Nacken (1946) and zeolites by Barrer (1948).Also following the production of quartz crystals and the molecular sieves, further studies were done to find new application areas of the hydrothermal technique both for science and technology (Byrappa and Yoshimura 2001).

After all these developments, many people from different branches of science including chemists, geologists, mineralogists, physicists, ceramists, biologists, material scientists, engineers, and hydro-metallurgists gave attention to the hydrothermal technique in their work to produce of a wide range of advanced materials carrying out their studies efficiently (Byrappa and Yoshimura 2001). These advanced materials synthesized by hydrothermal processing are often of a well-defined form; particle size,

crystal structure, and relatively high purity despite originating from a relatively low-grade source.

The hydrothermal technique has been used to produce many minerals and crystals both in nature and laboratory for many applications in materials science and solid state chemistry. The method is both technologically and scientifically popular in several countries particularly in the last decades; Figure 1.3 shows the countries having the greatest number of papers on hydrothermal research in materials. The method is the only way to produce some inorganic solid materials. Quartz (SiO_2), berlinite ($AlPO_4$), gallium phosphate ($GaPO_4$), potassium titanyl phosphate ($KTiPO_4$), calcite ($CaCO_3$), many other carbonates containing Mn, Fe, Cd, Ni, potassium titanyl arsenate ($KTiAsO_4$), and zeolites are important solids that have been synthesized by the method. Some other synthesized advanced materials are illustrated in Table 1.1 (Byrappa and Yoshimura 2001).

.

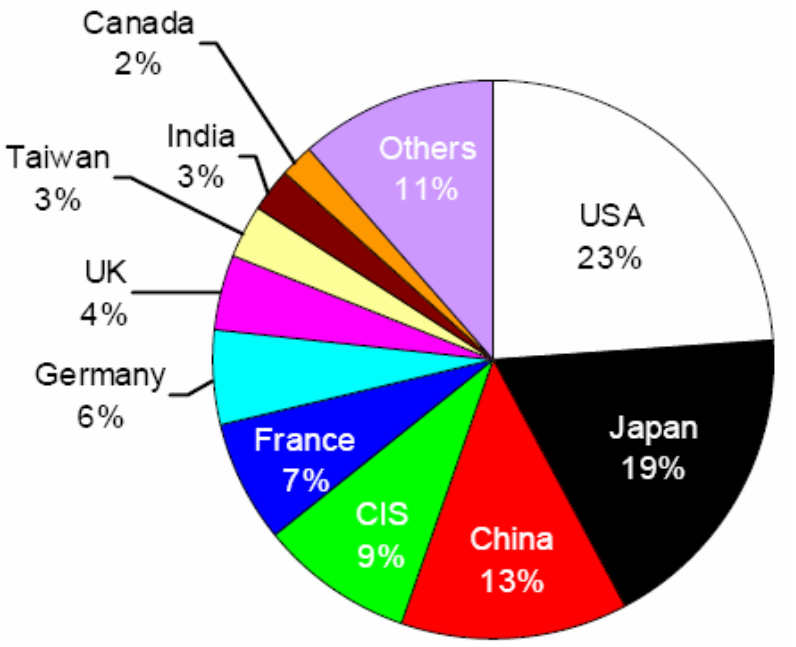

Figure 1.3. Number of papers on hydrothermal research in materials (Source: Byrappa and Yoshimura 2001).

Table 1.1. Summary of high performance material applications of hydrothermal synthesis

(Source: Goodenough et al.1972)

Fuction	Material	Application
Electrical Insulator	Al_2O_3	IC circuit substrate
Ferroelectirc	$BaTiO_3$, $SrTiO_3$	Ceramic capacitor
Piezoelectric	$Pb(Zr, Ti)O_3$,a-SiO_2	Sensors, transducers, actuators
Optical	$(Pb,La)(Zr,Ti)O_3$	Electro-optic video display and storage, light modular
Thermal insulator	$CaAl_2O_4$ calcium silicate	Refractory
Metal alloys	Cr, Co, Ni	High performance metal alloys
Semiconductor	$BaTiO_3$, ZnO-Bi_2O_3, transition metal oxides	Thermistors and varistors
Chemical	ZnO, Fe_2O_3, ZrO_2, TiO_2, zeolites	Chemical sensor, catalyst, catalyst substrate, desiccant, gas adsorption / storage
Structural	ZrO_2(TZP), cordierite, Al_2TiO_5, mullite,xonotlite	Automotive, heat exchangers, metal filters, light modulator
Biological	Hydroxyapatite	Artifical bone
Colorant	Fe_2O_3, Cr_2O_3, TiO_2-(Ni,Sb), $ZnFe_2O_4$, aluminates, chromites, cobaltites	Ceramic pigments, paints, plastic colorants
Eletroni conductor	Precious metals and alloys, indium tin oxide	Electrode layers, transparent conductive films
Magnetic	y-Fe_2O_3, Fe_sO_4,$BaFe_{12}O_{ls}$, garnets	Magnetic pigment (data / audio / visual) storage

Hydrothermal reactions can occur in both closed and open medium. Since water is used, for the closed system hydrothermal reactions the P-T relations of water at constant volume are very important (Figure 1.4). The hydrothermal method is different from other methods in which pressure is used. In many high pressure methods the reactants are placed between the jaws of opposed rams or anvils whereas in hydrothermal methods water is present in reaction vessels called autoclaves. The water is utilized under pressure and at elevated temperature above its boiling point to speed up the reaction between the solid particles in a closed system.

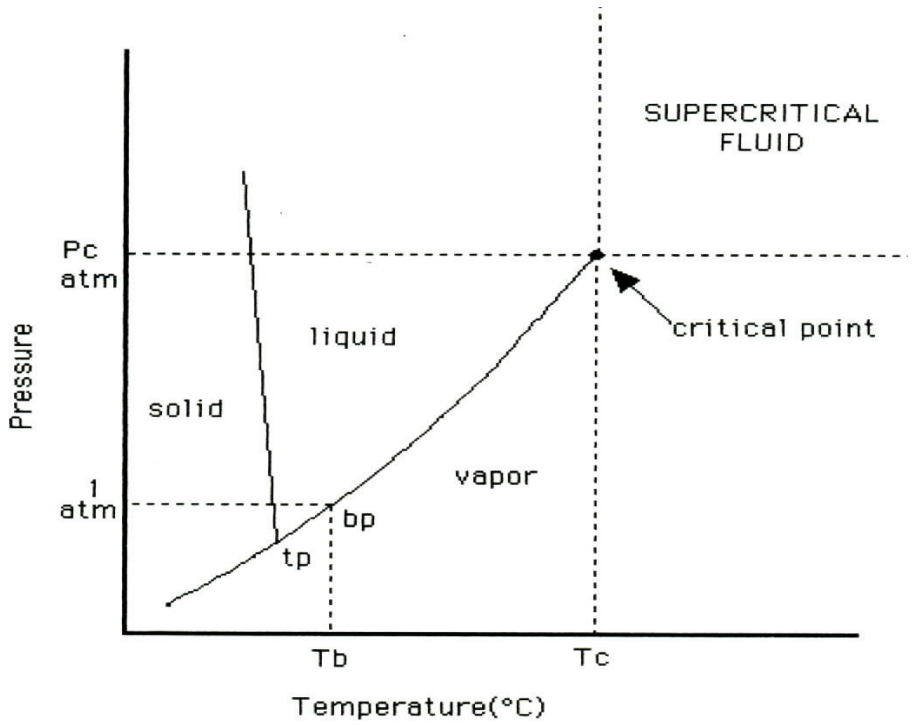

Figure 1.4. Phase Diagram of Water
(Source : Jessop and Leitner 1998)

Water has many significant actions (Table 1.2). Water may form two different phases, as liquid a vapor between the applied temperature and pressure. Whatever the phase is, water can serve as pressure transmitting medium. Besides this, water is used as solvent. Solids do not react with each other at room temperature; high temperature is needed for the kinetics of reaction. Some or all of the solids partially or truly dissolve in water under applied pressure and temperature. The solubility of reactants under these conditions can cause reactions to take place easily. Otherwise in the absence of water the reactions would occur with low yields or they may require much higher temperatures. Therefore, phases, which are unstable at high temperatures, may be synthesized by the hydrothermal method. Water is defined as being supercritical if it is at conditions above its critical temperature and pressure. It exhibits unique properties, especially under supercritical conditions (Jessop and Leitner 1998).

Table 1.2. Action of Hydrothermal Fluid on Solid State Materials
(Source: Byrappa and Yoshimura 2001)

Classified	**Action**	**Application**
1. Transfer Medium	Transfer of Kinetic Energy, Heat and Pressure Forming, etc	Erosion, Machining Abrasion
2. Adsorbate	Adsorption / Desorption at the Surface	Dispersion, Surface Diffusion, Catalyst, Crystallization, Sintering, Ion Exchange, etc.
3. Solvent	Dissolution / Precipitation	Synthesis, Growth, Purification, Extraction, Modification, Degradation, Corrosietc.
4. Reactant	Reaction	Formation / Decomposition (hydrates, hydroxides, oxides)

In the Figure 1.4, the critical point shows the end of liquid-vapor coexistence curve at the critical temperature, T_c, and pressure, P_c, for water. The properties of all supercritical fluids (SCFs) (Table1-5) vary depending on the pressure and temperature and are frequently described as being intermediate between those of a gas and a liquid. A supercritical fluid is neither a liquid nor gas above its critical point, and both phases become indistinguishable having properties between a gas and liquid. With increasing temperature, the liquid form becomes less dense because of thermal expansion and at the same time the gas form becomes more dense. At the critical point T_c, both phases coexist in equilibrium and one density (Figure 1.5)

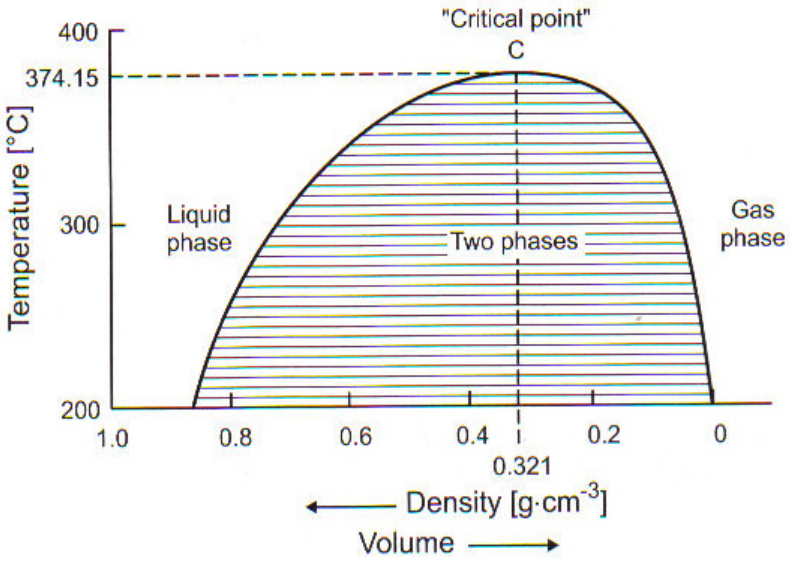

Figure 1.5. Volume (density) / temperature dependence of water
(Source: Schubert and Husing 2000)

Diffusivity and viscosity affect mass transfer. Diffusivity of species in an SCF may occur faster than in a liquid solvent. High diffusivity, low viscosity and intermediate density increase the rate of the reaction (Jessop and Leitner 1998, and Eanes 2000). Thus supercritical water is a good reaction medium for easy transport, synthesis of metastable phases, and the growth of good quality single crystals.

Water is one of the most important solvents in nature and its usage is environmentally beneficial. It is nontoxic, nonflammable, noncarcinogenic, nonmutagenic, and thermodynamically stable, and it is reasonably volatile, so as to be removed from the product (Eanes 2000). Water is a polar solvent and its polarity can be controlled by temperature and pressure. This can be an advantage over other solvents.

For hydrothermal synthesis, the P-T behavior of water changes under various conditions of pressure, volume, and temperature. Laudise studied the details of pressure-temperature behavior of water (Laudise 1987). According to his study, if container, the autoclave, is filled initially to 32%, the liquid level remains constant until the critical temperature is as shown in Figure 1.6. At 374.15°C, is critical point of water, the densities of both the gas and liquid phases are the same and equal to 0.32g/cm^3. Filling less than 32% results in decreased liquid level as temperature rises and gas fills the autoclave at temperatures below the critical temperature (i.e. liquid is lost). When

filled to more than 32% with water, the autoclave is filled at temperatures before the critical temperature. As the filling percentage of containers is increased, the autoclaves will be filled at lower temperature (Laudise 1987). Hydrothermal crystallization is performed with degrees of filling of 32% with pressures of 100bar and more successfully above 65% with pressures of 200-3000bar (Laudise 1987).

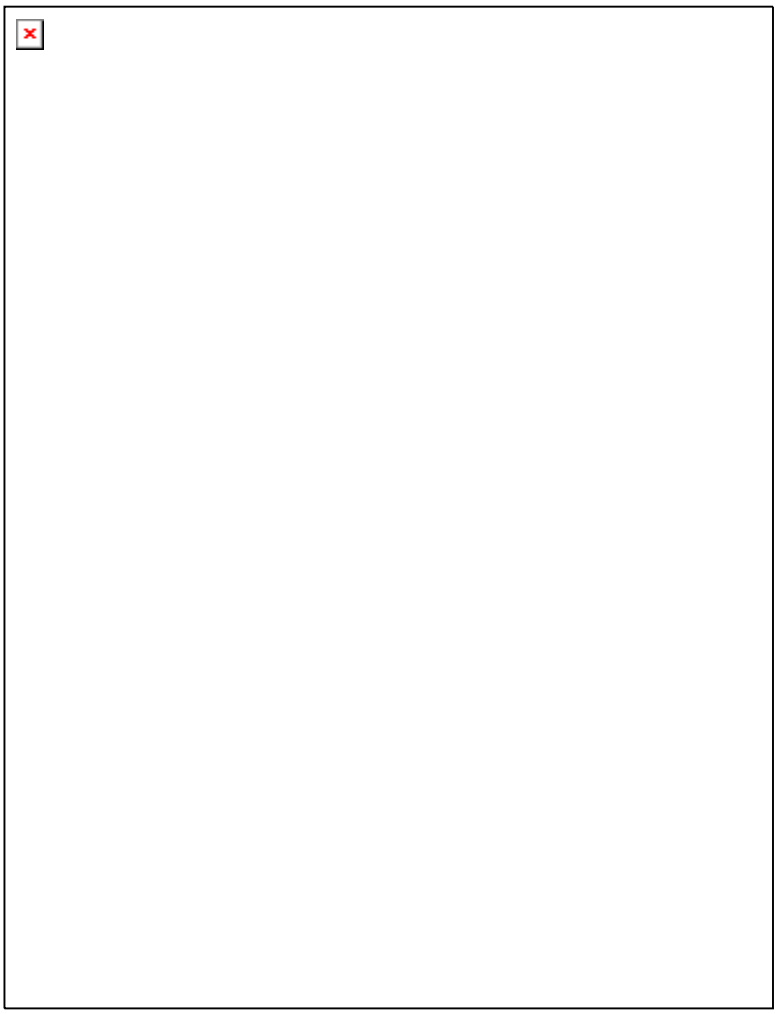

Figure 1.6 Presentation of the P-T behavior of water at various degrees of fill (Source: Laudise 1987).

There are many non-aqueous solvents (Table 1.3) that can be used as superheated fluids. Ammonia is a common solvent in solvothermal reactions and the reactions containing ammonia as solvent are called as ammonothermal reactions (Schubert and Husing 2000). Ammonia, NH_3, even though it is less polar and less protic than water, is a good medium for inorganic synthesis in high pressure fluids because many inorganic reagents are soluble in it. Carbon dioxide, CO_2, is another solvent for the synthesis of several inorganic, organometallic complexes and inorganic aerogels

(Loy 1997). Methanol, CH_3OH, is a solvent for most inorganic compounds despite its smaller polarity than water. Many metal carbonates have been prepared by using CO_2 / water mixture as solvent (Loy 1997, Ikornikova and Lobchev 1971). The combined mixture forms carbonic acid which is polar enough to dissolve inorganic solids.

Table 1.3. Critical Temperatures and Boiling Points for Selected Solvents (Source: Rabenau 1985).

Solvent	**Tc (°C)**	**Bp (°C)**
Water	374.1	100
Ethanol	243	78.3
Carbon dioxide	31.3	-78.5
Chlorine	144	-34.6
Hydrogen sulfide	100.4	-60.2
Ethylenediamine	320	116.9
Sulfur dioxide	157.8	-10
Carbon disulfide	279	-46.5
Hydrogenchloride	51.4	-85.05
Ammonia	132.3	-33.5
Methylamine	156.9	48
Methanol	240	65

Supercritical fluids (SCF's) have the ability to solubilize and to transport low concentrations of reactive intermediates. Relative stoichiometry, reaction time, solvent polarity, acid concentration and mineralizer affect the route of the reactions in SCF's. When controlling all these parameters, the hydrothermal method can be used for single crystal growth as well as for the crystallization of materials, materials processing, thin film preparation, and etc. (Byrappa and Yoshimura 2001).

Many compounds do not show high solubility in water even at supercritical temperatures; therefore, the size of the crystals or minerals obtained will not be big enough for X-ray diffraction measurements necessary for crystallographic studies and technological applications. Chemical structure in almost all types of compounds (organic, inorganic, biological) has been the basis for the spectacular advances in nearly all physical sciences in the last nearly 100 years. The determination of structure in the

vast majority of cases is due to the development of single crystal and powder X-ray crystallographic techniques.

In order to form soluble species, a small ionic, soluble molecule known as a mineralizer is added to an aqueous solution to speed up crystallization, and to increase the solubility of the solute by attacking the starting material (Schubert and Hüsing 2000). Even a small percentage of mineralizer is enough to observe reactivity. The more mobile the species, the more the reactants dissolve and the larger the products of precipitation. But sometimes under the hydrothermal conditions, fast diffusion results in super saturation and then dendritic growth that increases the chance of impurities (Eanes 2000). Impurities bring about low quality crystals. By controlling not only the temperature but also the temperature gradient, the effect of impurities can be removed. The reactants dissolve at the hot end and then reprecipitate at the cooler end of the container by arranging the temperature gradient to be present in the reaction container (Figure 1.7). Hydroxides, chlorides of alkali metals carbonates, alkali salts of weak acids, and halides can be used for this purpose.

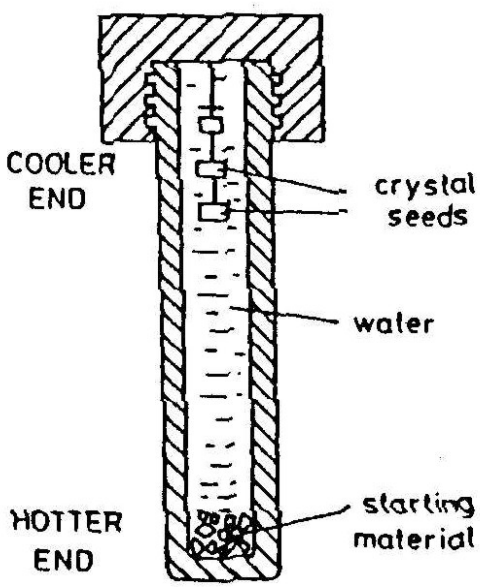

Figure 1.7. Schematic of hydrothermal bombs
(Source: Schubert and Hüsing 2000).

The use of high pressures in the hydrothermal method provides an additional parameter for getting information about structures, properties and behaviors of solids. Today there are many examples of commercial equipment capable of use under high

pressure and temperature conditions. The hydrothermal method is often employed in the 1-10kbar pressure range either in an open or a closed system. In an open system, the solid is in direct contact directly with the reacting (pressure intensifier) gas (F_2, O_2, or N_2). Bradley and Munro (1965) reported an early application of the hydrothermal process in their studies concerning the synthesis of crystals of quartz for piezoelectric applications. Recent applications have also been reported by Dawson and Han (1993), all in relation to production of a wide range of so-called advanced materials. For open systems, generally gold vessels have been used. RhO_2, PtO_2 and Na_2NiF_6 have been synthesized by open system hydrothermal methods (Mambote et al 2000).

Hydrothermal high pressure synthesis under closed system conditions have also been used for the preparation of higher valence metal oxides, such as pyrochlores of palladium(IV) and platinum(IV), rare earth metal oxides, and a family of zero thermal expansion ceramics ($Ca_{0.5}Ti_2P_3O_{12}$) (Rao 1994). In the closed system an internal oxidant (e.g., $KClO_3$) decomposing under reaction conditions is added to the reactants to provide necessary oxygen pressure (Rao and Raveau 1998). Synthesis in a closed system has been used to prepare metal oxides of high valence number. Hydrothermal reactions in a closed system are important especially for synthesis of a class of catalytically relevant oxides such as which are zeolites and related compounds. A variety of materials have been synthesized by the hydrothermal method such as $KTiOPO_4$ (Bierlein and Geir 1976), tungstates, Tl- superconductors (Chen et al. 1994), layered compounds (Sugita et al. 1990), and artificial gems (Hosaka 1991).

Hydrothermal methods are generally used for the synthesis of materials that cannot be obtained otherwise. This is an advantage of the hydrothermal method over conventional solid state. According to thermodynamic rules, for the formation a new compound from its initial components, the formed compound must have lower free energy than the sum of the energies of the initial components. In other words, there must be lowering in the free energy at the end of the reactions. Goodenough and coworkers gave explanations to question how pressure promotes the decreasing of the free energy (Goodenough et al. 1972). One of the explanations is that pressure delocalizes the valence d electrons in the transition metal compounds by increasing the magnitude of coupling between the d electrons on the cations, thus lowering free energy, e.g., in $ACrO_3$ (A=Ca, Sr, Pb) perovskites. Another explanation is the stabilization of higher valence states of transition metals by pressure. The stabilization results in promotion of new phase formation with lower free energy.

$CaFeO_3$ (Fe^{4+}) can be given as an example. Suppressing the ferroelectric displacement of cations as in the example of MoO_3 which is stabilized by a ferroelectric distortion of MoO_6 and inducing of the crystal structure transformations to more close-packed arrangements are the other explanations for the effect of pressure on energy (Goodenough et al. 1972).

CHAPTER 2

EXPERIMENTAL METHOD

The experimentation part can be classified into three sections. First part of the experimentation includes reactants, containers and proper heat treatment. Characterization of the solid is the second part. In this part Diffraction Techniques including both single and powder X-ray diffraction which are necessary to characterize the solids and Microscopic Technique which is the scanning electron microscope (SEM) analysis in order to get information about elemental compositions and morphology of the solids are used. After getting enough information about the novelty solids ShelX-97 computer software program has been used to solve the solids structure by using its data.

2.1. Synthesis

2.1.1. Reagents and Solvents

Depending upon the planned reaction the source of transition metal and phosphate groups were changed. Distilled water used as solvent. In most of the reactions ortho-Phosphoric acid (H_3PO_4, Merck 99%), sodium hydrogen phosphate (NaH_2PO_4, Merck 99%), manganese chloride ($MnCl_2$, Aldrich 99%), boron phosphate (BPO_4, Aldrich 99.5%) were used. As transition metal sources, Manganese(III) oxide (Mn_2O_3, Aldrich 99%), Manganese(II) carbonate ($MnCO_3$ Aldrich 99%), and manganese nitrate ($Mn(NO_3)_2$, Aldrich 99%), Vanadium(III), (IV), (V) oxides (V_2O_3, Alfa 99%; VO_2, Alfa 99%; V_2O_5, Aldrich 99.5%), alkali vanadium oxides ($LiVO_3$, Alfa 99.9%; $NaVO_3$, Fluka 98%) were chosen. In some reactions ethylenediammine ($C_2H_8N_2$, Merck 99%) was used as an organic component. Distilled water and acetone were used to wash products.

2.1.2. Reaction Containers: Autoclaves

Teflon-Lined Acid Digestion Parr Autoclaves were used for the synthesis. Parr acid digestion bombs were purchased from Parr Instrument Company. The containers are lined with a removable Teflon insert and posses a maximum operating temperature and pressure of 250°C and 1800psi, respectively. The closure design consists of a spring-loaded, broad flanged closure that is sealed by tightening the bomb cap with a hook spanner wrench (Figure 2.1). The Teflon will expand and contract depending on heating and cooling cycles.

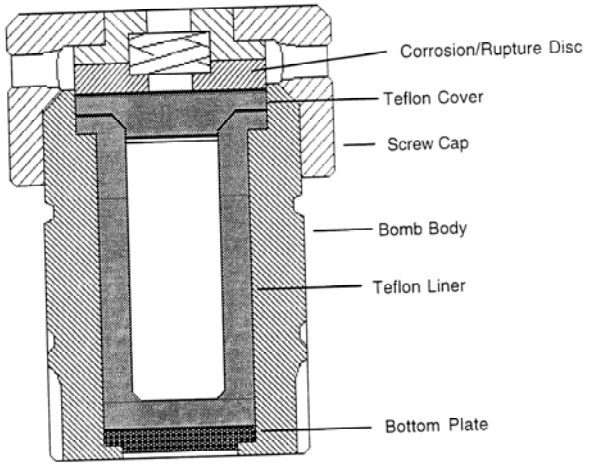

Figure 2.1. Schematic representation of an autoclave.
(Source: Parr Instruments Catalog)

Inner parts of the acid digestion bomb are made from polytetrafluoroethylene (PTFE) and outer parts of that made of steel are shown in Figure 2.2. These Teflon inserts are completely inert to aqueous base and fluorides it makes them a workhorse for the zeolite industry. Also the PTFE bombs provide a convenient medium in order to dissolve samples rapidly in strong alkalines or acids except perchloroic acid due to unpredictable behavior of the perchloric acid in a closed system. The bombs are useful at the temperature ranges of hydrothermal synthesis but care should be taken in selecting the operating temperature depending on used acid. Temperatures in the range of 150 to 220ºC range are quite applicable.

(a) An acid digestion bomb

(b) PTFE cup with its cover

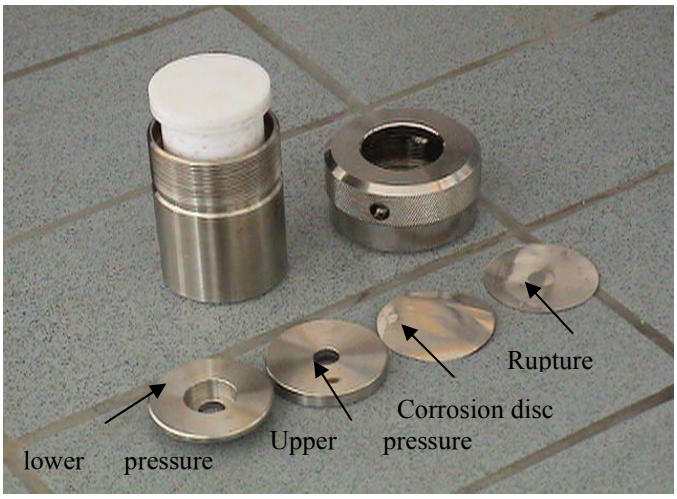

(c) PTFE cup with cover, acid digestion bomb body, screw cap and its parts

Figure 2.2. An acid digestion bomb, PTFE cup with its cover and pieces of the bomb.

PTFE has two characteristics which make it somewhat less than perfect for its application. First PTFE has a tendency to creep or flow under pressure or load. This is present even at room temperature and emphasized at higher temperatures. At temperatures below 150ºC the creep effect will become more pronounced, making it difficult to maintain tight seals and resulting in deformation and shorter life for PTFE components. The creep effect is proportional to maximum operating temperature. Secondly PTFE is a porous material. There can be vapor migration across the cover seal and through the wall of the liner itself. Parr can minimize the problems by machining the seal and the wall of the liner to reduce any porosity to an absolute maximum. Also

the thick wall and long path seals in the Parr bomb liners can help to reduce the undesired properties. According to done experiments amount of solute lost in this manner during a normal digestion is negligible, but vapor migration will occur and frequently it will produce discoloration on the inner metal walls of the bomb body and the screw cap.

A new autoclave must be pre-treated carefully prior to heating. Before using a new PTFE cup and cover, these parts should be heated in a bomb with a charge of pure water. This pre-treating will help to develop the required seals and it may prevent annoying leakage in subsequent procedures. The amount of water used in this pre-treatment should not exceed 40 percent of the capacity of the cup. Since the autoclaves used in our laboratory (Parr Instruments, model 4749) have 23mL capacity, it is necessary to use 9mL of H_2O providing 32% filling for pre-treatment. Maximum charges for inorganic and organic samples are 1.0 and 0.1gram respectively. These autoclaves can be heated up to 250°C and 1800psig pressure.

These bombs can be used safely and routinely for treating a great variety of samples with different digestion media under a wide range of operating conditions. The pressure generated within bombs, filling level and the amount of heat applied to promote the reactions are dependent upon the nature of materials being treated.

After designing a reaction, proper amount of starting materials and solvent are added to the containers, than the pieces of autoclave, which are shown in Figure 2.2c, are placed in the order of first corrosion disc (thinner one), then rupture disc (thicker one). After closing the autoclave, it is placed into the Carbolite CWF 1100 (Figure 2.3) furnace for at least 1 day at 170-220°C. After the reaction time is completed, the autoclave is allowed to cool slowly in the furnace. Cooling must proceed slowly. It should be avoided to submerge the bombs in a sink on an aluminum plate and to accelerate the cooling by placing the bomb in the air flow.

Figure 2.3. Carbolite CWF 1100 oven

2.2. Characterization Techniques

After synthesizing a solid, the most important question coming into mind is what the solid is. Depending upon nature of the substance, many methods are used to get answer for this question. For molecular materials spectroscopic methods and chemical analysis can be used for identification. If the obtained substance is non-molecular and crystalline, identification is usually carried out by X-ray crystallography in which case information is also obtained on the way where the molecules pack together in the crystalline state (Pope and Muller 1991) and the identification is supplemented by chemical analysis.

The crystalline solids can be in the form of: a *single crystal* that is pure and free from defects, *a single crystal* whose structure can be modified by defects and specific impurities, a *powder,* i.e. a large number of small crystals, *a polycrystalline solid piece*, e.g. a pellet or a ceramic tube in which a large number of crystals are present in various orientations or a thin film (Muller et al. 1998). The noncrystalline solid materials can be glass or amorphous. Noncrystalline solids may be prepared in various forms as tubes, pellets or thin films (West 1984).

In chemistry concerning solids, the two primary pieces of information most often sought are the structure of the material and its reactivity. Each solid has its own

characteristic X-ray pattern which may be used as a 'fingerprint' for its identification. The X-ray diffraction patterns of most inorganic solids are known and the solids can usually be identified rapidly and unambiguously by matching the patterns of unknown solids with that of known one. X-ray diffraction methods that can be used to study single crystals, powders and other forms of solids (Tanaka and Suib 1999) are the most powerful characterization tools known by scientists. If X-ray powder pattern of the substance is not match with of the known phase, next step is collecting single crystal X-ray data.

Structural properties are often responsible for several physical and chemical properties such as electrical conductivity, chemical stability, toughness and others (West 1984). No single technique is capable of providing a complete characterization of a solid. Diffraction, microscopic and spectroscopic techniques are three main categories of characterization techniques which may be used to characterize solids.

2.2.1. Diffraction Techniques

There are two different diffraction techniques to characterize crystalline materials. These are powder X-ray diffraction and single X-ray diffraction methods.

X-ray powder diffraction method which is the most powerful technique can be used to study the degree of crystallinity of a material, to determine the basic structure of the material, and to elucidate the degree of purity and crystallinity of the sample under interest. X-ray diffraction methods can be used to study single crystals, powders and other forms of solids such as thin films, wires, fibers and other similar forms of materials (Tanaka and Suib 1999). The powder method has also some other uses such as characterization of materials, qualitative and quantitative phase analysis, determination of crystal size, study of distortion by stress, crystal structure determination (West 1984).

An X-ray powder diffraction pattern is a set of lines or peaks, each of which are in different intensity and position (d-spacing or Bragg angle, θ) on a strip of photographic film or chart paper as shown in Figure 2.4. For a given substance, the characteristic powder pattern or the line positions are fixed and characteristic for that substance. The intensities may vary from sample to sample depending on the method of sample preparation and analysis conditions. The thermal motion of atoms which is inevitably present in all substances above absolute zero causes a reduction in peak

intensities and an increase in the background radiation. This is mostly noticeable at high temperatures and as the melting point of the sample is approached.

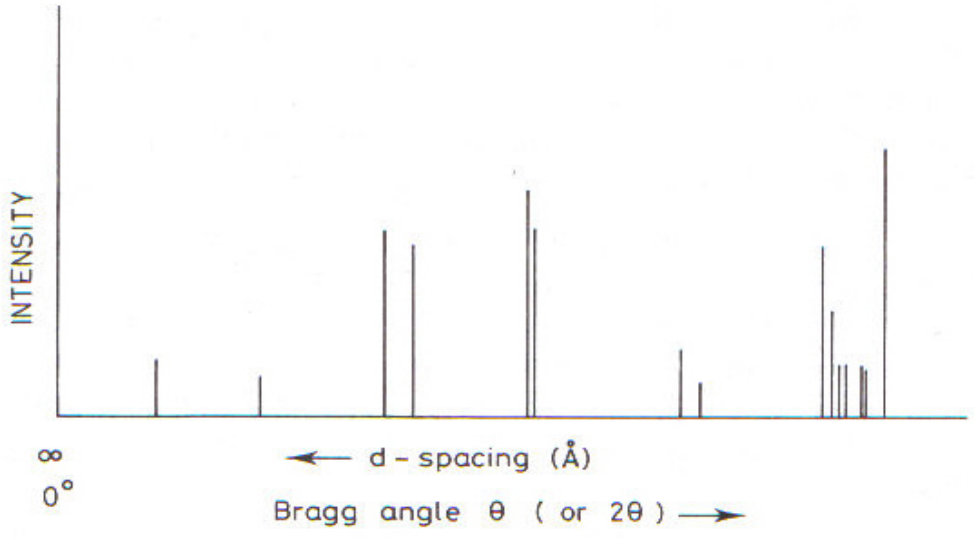

Figure 2.4. Systematic X-ray powder diffraction pattern
(Source: West 1984).

The powder method is based on the principles that a monochromatic beam of X-rays strikes a finely powdered sample having crystals randomly arranged in every possible orientation and also having various lattice planes in every possible orientation. The x ray diffraction is explained by Bragg. The Bragg approach to the diffraction is to regard crystals as constructed from in planes or layers which act as a semi-transparent mirror. Some of the X-rays are reflected off a plane with the angle of reflection that is equal to the angle of incidence rays and reflected beam are interfere constructively. So diffraction occurs for the crystals and planes which are oriented at the angle of incidence beam called as Bragg angle, θ, with the planes (West 1984). The diffracted beams can be detected either by surrounding the sample with the strip of photographic film or by using a movable detector.

Usually the powder or other sample form whose crystal size is less than 2000Å is attached to a glass slide by some noncrystalline material such as vaseline. The lines in a powder diffraction pattern are of finite breadth but if the particles are very small the lines are broader than usual. The broadening increases with decreasing particle size. The limit particle size to be seen is about 20 to 100Å (West 1984).

A diagram of an X-ray powder diffractometer is given in Figure 2.5. X-rays are produced in the X-ray tube and are collimated onto a sample. In most cases CuK_{α} radiation is used for studies of powders. The sample is usually moved at angles between 2θ=5-70 degrees or larger. A proportional counter is used as a detector and the intensities of the diffraction peaks are recorded on a chart recorder or stored on a computer.

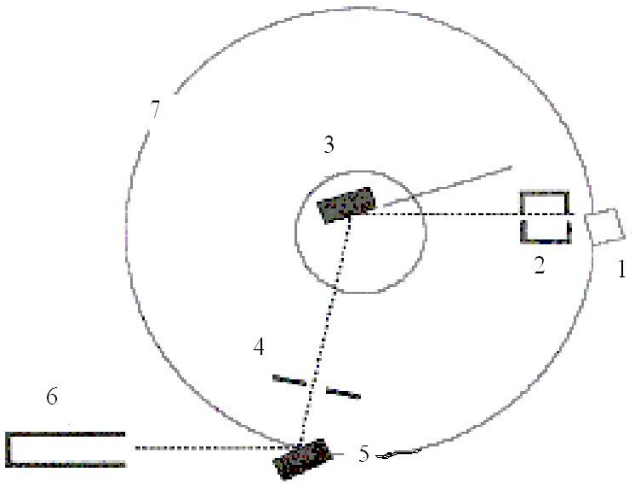

Figure 2.5. Diagram of an X-Ray Diffractometer. Various parts: 1= X-ray Source, 2= Collimator, 3= Sample, 4= Slits, 5= Monochromator, 6= Detector, 7= Focus circle.

(Source: Tanaka and Suib 1999)

It is also important to press the powdered sample onto such a slide because a random orientation is necessary in order to get all of the diffraction from the different planes. During the analysis it is important to compare the peak positions, relative intensities and the general shape of the background signal (Tanaka and Suib 1999).

Crystalline solids give diffraction patterns that have a number of sharp lines. Noncrystalline solids like glasses, gels give diffraction patterns that have a small number of very broad lines with low intensity (Figure 2.6). The detection limit of X-ray powder diffraction method is typically around 5%. Once the 2-theta values are collected they can be converted to theta and by using Bragg's law values of the d-spacings can be obtained (Cullity 1978).

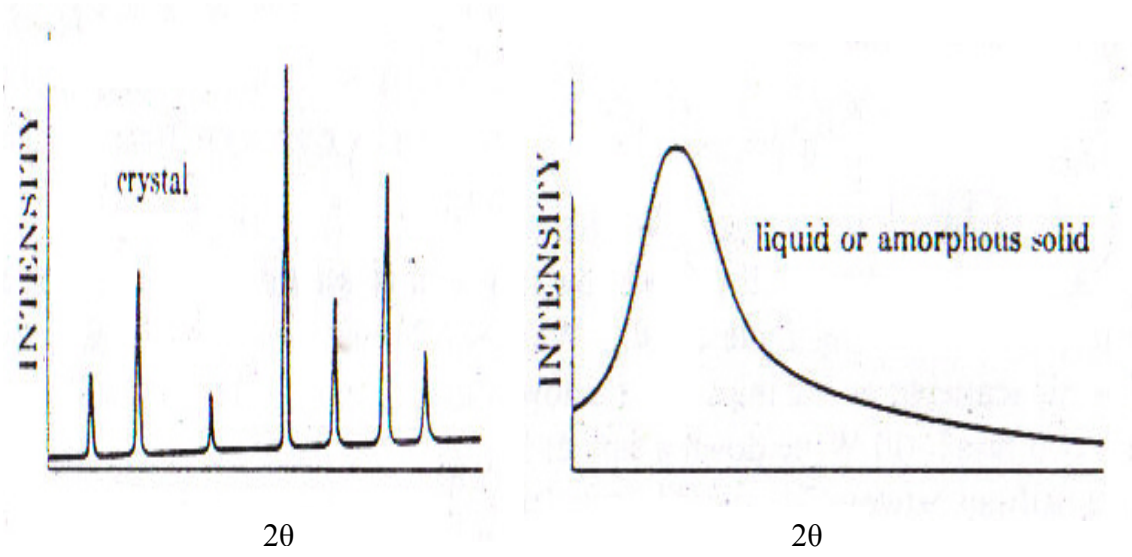

Figure 2.6. Comparative X-ray scattering by crystalline solids and amorphous solid or liquids. The two vertical axes are not equal
(Source: Cullity 1978).

If the obtained substance is a common type then the experimental X-ray powder diffraction pattern can be compared to known published patterns such as those found in the ASTM (American Society for Testing and Materials) tables (Tanaka and Suib 1999). Standard patterns of crystalline substances are given in the Powder Diffraction File, JCPDS (Joint Committee on Powder Diffraction Standards) or ASTM File. The inorganic section of this file now contains over 35000 entries and is increasing at a rate of about 2000 per year (West 1984). If a powder pattern has never been collected before, analogies to known structural types can be made.

In these study X-ray powder diffraction patterns of the compounds were obtained by using a Philips *X'pert Pro* X-ray diffractometer. The grounded samples were placed on a zero-background silicon sample holder. Data was collected by using CuK_{α} (λ=1.5406Å) radiation at settings of -45kV and 40mA for 27 minutes. The scan rate was 0.1^{o}/sn and the data was collected for 2θ values of 5 to 70° (West 1984).

There are several single X-ray diffraction techniques. One of the most used one is the diffraction cameras and the results are the patterns of spots on photographic films as demonstrated in Figure 2.7. The centre, A, of the film correspond the position of the undiffracted beam of radiation. Diffracted X-ray beams results in the spots and the spots fall on the corners of an imaginary grid which may be rectangular, square or parallelogram .In this case rectangular shape. The size and shape of grid forms part of

what is known as the reciprocal lattice and the size and the shape of the unitcell is related inversely with the grid size and shape. a* and b* are the axes of the grid and from the distance apart from the spots the unitcell dimensions may be calculated (West 1984 and Cullity 1978).

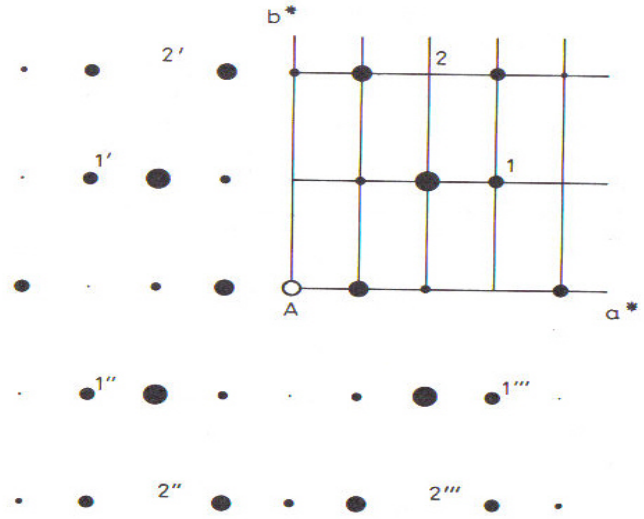

Figure 2.7. Systematic single crystal X-ray precession photograph through a section of the reciprocal lattice. Relative intensities are indicated by the size of spots (Source: West 1984).

Single crystal X-ray diffraction methods have several applications such as determination of unit cell and space group, crystal structure determination, electron distribution, atom size and bonding, crystal defects and disorder. The knowledge of crystal structures is important to understand crystalline materials, their structures, properties and applications (West 1984).

The first step in single X-ray diffraction method is to mount a single crystal on a goniometer which is usually to rotate the crystal in space with two mutually perpendicular arcs. In addition the goniometer can be rotated about a spindle axis. In many cases a precession photograph is taken and the crystal is moved in space until the crystallographic axes are aligned with the photographic detector which is behind the X-ray source and the sample. Usually MoK_{α} radiation is used in single crystal studies.

Data are then collected on the different diffraction peaks and the intensities are counted in a systematic fashion. The crystal system of a crystal may be determined from single crystal X-ray photographs. Basically by looking for a symmetrical arrangement of spots, one can find the symmetry of the unit cell. Once the unit cell is been

determined, the space group determination is done by looking for patterns of absent spots in the X-ray photographs. For instance alternate spots in a row or perhaps entire row may be absent. From the systematic absences, it is possible to determine the lattice type, face centered, body centered, etc. And whether or not the crystal has elements of space symmetry i.e. screw axes or glide planes (West 1984).

Crystal quality is the most important factor in determining the final precision for a given structural investigation. High-quality crystals give high-precise structural results. In order to get high precision, crystals should have some properties; such as they must be single which have no smaller crystals or powder attached to it, they must be of the proper size which is between 0.1 to 0.6mm on an edge and shape with well-defined and lustrous faces; they are of uniform color and contain no cracks or fracture lines. Also they must be ordered and diffract to reasonably high scattering angles (Tanaka and Suib 1999).

Figure 2.8. A mounted single crystal to a capillary with epoxy

Suitable single crystals were mounted in epoxy, and placed in a capillary as shown in Figure 2.8. Single crystal X-ray diffraction data were collected on a Bruker Smart 1000 CCD diffractometer under following conditions. A full reciprocal sphere corresponding to a total of 3x606 frames collected (ω-scan, 15s per frame, 0.3° oscillations for three different values of j). Monochromatic MoK_α (λ=0.71073Å) was employed.

2.2.2. Microscopic Techniques

Microscopes are can be divided into two groups as optical and electron. With optical microscopes, particles down to a few micrometers in diameter may be seen

under high magnification. The lower limit is reached when the particle size approaches the wavelength of visible light, 0.4 to 0.7μm. For submicrometer sized particles it is essential to use electron microscopy. By this way one can image diameters in a few Angstroms. Various kinds of microscopes are available.

2.2.2.1. Scanning Electron Microscopy

Electron Microscopy is a very useful technique capable of providing structural information over a wide range of modification. The Scanning Electron Microscope (SEM) has become one of the most widely utilized instruments for material characterization. Preparation of the samples is relatively easy since most SEMs only require the sample to be conductive. The SEM gives information about the texture topography and surface features of powders or solid pieces by using electrons rather than light to form an image. Features up to tens of micrometers in size can be seen because of the depth of focus of SEM instruments. The resulting pictures have a definite 3-D quality. The resolution of SEM is approximately between 100Å and 10μm (West 1984).

The most common accessory equipped with a SEM is the energy dispersive x-ray detector, EDX. This type of detector allows a user to analyze a sample molecular composition. The ideal specimen for EDX microanalysis is perfectly flat and polished. The results of EDX analysis are usually presented as a spectrum. In this graphical representation the *x*-axis represents the energy level - and therefore identifies the elements, and the *y*-axis provides the number of counts of each element detected.

In the study, the obtained products were analyzed with a Philips XL 30S FEG Scanning Electron Microscope. Although the conditions change from sample to sample approximately accelerating voltage, was 5kV, spot was 3, magnification was 1200, the detector type was Secondary Electron (SE) or Through the Lens (TLD) and the working distance was 4.5-6mm. In the SEM / EDX analyses of our samples, we can obtain the data only in 1-2μm distances from the surface. For the elements staying deeper, results may not be very reliable.

CHAPTER 3

TRANSITION METAL OXIDES CONTAINING PHOSPHATES

Oxygen is the most abundant terrestrial element and almost all elements except noble gases combine with oxygen to form different compounds (Chen and Zubieta 1992). A chemical compound of oxygen with other chemical elements is defined as an oxide. The main field of our investigations is the synthesis and the structural analyses of inorganic solids including transition metals.

Transition metal oxides constitute the most exciting family of materials due to the wide range of structures and variety of properties exhibited by them. There has been considerable effort to synthesize and characterize open-frame inorganic architectures including both metal oxides and phosphates.

Metal oxides are inorganic solids having vast structural chemistry. Simple metal oxides occur throughout nature, for example hydrogen oxide, aluminum and silicon oxide. Oxides can be as discrete binuclear molecular species and polymeric species as chains, layers and three dimensional network structures (Chen and Zubieta 1992). Oxo-metal solid structures can be constructed from metal polyhedra having formula $M_xO_y^n$ in combination with oxygen or oxygen containing groups such as phosphates, arsenates, borates…

In the literature; there are many examples of synthesized inorganic oxides and most of them have been prepared by hydrothermal reactions in crystalline form (Chen and Zubieta 1992, Cheetham et al. 1999, and Hagrman et al. 2001). Metal oxides which are crystalline inorganic oxides are important class of materials with many technological uses. They are extensively studied due to their interesting redox, electrochemical, catalytic or magnetic properties (Hagrman et al. 2001).

In this study we are interested in the synthesis of transition metal oxides including oxoanionic group such as phosphate. Transition metal oxides constitute one of the most fascinating classes of inorganic solids. They show a wide variety of structures, properties, and phenomena. The main reason for the unusual properties of transition metal oxides is the unique nature of the valence d electrons. They have several types of

complex structures which have been characterized in recent years and they may be in the form of simple perovskite, spinel, hexagonal ferrite or complex octahedral tunnel structures depending upon the coordination and the radii of elements present in the oxide (Rao and Raveau 1998).

Actually the metal oxides have simple formula small unit cells despite having complex structures. Many ores, silicates, rocks and soil are examples of these materials in nature. Not only are most ores and gems examples of solid state oxides, but also bones, shells, teeth and wood represent structurally complex oxides fashioned through biomineralization (Li et al. 1999).

Metal oxides containing M-O or M-P-O systems, where the M is metal, may show different structural chemistries and cations (M) used to synthesize these systems include elements from group 1 alkali metals to group 14 of the periodic table, transition metals and even rare earth elements (Chunga et al. 2005). Especially systems having zeolite-like structures have been of great interest scientists due to their useful chemical properties resulting from their special architectures. Most of the transition metal oxides and especially phosphates are described as being microporous or displaying open frameworks and they contain regions of unoccupied spaces. These spaces are large enough to accommodate small molecules. Structures of the phosphates solids resemble those of zeolite materials.

Inorganic porous materials have open framework structures that contain voids in the system and porous solids can be classified into three categories according to their pore dimensions: as microporous solids with pore diameters less than 2nm, as mesoporous solids with pore diameters 2-50nm, and as macroporous solids with the pore diameters greater than 50nm. Manganese phosphates, MCM-41 and vanadium phosphorus oxides can be given as examples for each group, respectively. (Suib 1996).

Open-framework materials currently form an amazingly active field of research (Chippindale et al. 1994 and Wilson et al. 1982). Aluminosilicate zeolites and aluminophosphates with channels and cages of various dimensionalities and sizes were the first studied in these fields. Various families of microporous solids, starting from aluminosilicates and aluminophosphates (Yu et al. 2005 and references therein and Wilson et al. 1982), have been synthesized. Zeolite materials are the most widely known examples of the open framework solids family. Zeolites are crystalline aluminasilicates of alkali and alkali earth elements such as Na, K, Mg, and Ca with the empirical formula $M_{2/x}OAl_2O_3{\cdot}ySiO_2{\cdot}zH_2O$ where x is the cation valence, z is the

number of waters of hydration accommodated in the pores of the zeolite and y changes from 2 to 10, representing the amount of silica in the compound (Meier et al. 1996).

Structures of zeolites are complex and based on an infinite extending through three dimensional frameworks. The frameworks contain AlO_4 and SiO_4 tetrahedras linked to each other via oxygen atoms to form rings (holes) and the formed framework has a negative charge due to the tetrahedral groups. The net negative charge of the framework is balanced by the mobile cations occupying the holes in the framework. The size of the holes changes with the numbers and sizes of the ring members.

Microporous zeolite are well-ordered nanoporous materials used in many areas of chemical science and technology including many process including catalytic, adsorption and separation processes (Cheetham 1999), gas storage and ion exchange (Rowsel and Yaghi 2004). There are many research efforts which have been performed both experimentally and theoretically on this class of materials. The efforts are not only because of their technological importance but also because of their model systems. Indeed, porous materials offer the greatest possibilities for investigating their adsorption properties as a function of many parameters like size and shape of the pores, chemical composition of the framework and nature of the extra-framework cations (Davis and Lobo 1992).

Some important applications of aluminosilicate zeolites are ion-exchange with hydrated zeolites, detergency (e.g. zeolites Na-A and Na-P),water softeners, animal feeds, radwaste remediation (e.g. Cs, Sr with clinoptilolite), molecular sieving with dehydrated zeolites, air separation (N_2 from O_2), drying agents (e.g. double glazing, air conditioning), sulfur removal from natural gas, separation of HFCs (CFC substitutes), catalysis with dehydrated zeolites, catalytic cracking (gasoline production), butene isomerization (Cheetham et al. 1999, Ackley et al. 2003).

At the beginning of the 1980s the aluminasilicate zeolites and the related compounds were represented as the dominant part of open framework materials with three dimensional crystalline structures. Following the extensive development of microporous aluminosilicates, research has gradually shifted towards the aluminophosphates ($AlPO_4$) which have framework compositions of the general formula $(Si_xM_wAl_yP_z)O_2$; where x varies from 0 to 0.20, w takes values from 0 to 0.25, and where the silicon substitutes preferentially at the phosphorus site whereas the metal substitutes exclusively for aluminum (Cheetmam et al. 1999).

Because of the discovery of the open-framework structure alumina-phosphate (Wilson et al. 1982), vast numbers of novel metal phosphates have appeared in the literature. The Zubieta research group synthesized the first example of a non silicate transition metal phosphate TMPO, open framework inorganic oxide with hosted cations in the molybdenum phosphate system in 1989 (Occelli and Robson 1989). The compound $(Me_4N)(H_3O)[Mo_4O_4(PO_4)].xH_2O$ which has a zeolite-like structure was formed from octahedral-tetrahedral Mo_4-oxoclusters and tetrahedral PO_4 groups which are connected each other via oxygen. The formed anionic framework is charge compensated by the cationic organic group Me_4N^+.

Analogous studies with both main group and transition metals were done which have shown that as many as 25 elements of the main block and transition series can be combined to form gallophosphates (Parise 1985 and Ferey 1995), titanosilicates (Chapman and Roe 1990), as well as beryllium (Gier and Stucky 1991), zinc (Neeraj and Natarajan 2000,), titanium (Ekambaram and Sevov 1999), cobalt (Natarajan et al. 2000), iron (Lii et al. 1998), vanadium (Soghomoniam et al. 1995), and molybdenum phosphates (Haushalter 1992), and many others. All the phosphate solids have very interesting structures. Three examples of the phosphate structures including the transition metals cobalt, iron, and zinc are shown in Figures 3.1, 3.2, and 3.3.

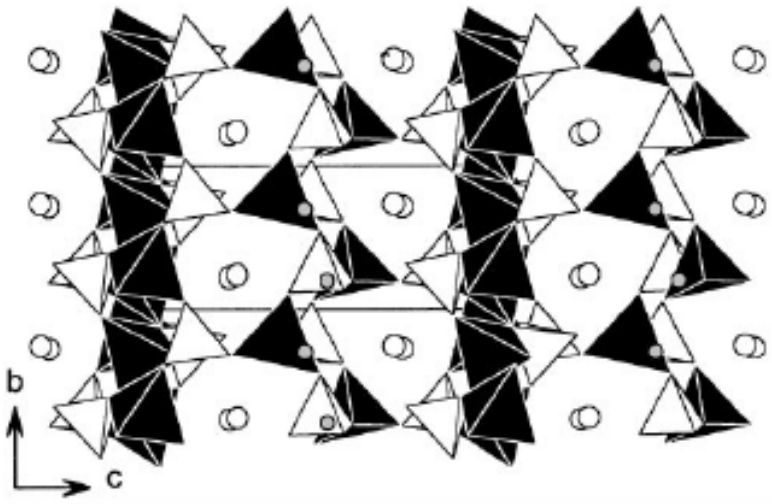

Figure 3.1. Polyhedral view of $Cs_2Co_3(HPO_4)(PO_4).H_2O$ showing the 6-ring tunnels along the [100] direction: CoO_4, dark tetrahedral; PO_4, light tetrahedral; cesium, large circle; water, small circle.

(Source: Chiang et al. 2001)

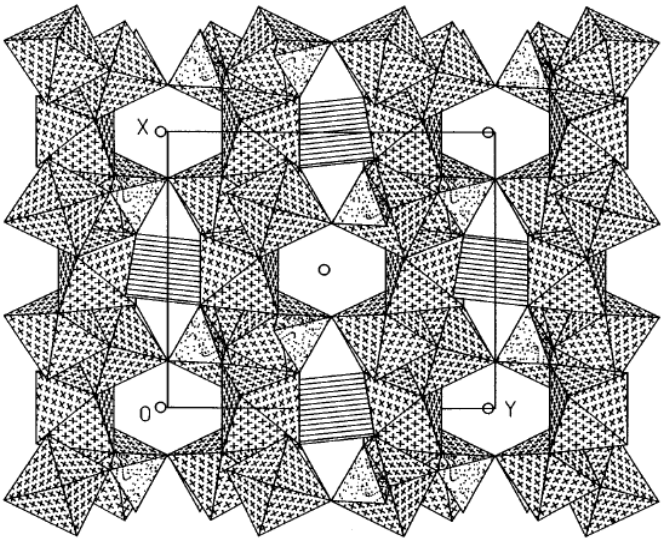

Figure 3.2. Polyhedral representation of the $NaFe_{3.67}(PO_4)_3$ unit cell showing the open-framework channel structure propagating along [0,0,1]. The FeO_6 and PO_4 polyhedra are filled by lined and dotted patterns, respectively. The sodium ions occupy the cavities at the face center.

(Source:Korzenski et al. 1998)

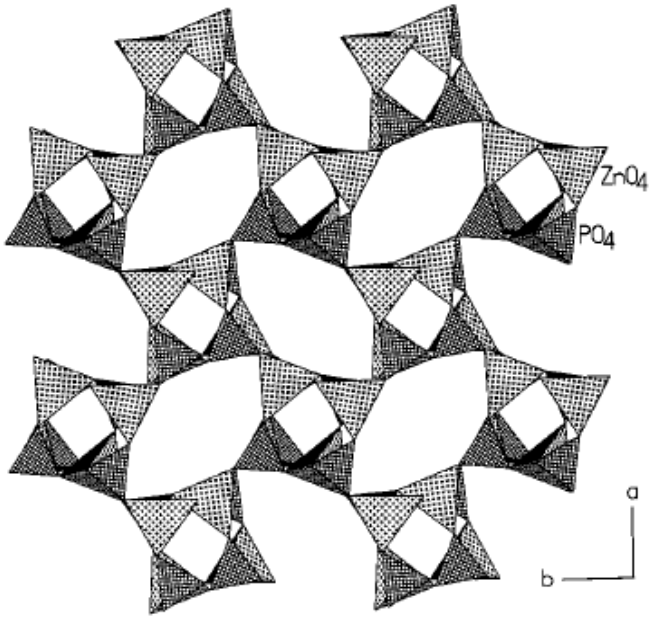

Figure 3.3. Polyhedral view of $[N_2C_3H_{12}]_2[Zn_4(PO_4)_4]$, along [0,0,1] axis. Note that the connectivity creates eight-membered channels. The amine molecule occupies these channels (not shown).

(Source: Neeraj and Natarajan 2000)

Porosity and solid composition are two critical factors which determine chemical properties (Suib 1996). Open framework phosphates containing transition metals are of particular interest because they show high chemical activity which results from the ability of metals to possess more than one oxidation state have high thermal stability (Morozov et al. 2003). In addition to this, the phosphates have some advantages over aluminosilicate materials for use in electromagnetic, photo electronics, and catalysis because transition metal atoms can exist in various oxidation states (Tian et al. 1992).

Microporous materials hosting transition metal elements offer special chemical properties as mentioned above which are inaccessible to zeolites and other frameworks based on main group elements (Brock et al. 1998 and Iwamoto et al. 1986). During consideration of zeolites, porous oxides and transition metal phosphates the phenomena that influence their formation should be considered. Many open-framework and microporous M–O and M–P–O systems that have been synthesized hydrothermally are expected to be meta-stable rather than thermodynamically-stable because most thermodynamically stable phases are dense solids. Metastable phases have a higher free energy than other phases with similar compositions. Since the hydrothermal temperature range allows the reaction a limited amount of energy, the reaction is showed that in its progression towards the thermodynamic product and the result is the formation of metastable product. Open framework solids can be isolated as a result of their ability to produce metastable phases.

In addition to the promise of properties arising from the partially filled d-orbitals, the transition metals also exhibit a great deal of flexibility in coordination and a tendency to form metal–oxygen–metal linkages. These properties of transition metals usually make the formation of zeolite-type architectures in these compounds difficult, but there is the promise of forming novel framework solids from combinations of various metal–oxygen polyhedra (Neeraj 2002).

Hydrothermal methods can be used to provide a rich source of new materials containing both traditional inorganic framework and metal organic framework systems (Cheetham et al. 1999). Unfortunately it is not possible to predict with confidence which compound is going to form during the hydrothermal process despite there being present some degree of designability particularly in metal organic frameworks (Ferey 2000). The main reason of non-predictibility of formed product is the wide range of synthetic variables including reaction time, temperature, pressure, reactant source,

stoichiometry, concentration of reactants, pH, and water which itself can also be a useful synthetic variable in the hydrothermal chemistry of zeolites (Camblor 1999).

In studies where the incorporation of hydrogen bonded molecules via the hydrothermal method has been done successfully it was recently demonstrated that it is a very general method for the preparation of a large variety of novel phosphates, phosphonates, and oxides with a large variety of transition metal ions (Haushalter et al. 1992, Zhang et al. 1996, Zapf et al. 1996, deBord et al. 1996 and Khan et al. 1994). By optimizing the variables of a hydrothermal reaction such as temperature, stoichiometry, and reaction time, the production of transition metal phosphates has been achieved successfully (Yu et al. 2005).

Another strategy is to synthesize solids with voids, templates which generally organize an assembly of atoms in order to achieve a particular linking between the atoms are used (Rajic et al. 2004). Templates may be either organic or inorganic which causes the structure of solid to adopt the geometric and electronic configurations that are unique to the templating molecule, the structure directors organize the growing framework and result in the production of phases and space fillers which function only to lower the thermodynamic stability of the product. Traditionally, structure directing agents are added to the hydrothermal reaction medium to provide a degree of control over the structure formed (Chen et al. 1999).

The literature includes examples of extensive work on open-framework titanium, cobalt, iron, vanadium and zinc phosphates. In contrast not many open-framework manganese phosphates systems have been reported (Song et al. 2003). So in this work we have sought to extend the range and the composition of materials built from manganese and also vanadium in which the structure and arrangement of inorganic oxide components show a porous architecture.

3.1. Mn-O and Mn-P-O Systems

Mn/O and Mn/P/O phases are excellent examples of the variability encountered in solid-satate inorganic syntheses. Zeolite-like materials containing transition metals are of both academic and practical interest (Tong et al. 2002). Mixed metal phosphates with alkali-earth cations and transition metals especially iron (Morozov et al. 2003), vanadium (Cherneya et al. 2004), cobalt (Chiang et al. 2001), and copper (Belik et al.

2001) have been studied extensively and have shown to possess a rich structural chemistry.

The basic building units of the manganese oxides are in the form of the monomeric or polymeric corner, edge and/or vertex-sharing manganese polyhedras MnO_5 or MnO_6 which are shown in Fig. 3.4.

Figure 3.4. Ball and stick representation of MnO_5 (a) triangular bipyramid and MnO_6 (b) octahedra.

The structures of manganese oxides whose main building blocks are mostly MnO_6 octahedras having bond angles of about 90º and 180º are very limited when compared with zeolite-like materials in which the building parameters are tetrahedras with bond angles of 110º. The rigid connectivity between octahedras causes manganese oxides to have layered or one dimensional tunneled structure (Tong et al. 2002).

Of all the elements in periodic table, manganese has the greatest number of oxidation states (Tong et al. 2002). However manganese has only the +2 oxidation state in many reported porous structures, as in the manganese phosphates $SrMn_2(PO_4)_2$ (El-Bali 2000), $NaMn_4(PO_4)_3$, $KMn_4(PO_4)_3$ and $Ba(MnPO_4)_2.H_2O$ (Daidouh et al. 1999 and Escobal 1999). The reasons for the +2 oxidation state of manganese in many materials are the easy reduction of materials of Mn^{+3} and Mn^{+4} to that of Mn^{+2} at high temperatures and the low solubility of compounds including Mn^{+3} and Mn^{+4} in solution which causes difficulties in the hydrothermal synthesis of open structural materials with high crystallinity (Tong et al. 2002). Availability of the various oxidation states of manganese may lead to synthesize new materials for science and technology.

There are many natural manganese oxide materials having tunneled structures which are known as cryptomelane (potassium cation in the tunnel, KMn_8O_{16}), as hollandite (barium cation in the tunnel, $BaMn_8O_{16}$), as manjiroite (sodium cation in the

tunnel $NaMn_8O_{16}$) and as coronadite ($PbMn_8O_{16}$) in which manganese is in the Mn^{+3} or Mn^{+4} states necessary for catalytic applications such as in the catalytic oxidation of carbon monoxide and reduction of nitric oxide with ammonia (Krishnan and Suib 1999, Zhou et al. 1998). Manganese phosphates are also found in nature as minerals like Bermanite $\{[Mn(PO_4)(OH)]_2\}$, Triplite $[Mn_2(PO_4)(OH)]$, Hurealute $\{Mn_5(PO_4)_2[PO_3(OH)]_2.4H_2O\}$, and Triphylite $[Li(Fe, Mn)PO_4]$ (Kohn et al. 2002).

In many studies, in order to synthesize solids with void; a templating, a structure directing or a space filling agent has been used. The agents are usually organic compounds and sometimes inorganic. $[NH_4][Mn_4(PO_4)_3]$ (Neeraj et al.2002), $Mn_3(PO_4)_4.2(H_3NCH_2CH_2)_3N.6(H_2O)$ (Thoma et al. 2004), $[CH_3NH_2CH_3][Mn_2(OH_2)(HPO_4).(C_2O_4)_{1.5}]$ (Yu et al. 2005), $Mn_2(H_2PO_4)_2(C_2O_4)$ (Zoe et al. 2004), $(C_2N_2H_{10})Mn_2(PO_4)_2.2H_2O$ (Song et al.2003), $Mn_6(H_2O)_2(HPO_4)_4(PO_4)_2.C_4N_2H_{12}.H_2O$ (Kongshaug et al. 2001), $(C_2H_{10}N_2)[Mn_2(HPO_4)_3(H_2O)]$ (Escobal et al. 2000), are examples of compounds synthesized by using variable organic components such as ammonia, ethylenediammine, oxalate and piperazine. Organically templated manganese phosphates (Mn/P/O) and (Mn/O) are of particular interest because of their rich structural chemistry and they can exhibit 1-D chain structures, 2-D sheet structures, and 3-D structures. Examples are the structures of $[NH_4][Mn_4(PO_4)_3]$ and $[CH_3NH_2CH_3][Mn_2(OH_2)(HPO_4).(C_2O_4)_{1.5}]$ as shown in Figures 3.5 and 3.6.

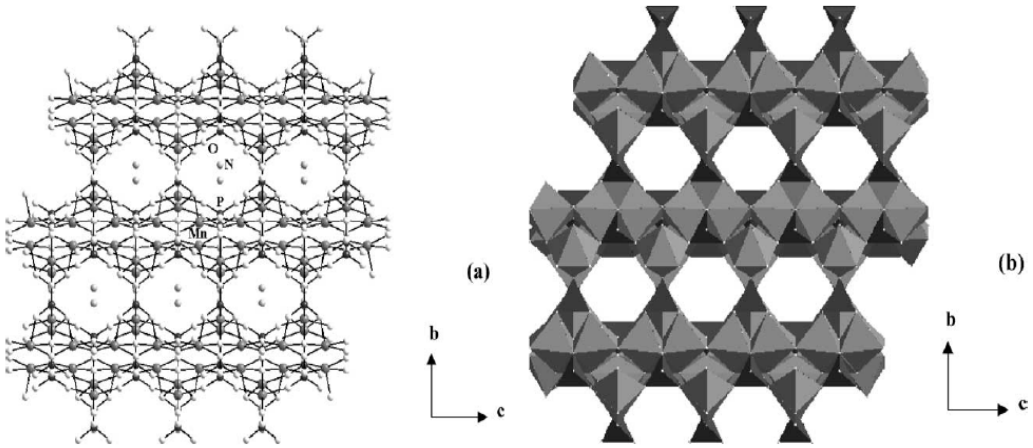

Figure 3.5. (a) Ball and stick view of $[NH_4][Mn_4(PO_4)_3]$, showing one-dimensional channels containing ammonium ions along the *a*-axis. (b) Polyhedral view of the channels. The Mn–O polyhedras are shaded light grey whereas the phosphate tetrahedras are dark grey in color

(Source: Neeraj et al. 2002).

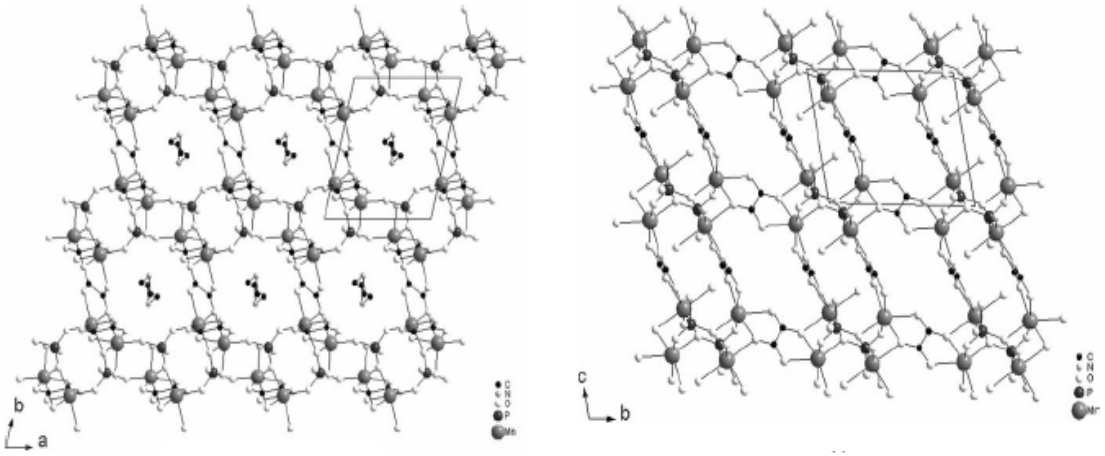

(a)

Figure 3.6. (a) Stick-and-ball representation $[CH_3NH_2CH_3][Mn_2(OH_2)(HPO_4)(C_2O_4)_{1.5}$ showing the framework structure formed by the one-dimensional chains made of the $[Mn_2O_{10}]$ dimers and the PO_4 tetrahedra along the a axis together with the C_2O_4 groups. 10-membered-ring channels running along the c axis with organic template lying inside the channels are seen. (b) Stick-and-ball representation of the same structure with the 10-membered-ring seen in the bc plane.

(Source: Yu et al. 2005)

Manganese oxides having open structures are strong oxidative catalyst and they can be used in total oxidation reactions of carbon monoxide (Xia et al. 1999) and benzene (Luo 2000). The basic features of manganese oxide open structures are edge sharing chains and/or planes (Post et al. 1982). Synthetically without using any template, many pure Mn phosphates; an orthophosphate $Mn_3(PO_4)_2$, a diphosphate $Mn_2P_2O_7$, two polyphos-phates $Mn(P_3O_9)$ and $Mn_2(P_4O_{12})$, the ultraphosphate MnP_4O_{11} (Massa et al. 2005) have been synthesized up to now.

Also in some studies especially in the case of inorganic oxides, alkali and alkali earth cations such as Na, K, Sr, Ba have been used as templating agents, serving as space fillers and charge balancing the anionic frameworks (Tong et al. 2002, Morozov et al. 2003, Escobal et al. 1999, El-Bali 2000).

3.2. V-O and V- P-O Systems

Vanadium compounds are widely studied due to their interesting chemical properties including redox, electrochemical, catalytic and magnetic properties. For example, among the oxides, the layered lithium vanadates are used as electrode material in lithium batteries (Whittingham et al. 1996), and some vanadates show catalytic activities in the oxidative dehydrogenation of hydrocarbons (Bahranowski et al. 1999, Baerns et al. 1996). The design or manipulation of oxide architecture remains a significant challenge in solid state chemistry (Hagrman et al. 2001).

Similar to vanadium oxides, vanadium phosphates offer catalytic and magnetic properties (Boudin et al. 2000). For example, $(VO_2)_2P_2O_7$ (Centi 1993) is used as a catalyst for selective O and N insertion reaction of aliphatic and methyl aromatics due to oxidation states of V. Numerous oxovanadium phosphate hydrates MVPO's with M as inorganic or organic cations have been synthesized during the last decade since the discovery of the efficient catalyst $(VO)_2(P_2O_7)$. A critical feature of $(VO)_2P_2O_7$ for selective oxidation of *n*-butane appears to be the presence of vanadyl dimers. The vanadium phosphates are important oxidation catalysts and the vanadyl hydrogen phosphate $VOHPO_4{\cdot}0.5H_2O$ is the precursor for catalysis. This compound has been used for the commercially important and scientifically fascinating 14 electron selective oxidation of butane to maleic anhydride (O'Mahony et al. 2003).

Hydrothermal reactions are very useful for preparing low-density open-framework solids in crystalline form (Khan 2003). The hydrothermal method is a convenient method for the preparation of mixed valence polyvanadates stabilized by oxygen donor ligands as well as a variety of zeolitic vanadium phosphates (Zhang et al. 1998). Oxovanadium solid state structures are often constructed from vanadate polyhedra in combination with other oxyanion tetrahedras, such as (PO_4) and (SO_4).

The vanadium phosphates; A-V-P-O, (A: Li, Na, K, Rb, Cs, Ag, Tl, Ca, Sr, Ba, Cd, Co, Cu, Hg, Mn, Ni, Pb, Zn) form a huge family of compounds with complicated structures (Boudin et al. 2000). Vanadium oxide chemistry is characterized by several general families of compounds: binary oxides, bronzes, and molecular polyanions and the chemistry of polyanions has been studied recently (Muller et al. 1995, Boudin et al. 2000, Hagrman et al. 2001).

The polyanions contain various kinds of metal atoms fused together with oxide ligands presented in some bridging modes (Khan 2000). A number of polyvanadates that contain 3 to 34 vanadium atoms has been synthesized and characterized (Pope and Muller 1991, Klemperer et al. 1992, Muller et al. 1998). Generally, vanadium adopts the basic structural unit of $\{VO_6\}$, $\{V_2O_{11}\}$, $\{V_2O_{10}\}$, $\{V_2O_9\}$, $\{V_4O_20\}$, $\{V_5O_{17}\}$ in the finite clusters and $\{VO_5^{\infty}\}$, $\{V_4O_{18}\}^{\infty}$, $\{VO_4\}^{\infty}$, $\{V_3O_{13}\}^{\infty}$,$\{V_2O_9\}^{\infty}$ linking modes in the infinite chains, and the phosphorus atom usually exhibits $\{PO_4\}$ tetrahedral coordination mode (Figure 3.7). Examples are $\{P_3O_{10}\}$, $\{P_4O_{13}\}$, $\{P_5O_{16}\}$, $\{P_8O_{24}\}$, $\{P_8O_{23}\}$, $\{P_{12}O_{36}\}$ (Duan et al. 2003).

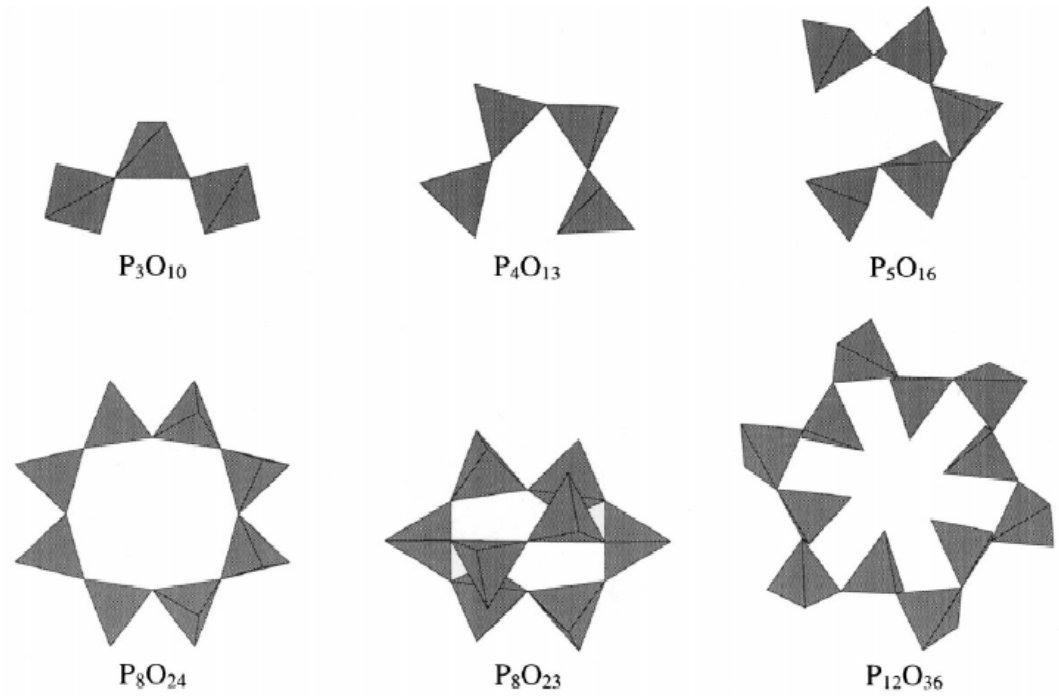

Fig.3.7. Different arrangements of the P–O tetrahedra different from mono and diphosphate found in the vanadium phosphates
(Source: Boudin et al. 2000).

Vanadium polyanions with the formula $V_xO_y^{n-}$ are composed of vanadium chains and layers and in these compounds vanadium atoms can adopt different oxidation states from III to V and different environments from octahedral to tetrahedral (Boudin et al. 2000). Complex vanadium oxides and phosphates where vanadium is in its low oxidation state often exhibit interesting magnetic properties and have become an

object of heightened attention of the investigators are the in the last few years (Chernaya et al. 2004). The vanadium phosphates have numerous arrangements with varied A/V/P ratios, different A cations, different environments for vanadium (octahedral, square pyramidal, trigonal bipyramidal, tetrahedral), and different oxidation states of vanadium (III, IV, V) as shown in Figure 3.8.

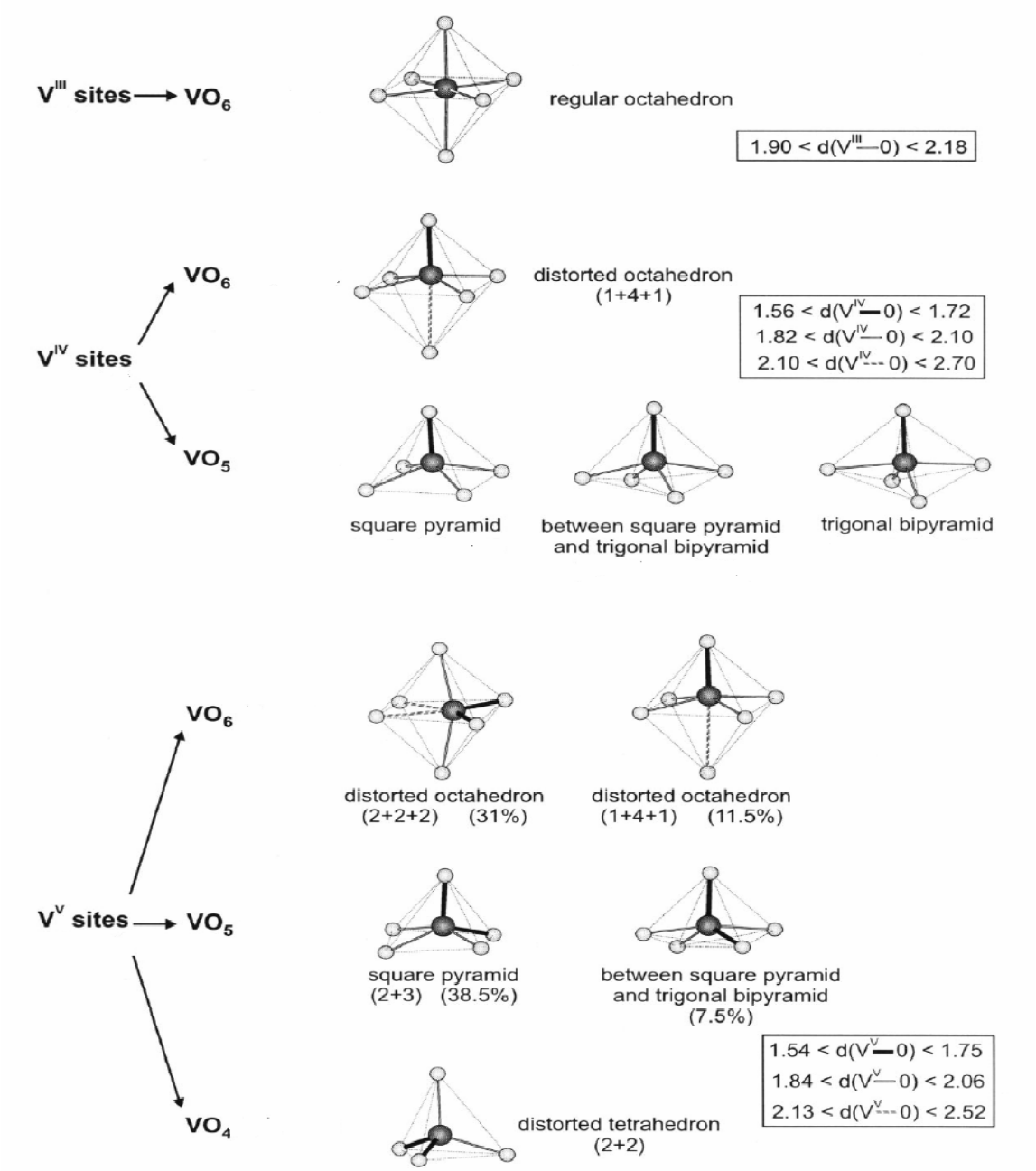

Figure 3.8. Different environments of vanadium encountered in the vanadium phosphates with metallic cations. The V–O distances are given in Å. (Source: Boudin et al. 2000).

The vanadium phosphates even the whole field of metal phosphates have been extensively studied and explored for more than two decades. The continuing interest in the design and synthesis of vanadium phosphate comes from not only their practical application such as catalysts, inorganic ion exchangers and their versatile intercalators but also their fundamental chemistry which is characterized by a concomitant diversity of electronic and magnetic properties and unusual structural complexity. But the phosphate structures consisting of larger odd number rings are still rarely reported, because the strict alternation of M polyhedra and P tetrahedra in MPO's define an even-number ring of T atoms such as 8, 10, 12, 14, 18, and 20, which prevents the occurrence, for example, of five-ring units commonly encountered in aluminosilicate zeolites (Cui et al. 2005). Cui and co-workers have synthesized new vanadium phosphate, $(C_6H_{16}N_2)_3(VO)(V_2O_4)_2(PO_4)_4{\cdot}2H_2O$ which has an odd number of rings it has 3-, 6-, and 7-membered rings (Fig.3.9). In V–P–O frameworks, vanadium is connected in different ways through phosphate groups as 126 different vanadium phosphates which were synthesized up to year of 2000 (Figure 3.10).

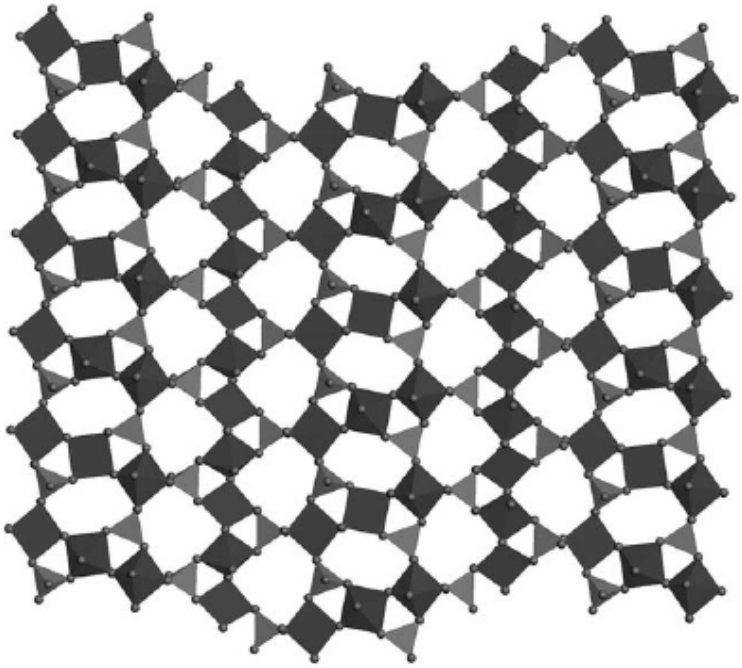

Figure 3.9. The inorganic sheet with 3-, 6-, and 7-membered rings built up by the alternate linkages of two kinds of 1-D chains in $(C_6H_{16}N_2)_3(VO)(V_2O_4)_2(PO_4)_4.2H_2O$

(Source: Cui et al. 2005).

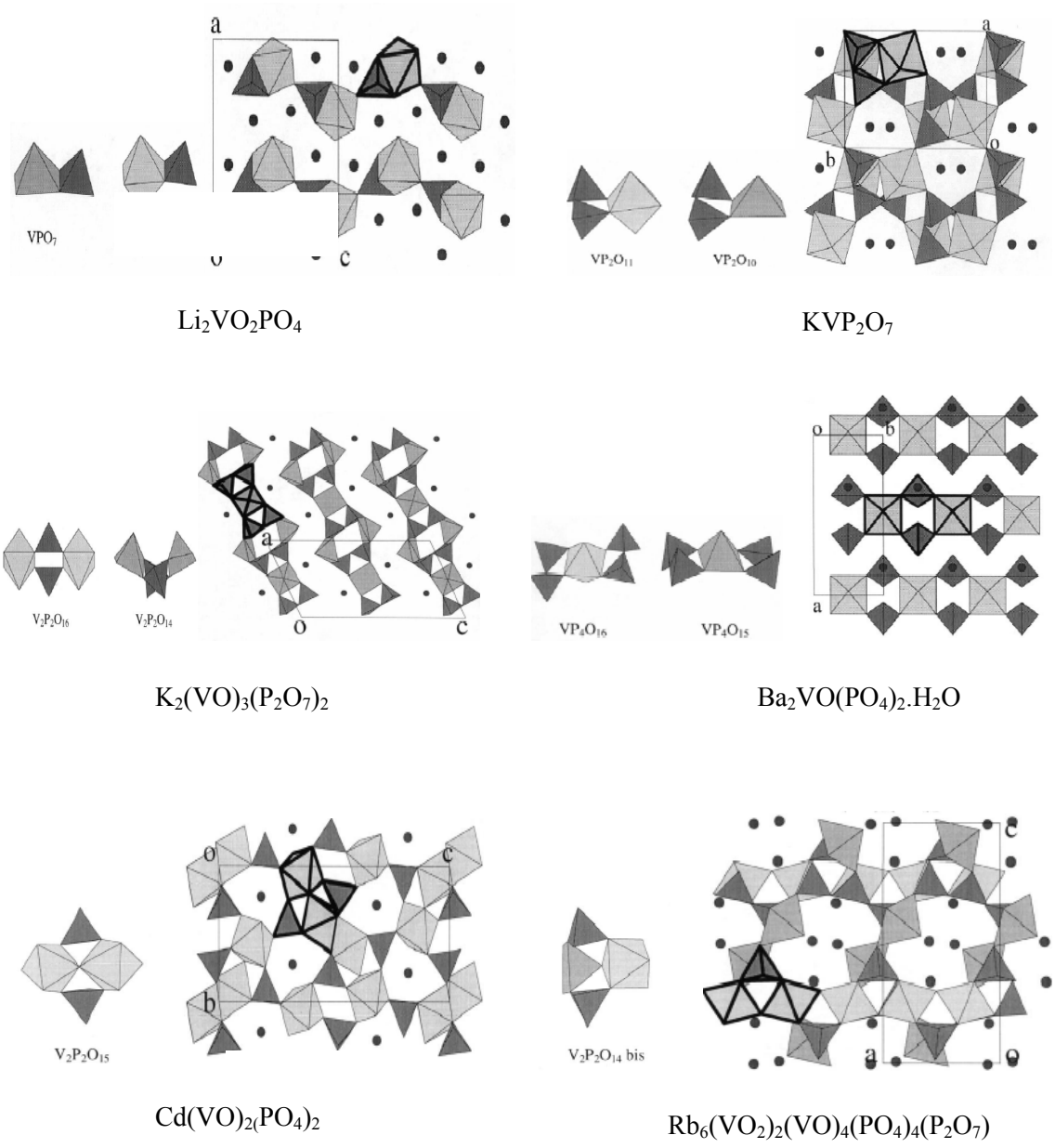

Figure 3.10. Some of the most common mixed units composed of one VO polyhedra and examples of AVPO structures where they appear. The VO_6 and VO_5 polyhedras are represented in light and middle gray and the PO_4 tetrahedra in dark grey. The A cations are in dark gray circles from two VO polyhedra and examples of AVPO structures where they appear. (c) Most common mixed chains and examples of AVPO structures where they appear.

(Source: Boudin et al. 2000)

CHAPTER 4

CRYSTALLOGRAPHY

Crystal structure solution is done via commercial software programs. In order to get the detailed structural information of our synthesized materials, SHELX (Sheldrick 1997) and CRYSTAL STRUCTURE (Molecular Structure Corparation / Germany 2004) were chosen.

After getting the data obtained from single X-ray diffractometer, data is transferred to these crystal solution programs. The transferred data include the intensity of diffraction values of X-rays from the each atom in different *hkl* planes of crystals, unit cell parameters of crystals are obtained from these atoms. The simple definition of miller indices, hkl, is the reciprocals of the fractional intercepts which the plane makes with the crystallographic axes (Cullity 1978). The most important part in the solution of crystals shapes is hkl data of synthesized crystals. Then by the help of the probability functions with the regression analysis, the position of the atoms in the unit cell is obtained. Due to the various results of positions in the unit cell deciding the most appropriate one is made by the help of the 'R' values of design results. The R value represents the error of the model that occurred in the end of the regression. To obtain a good solution the R value should be as near as zero. In summary both of these programs use the electron densities that belong to the atoms.

SHELX software runs in a DOS system which requires using command to solve the structure. Every analysis step requires opening a new screen (Figure 4.1). Input files are given in a system to solve the structure, at the end there will be out put files, include result of solution, created by SHELX programs (Figure 4.2)

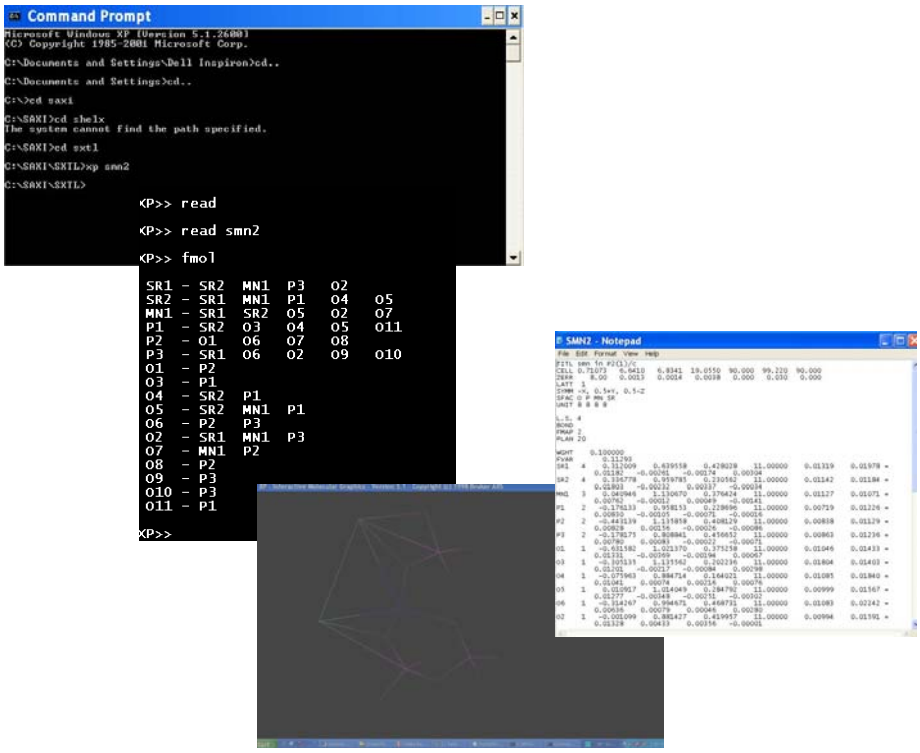

Figure 4.1. Screens of SHELX.

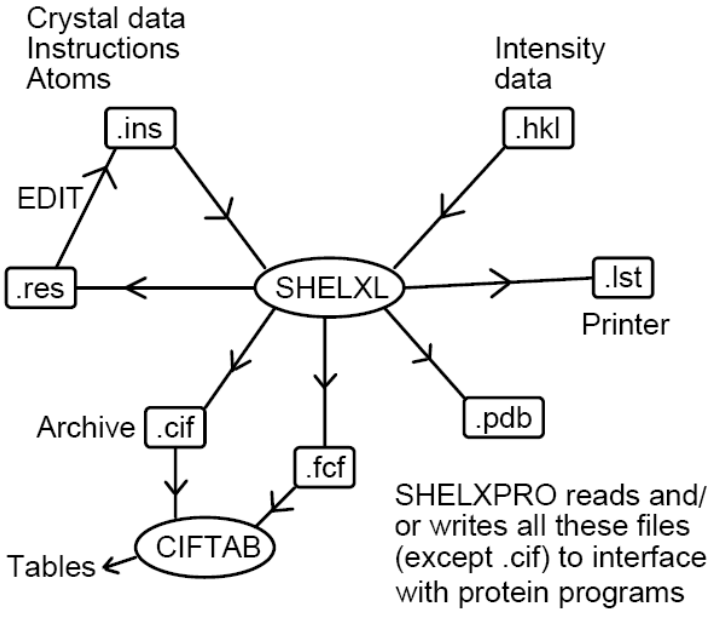

Figure 4.2. Schematic diagram of SHELX program.

The SHELX is the mostly used crystal solution program and many program developers take the main idea used in SHELX programming language. The crystal structure program is one of the examples of them. The crystal structure program includes several solution methods including SHELX-97 includes mainly 6 areas that include all the information in the same screen. These are the *graphic area*, *toolbar*, *menu bar*, *flow chart*, *status line*, and *message area* in the same screen. The *graphic area*, in which the molecular structure is developed and displayed, has the biggest area in the program window. *Toolbar*, above the *graphic area*, is used during model building and display, includes many commands such as zoom function, representing the unit cell position, bond distances and angles between the atoms, and coloring function, etc. At the very top is a *menubar*, providing access to a number of dialogs and utilities that may be used in analysis. On the left side is the *flow chart*, guides through the process of a crystal structure analysis. At the bottom of the screen is the *message area* where crystal structure sends information about processes that are executing. The *status* line at the very bottom is where help messages are displayed in for menu items. Fig. 4.3 shows the screen of this program.

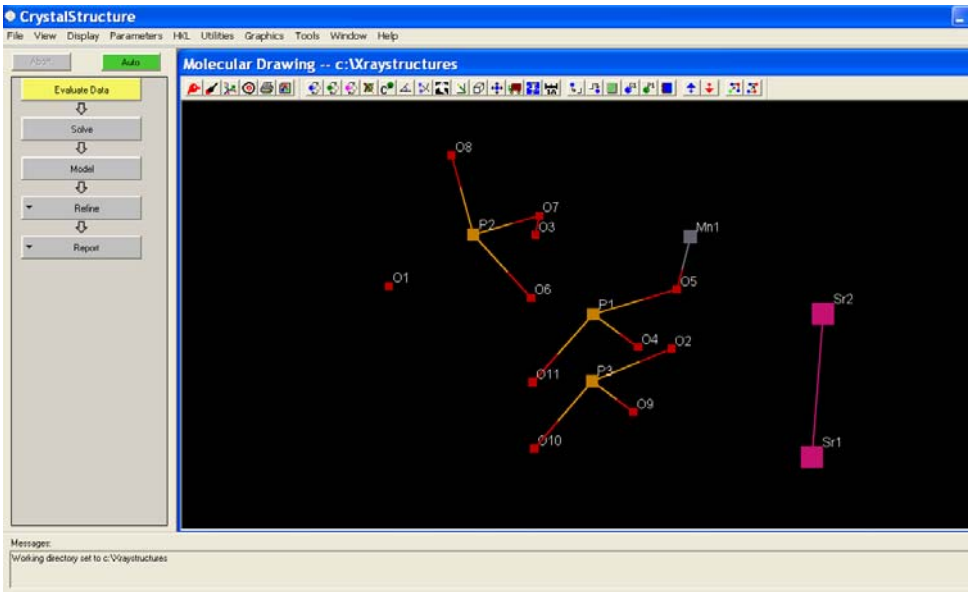

Figure 4.3. Schematic representation of the main areas of Crystal Structure information program.

First the f2.dot file (a type of .hkl file) is loaded to program to start structure solution. Then the program starts to evaluate these data by using different solution methods. SHELX is one of these solution methods. At the end of the probability calculations, the resulting parameters such as R values etc. are given in a report with a shape of the positions of the atoms in the unit cell (Figure 4.4).

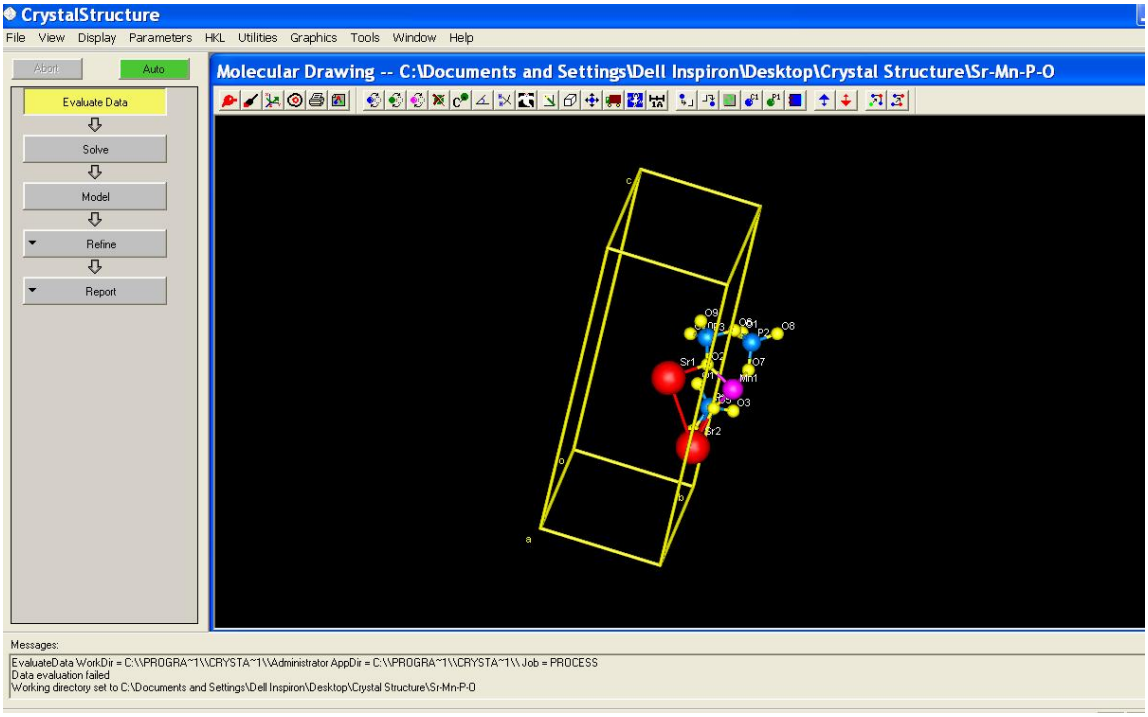

Figure 4.4. The atoms positions of a compound in its unit cell.

After logging on the program, the project is chosen with the proper file format. The loaded data file is generally in .hkl format. However the required file extensions should be *.dat* or *.cif*. Therefore the .hkl file should be converted into those file formats. The first task to be performed with any new data set is *Evaluated Data*. In this step, by the help of the accessing a dialog box, the parameters are modified and demands will be selected.

Crystal structure contains or support a multiple structure solution techniques. Solving the structure of crystal, the *solve* menu is chosen and then a multiple pop up menus will be occurred in order to choose the desired one (Figure 4.5). This is totally depended on the user. In this study generally SHELX97 was chosen. Also for each program, a default mode is available. Crystal structure creates simplest input file that is

required to execute the program. The *menu* option allows accessing a set of dialogs that can be used to make changes the instruction file.

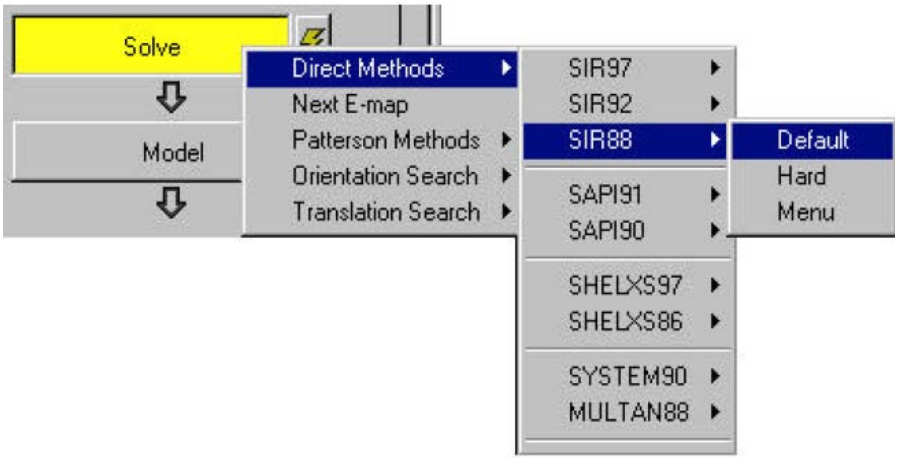

Figure 4.5. *Solve* command in the crystal structure program.

The peaks will be read in and displayed when the direct method program has finished running. These peaks are named with the numbers that indicate the relative peak heights and "1" shows the largest peak (Figure 4.6).

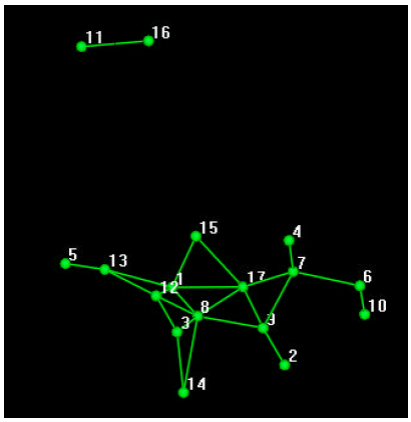

Figure 4.6. Scheme of a crystal with the relative peak heights.

Determining the actual peak height can be done either right-clicking on the peak and selecting *peak height* from the popup menu, or choosing the *utilities? List peak*. The peak menu not only displays the peak heights and coordinates; it also allows changing the covalent radius assigned to all peaks, which controls the computation of bonds. (Figure 4.7)

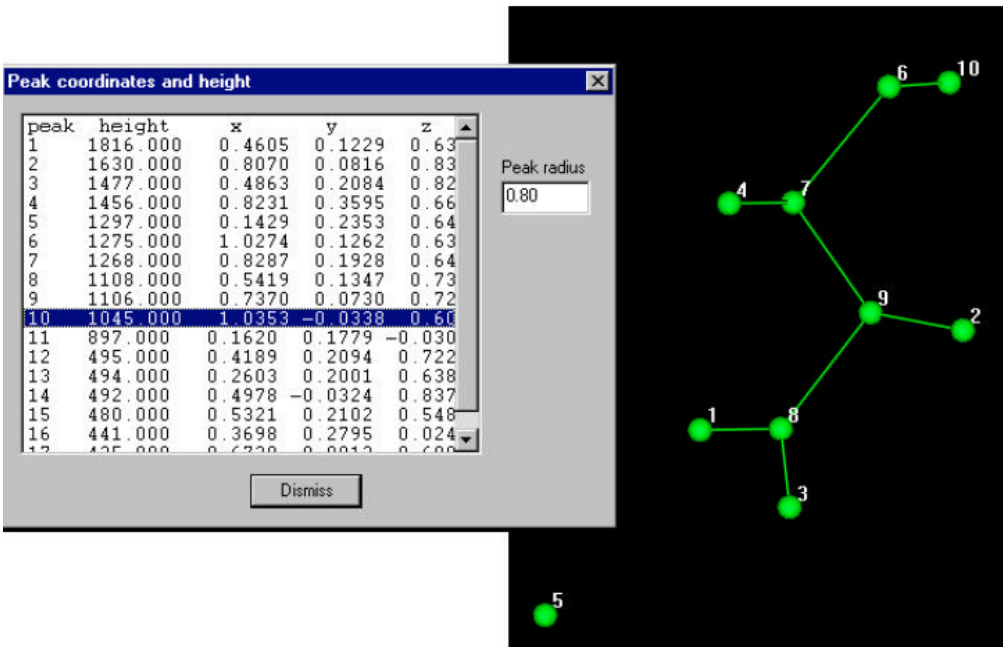

Figure 4.7. Scheme of peak heights and peak coordinates.

The next step is to assign the element types to the E-map peaks. By the help of the *naming* icon, the Name item dialog will be accessed. Then the element is selected from the list, which is created from the current formula. If the needed one is not in the list, from the "Parameters" icon "Formula" will be chosen to update the formula. The cursor will change to indicate the selected element. By clicking the peaks, the assignment of element type is done (Figure 4.8).

Even though there may still be missing atoms from the model, least squares refinement can be applied before completing all the missing atoms. The Refine command in the Flow Chart will be used to start refinement. The statistical report can be viewed at the end of the operation. Fourier calculations are done at the end of the refinement. The results are shown in Graphics area (Figure 4.9). The refinement result also is used to explain the peak heights. Based on the peak heights (intensities) atoms are named depending on crystal content.

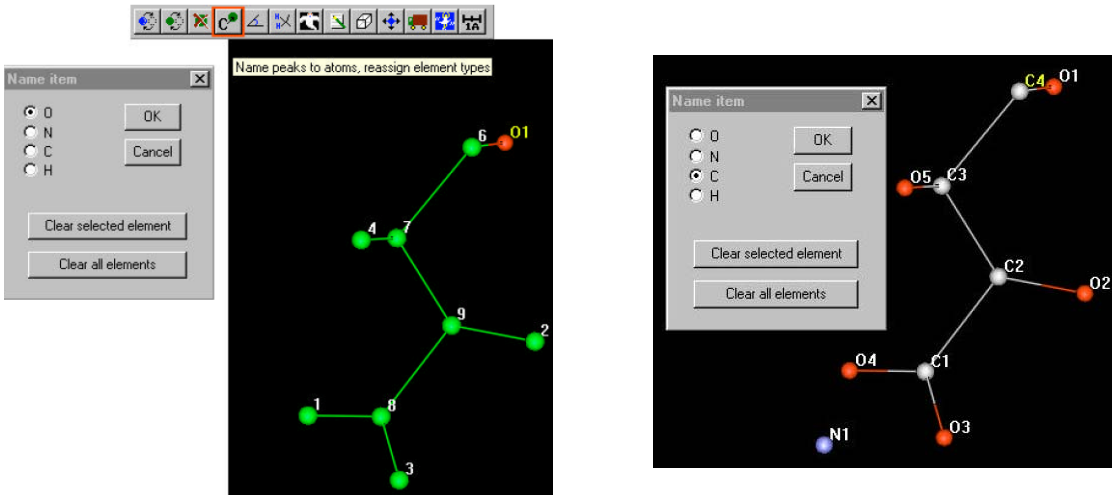

Figure 4.8. Scheme of Name Item dialog.

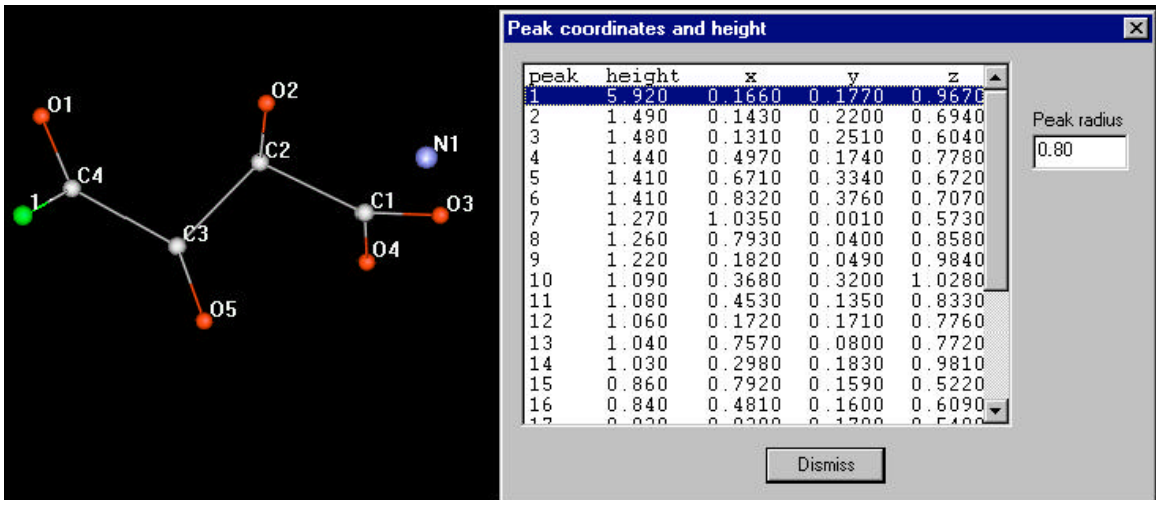

Figure 4.9. The report of the Fourier calculations.

If the crystal has hydrogen atoms, by taking the radius as “0.4”, the peak radius will be decreased and the hydrogen atoms can be located in the scheme (Figure 4.10). After that the bond angles and bond lengths will be displayed by the help of the geometrical tool. In addition hydrogen atoms can be found automatically by the program.

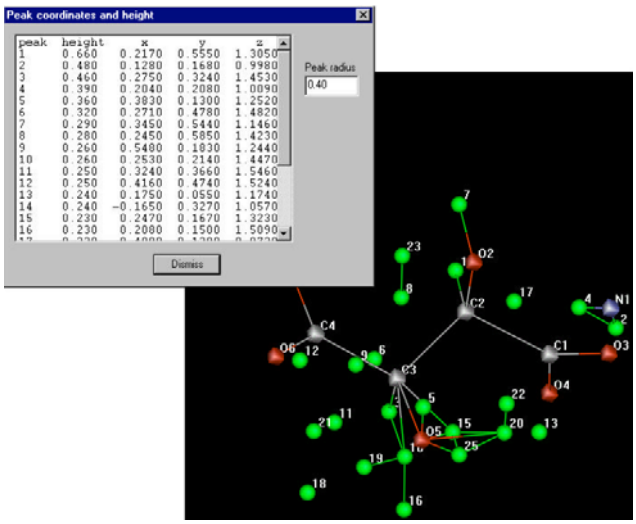

Figure 4.10. Replacement of Hydrogen atoms.

When the all refinement process is finished, the report will be prepared by the flow chart in order to get the *.cif* file format and the properties of crystals. The final report is depended on the users. At the end of the structure solution, the crystal will be seen in 3D mode and packing diagram can be drawn (Figure 4.11).

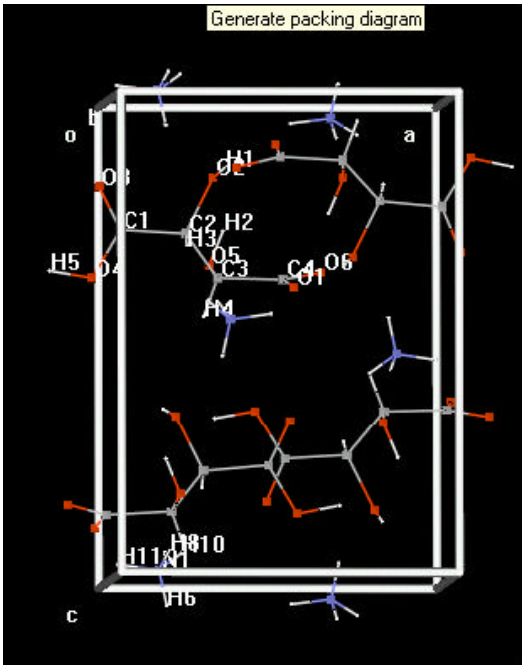

Figure 4.11. The packing diagram of a crystal.

4.1. Hydrothermal Synthesis and Structural Characterization of Strontium Manganese Phosphate ($Sr_2MnP_3O_{11}$)

4.1.1. Experimental

In this study the new manganese phosphate compound, $Sr_2MnP_3O_{11}$, in a powder form was synthesized in our laboratory by hydrothermal reaction of Mn_2O_3, $SrCO_3$, H_3PO_4, and H_2O at 230ºC for 5 days in Solid State Laboratory of İzmir Institute of Technology. It is the second compound in literature including Sr, Mn, and phosphates (El-Bali 2000). So the title material was tried to be synthesized in crystal form. The production of crystals by the hydrothermal synthesis method requires design of experiments. There are lots of factors affecting the reaction results. These experimental factors were stoichiometric ratio of the reactants, amount of solvent, the temperature of reaction from 150ºC to 230ºC, and the source of the reactants etc. Even the use of various types of oven affects the experimental results. The level of each factors impact on quality, quantity and types of products in an experiment. After hundreds of trials in different levels, various types of materials were obtained. During these trials many known manganese phosphate and oxides crystals were synthesized such as $MnHPO_4$, $MnPO_4.H_2O$, $MnSb_2O_4$, $MnHPO_4.(H_2O)_3$.

A good quality and the size crystals of this compound, ($Sr_2MnP_3O_{11}$), was done in Clemson University Chemistry Laboratory via the reaction of 59mg $SrCO_3$, 63mg Mn_2O_3, 0.2mL H_3PO_4 (85%), and 0.5mL H_2O (4-1). Stoichiometric amount of the reactants were loaded into a fused-silica tube under an Ar atmosphere in a glove box. It was then loaded into a high-pressure autoclave. The autoclave was heated at 375ºC for 3 days and then cooled to room temperature in a furnace. The product was obtained as maroon crystals. The powder diffraction pattern of the title compound is shown in Figure 4.12.

$$SrCO_3 + Mn_2O_3 + H_3PO_4 \xrightarrow[H_2O]{(\ 375ºC\ /\ 3\ days)} Sr_2MnP_3O_{11} \qquad (4\text{-}1)$$

4.1.2. Single X-ray Crystallographic Analysis

A crystal of $Sr_2MnP_3O_{11}$ was mounted on a glass fiber with epoxy glue and centered on a Rigaku AFC8 diffractometer equipped with a Mercury CCD area detector. Crystal data, details of the data collection and refinement are given in Table 4.1. The unit cell parameters and the orientation matrix were based on the centroids of 1709 reflections with F_0>4sig (F_0). Reflection indexing, Lorentz-polarization correction, peak integration, and background determination were performed using the *Crystal Clear* software (Crystal Clear 2001).

An empirical absorption correction was applied using the REQAB (Reqab 1998) routine in the *Crystal Clear* software package. The structure was solved by direct methods with the program SHELXS (Sheldrick 2000) and by refined full-matrix least-squares techniques using the program SHELXL (Sheldrick 1997) in the Crystal Structure software (Crystal Structure 2004).

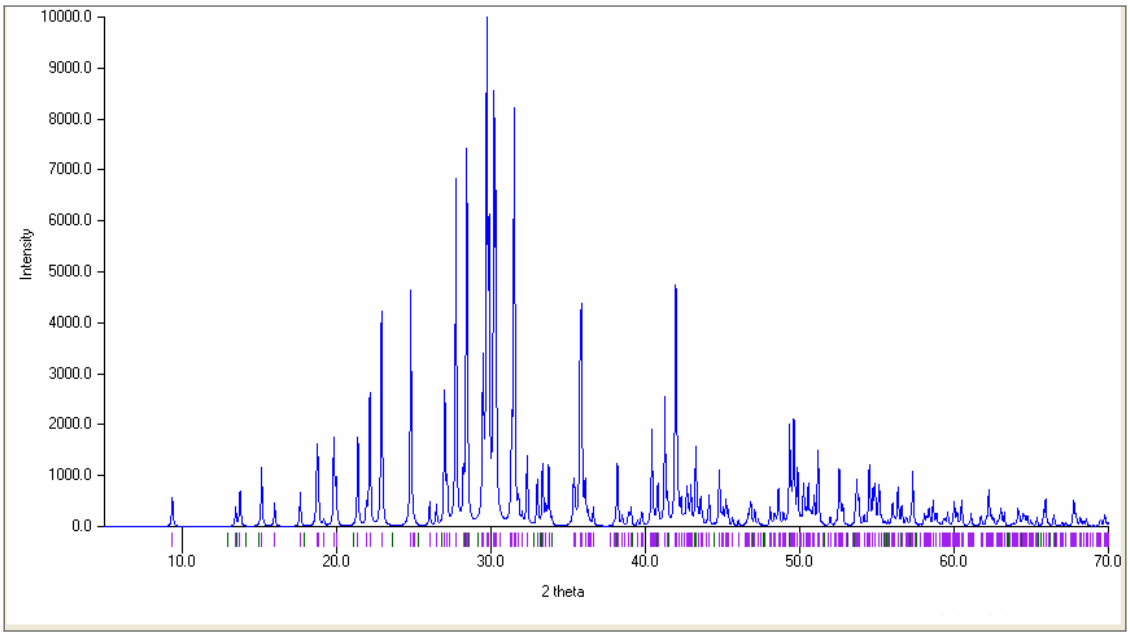

Figure 4.12. The powder X-ray diffraction pattern of $Sr_2MnP_3O_{11}$

Atomic coordinates and equivalent isotropic displacement coefficients, and anisotropic displacement coefficients were given in Tables 4.2 and 4.3, respectively. The selected bond angles were given in Table 4.4. And the selected bond distances and bond valence were given in Table 4.5.

Table 4.1. Crystal Data and Structure Refinements for $Sr_2MnP_3O_{11}$

Compound	$Sr_2MnP_3O_{11}$
F_W	498.98
Cristal System	Monoclinic
Space Grup	$P2_1/c$
Z	3
a, Å	6.6410(13)
b, Å	6.8341(14)
c, Å	19.055(14)
α = γ degree	90
β= degree	99.22(3)
V, $(Å)^3$	853.6(3)
T, (K)	293(2)
ρ_c, (gcm^{-3})	2.949
2θ range, degree	3.49 – 26.71
R	0.0494
R_w	0.0367

Table 4.2. Atomic Coordinates and Equivalent Isotropic Thermal Parameters of $Sr_2MnP_3O_{11}$.

Atom	**X**	**Y**	**Z**	**U_{eq}**
Sr1	0.31201 (12)	0.63956 (11)	0.42803 (4)	0.0153 (3)
Sr2	0.33678 (11)	0.95979 (11)	0.23056 (4)	0.0137 (3)
Mn1	0.04095 (18)	1.13067 (17)	0.37642 (6)	0.0100 (3)
P1	- 0.1761 (3)	0.9582 (3)	0.22870 (9)	0.0095 (4)
P2	- 0.4431 (3)	1.1359 (3)	0.40813 (10)	0.0095 (4)
P3	- 0.1782 (3)	0.8088 (3)	0.45665 (10)	0.0098 (4)
O1	- 0.6316 (8)	1.0214 (8)	0.3753 (3)	0.0131(11)
O3	- 0.3051 (9)	1.1356 (8)	0.2022 (3)	0.0151(12)
O4	- 0.0760 (9)	0.8847 (8)	0.1640 (3)	0.0132(11)
O5	0.0109 (9)	1.0141 (8)	0.2848 (3)	0.0133(11)
O6	- 0.3143 (8)	0.9947 (9)	0.4687 (3)	0.0133(11)
O2	- 0.0011 (8)	0.8814 (8)	0.4200 (3)	0.0128(11)
O7	- 0.2962 (9)	1.1787 (8)	0.3566 (3)	0.0134(11)
O8	-0.4918 (8)	1.3139 (8)	0.4490 (3)	0.0137(11)
O9	-0.0869 (8)	0.7401 (9)	0.5323 (3)	0.0128(11)
O10	-0.3071 (9)	0.6583 (9)	0.4142 (3)	0.0176(12)
O11	-0.3107 (9)	0.8064 (8)	0.2547 (3)	0.0152(12)

Table 4.3. Anisotropic Displacement Coefficients ($Å^2$) of of $Sr_2MnP_3O_{11}$.

Atom	U11	U22	U33	U23	U13
Sr1	0.0132 (4)	0.0198 (4)	0.0118 (4)	-0.0026 (3)	-0.0017(3)
Sr2	0.0114 (4)	0.0118 (4)	0.0180 (4)	-0.0023 (3)	0.0034(3)
Mn1	0.0113 (6)	0.0107 (6)	0.0076 (5)	-0.0001 (4)	0.0005 (4)
P1	0.0072 (9)	0.0123 (10)	0.0083 (9)	-0.0011 (7)	-0.0007 (7)
P2	0.0084 (9)	0.0113 (9)	0.0083 (8)	0.0016 (7)	-0.0003 (7)
P3	0.0086 (9)	0.0124 (10)	0.0078 (8)	0.0008 (7)	-0.0002 (7)
O1	0.010(3)	0.014(3)	0.013(3)	-0.004 (2)	-0.002 (2)
O3	0.018(3)	0.014(3)	0.012(3)	-0.002 (2)	-0.001 (2)
O4	0.011(3)	0.018(3)	0.010(3)	0.001 (2)	0.002 (2)
O5	0.010(3)	0.016(3)	0.013(3)	-0.004 (2)	-0.003 (2)
O6	0.011(3)	0.022(3)	0.006(2)	0.001 (2)	0.000 (2)
O2	0.010(3)	0.016(3)	0.013(3)	0.004 (2)	0.004 (2)
O7	0.016(3)	0.012(3)	0.013(3)	0.004 (2)	0.004 (2)
O8	0.011(3)	0.012(3)	0.018(3)	0.000 (2)	0.001 (2)
O9	0.015(3)	0.018(3)	0.005(2)	0.002 (2)	-0.001 (2)
O10	0.015(3)	0.020(3)	0.017(3)	-0.002 (2)	-0.001 (2)
O11	0.016(3)	0.010(3)	0.020(3)	-0.003(2)	0.005(2)

Table 4.4. Selected Bond Angles (degrees) in $Sr_2MnP_3O_{11}$

O5-Mn1-O7	87.2 (2)	O11-P1-O3	109.0 (4)
O5-Mn1-O2	91.4 (2)	O3-P1-O4	106.3 (4)
O2-Mn1-O7	89.5 (2)	O5-P1-O4	103.1 (4)
O7-P2-O1	113.8 (3)	O11-P1-O5	113.3 (3)
O8-P2-O6	104.0 (3)	O10-P3-O6	109.7 (3)
O7-P2-O6	104.6 (3)	O10-P3-O2	112.9 (3)
O8-P2-O1	113.4 (3)	O2-P3-O9	107.9 (3)
P2-O6-P3	113.4 (3)	O9-P3-O6	104.7 (3)

Table 4.5. Bond Length (Å) in $Sr_2MnP_3O_{11}$

Environment of Sr(1)			*Environment of Sr(2)*		
Sr1-O8	2.474(6)	*0.382(6)*	Sr2-O11	2.395(6)	*0.473(8)*
Sr1-O3	2.475(6)	*0.381(6)*	Sr2-O7	2.526(5)	*0.332(5)*
Sr1-O8	2.578(6)	*0.289(5)*	Sr2-O11	2.539(6)	*0.321(5)*
Sr1-O10	2.588(6)	*0.281(5)*	Sr2-O5	2.570(6)	*0.294(5)*
Sr1-O2	2.642(6)	*0.243(4)*	Sr2-O3	2.584(6)	*0.284(5)*
Sr1-O4	2.772(6)	*0.171(3)*	Sr2-O1	2.764(5)	*0.174(2)*
Sr1-O1	2.843(6)	*0.141(2)*	Sr2-O3	2.793(6)	*0.161(3)*
Sr1-O9	3.147(6)	*0.062(1)*	Sr2-O4	2.876(6)	*0.128(3)*
Sr1-O6	3.180(6)	*0.057(1)*	Sr2-O10	3.052(6)	*0.080(1)*
<Sr (1) – O>	2.745(6)		<Sr (2) – O>	2.038	
∑ij sij =		2.007(33)	∑ij sij =		*2.142(37)*

Environment of Mn (1)					
Mn1-05	1.900(6)	0.685(10)	Mn1-O2	1.934(6)	0.625 (10)
Mn1-04	1.929(6)	0.633(10)	Mn1-O9	1.931(5)	0.630 (8)
Mn1-O7	2.234(6)	*0.278(5)*	Mn1-O1	2.303(6)	*0.231 (5)*
<Mn(1) – O>	2.039				
∑ij sij =		*3.082(48)*			

Environment of P(1)			Environment of P(2)		
P1-O11	1.504(6)	*1.357 (21)*	P2-O8	1.507(6)	*1.346 (21)*
P1-O3	1.523(6)	*1.289 (20)*	P2-O7	1.519(6)	*1.303 (20)*
P1-O5	1.551(6)	*1.195 (19)*	P2-O1	1.523(6)	*1.290 (20)*
P1-O4	1.573(6)	*1.126 (18)*	P2-O6	1.637(6)	*0.947 (15)*
<P(1) – O>	1.538(6)		<P(2) – O>	1.547(6)	
∑ij sij =		*4.967 (78)*	∑ij sij =		*4.886(76)*

Environment of P(3)					
P3-O10	1.491(6)	*1.406 (22)*	P3-O9	1.544(5)	*1.218 (16)*
P3-O2	1.543(6)	*1.221 (19)*	P3-O6	1.597(6)	*1.056 (9)*
<P(3) – O>	1.544(6)				
∑ij sij =		*4.901(66)*			

4.1.3. Results and Discussion

The compound having a formula $Sr_2MnP_3O_{11}$ was prepared from the reaction of $SrCO_3$, Mn_2O_3, H_3PO_4, and H_2O as maroon crystals. The single crystal X-ray diffraction study of the title compound, $Sr_2MnP_3O_{11}$, showed that it possesses a three-dimensional structure composed of MnO_6, P_2O_7, PO_4 groups and strontium cations residing in the channels. The asymmetric unit shown in Figure 4.13 consists of 17 unique atoms.

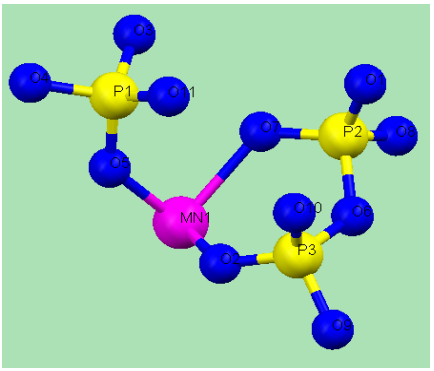

(a)

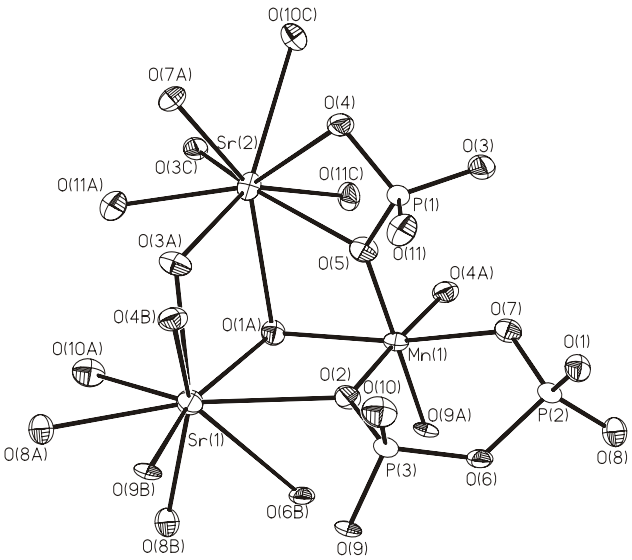

(b)

Figure 4.13. (a) Unique atom coordination (b) ORTEP plot of the asymmetric unit of $Sr_2MnP_3O_{11}$. Thermal ellipsoids are given at 70% probability.

There are crystallographically independent three phosphorus atoms and one manganese atom. Of the 11 oxygen atoms present in the asymmetric unit, two [O(8), O(11)] are two-coordinated, six [O(2), O(3), O(5), O(6), O(7), O(9), O(10)] are three-coordinated, and two [O(1), O(4)] are four-coordinated. Mn(1) is 6-coordinated with oxygen atoms forming distorted octahedra. The interatomic distances for the manganese atoms, Mn–O, lie in the range of 1.900(6)-2.234(6)Å and the O–Mn–O bond angles range from 87.2(2) to 91.4(2). The variation in bond distances and angles explain the slight distortions in the manganese–oxygen octahedra. All the P atoms are tetrahedrally coordinated to oxygen atoms and the P–O distances ranging from 1.491(6) to 1.637(6)Å, the O–P–O angles are in the range 103.1–113.8°. The three oxygen atoms around the phosphorous; O(8), O(11), and O(10); are not shared with manganese atom, but they have direct interaction with the two strontium cations which occupy the channels in the structure. Avarage distance between strontium and oxygen atom is 2.0745Å.

The valence sum calculations indicating that all Mn are trivalent, all oxygens are divalent, all phosphorous are pentavalent and Sr atoms are divalent (Table 4.5) has been done using the empirical relationship developed by Brown and Altermatt (Brown and Alternatt 1985). These oxidation states are consistent with the overall charge balance of the compound. As shown in Table 4.4, the oxidation state of Mn calculated according to this assignment has the value of 3.082.

The relation between bond length and bond valence were studied to show formal charge on the atom. The valence of a given atom is calculated from sum of the individual bond strengths of M–L bonds. Bond valence calculations have been performed also for Sr^{2+} cations and P^{5-} anions obtaining the values of 2.007 and 2.142 for Sr(1) and Sr(2), and 4.967, 4.886, and 4.901 for P(1), P(2) and P(3) respectively. All valence calculation results were given in Table 4.4.

Manganese can have three different oxidation states in minerals: 2+, 3+, 4+ and oxidation state of +2 is mainly observed in reported Mn–O and Mn–O–P systems, such as in manganese $SrMn_2(PO_4)_2$ (El-Bali 2000), $NaMn_4(PO_4)_3$, $KMn_4(PO_4)_3$ and $Ba(MnPO_4)_2.H_2O$ (Daidouh et al. 1999 and Escobal 1999). Trivalent Mn has the electron configuration $3s^23p^63d^6$ and occurs mainly in octahedrally coordinated manganese. As mentioned before, manganese with charge higher than +2 can easily be reduced to +2 under hydrothermal conditions and also the solubility of Mn^{+3} species in solution is low. However the Mn_2O_3 in the presence of phosphoric acid under supplied

hydrothermal conditions, dissolved easily and new manganese phosphate system including Mn^{+3} has formed.

The title compound crystallizes in a new structure type having the space group P 21/c of the monoclinic system with lattice parameters of a=6.6410(8)Å, *b*=6.8341(8)Å, *c*=19.0554(8)Å, *V*=857.00(15)Å^3. The unit cell of the title compound contains three $Sr_2MnP_3O_{11}$ formula groups (Figure 4.16). The Mn atom is coordinated by six oxygen atoms which are also directly bonded to phosphorous atoms.

Each MnO_6 octahedra shares six oxygen atoms with the tetrahedras; two PO_4 and two di-phosphate P_2O_7 groups. There is no Mn–O–Mn bond in the structure. Tong and his co-workers have stated that the presence of Mn–O–Mn bonds is necessary for the catalytic application of manganese oxides (Tong et al. 2002). In this compound there is no direct bond due to the connectivity of MnO_6 octahedra to PO_4^{3-} and $P_2O_7^{4-}$ groups. The $P_{(2)}O_4$ and the $P_{(3)}O_4$ tetrahedras form $P_2O_7^{4-}$ groups by sharing edges or corners. Connection between the tetrahedras is shown in Figure 4.13 (a, b).

A polyhedral representation of the structure along the [010] direction is shown in Figure 4.16. The structure is made up of PO_4 tetrahedra and P_2O_7 groups that connect MnO_6 octahedra into a 3D framework via common edges.

The three dimensional structure has microporous structure whose void size is less than 2nm. Looking down the a-axis, it has 24 membered channels containing 6 MnO_6 and 6 PO_4 polyhedras. From b side of the unit cell there are 2 different channels, one of which has twelve members and the other is 14 membered. These channels can be seen easily in Figure 4.14a and Figure 4.14b respectively.

Even though compound has channeled structure, for simplicity it can be considered as layered. The separate layers can be seen in Figure 4.14 and they are connected to each other through PO_4 tetrahedras as seen in Figure 4.15.

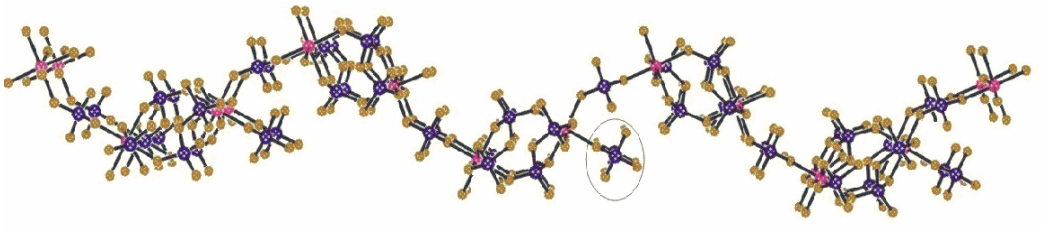

Figure 4.15. View of the Mn/P/O layers of $Sr_2MnP_3O_{11}$ along the c axis.

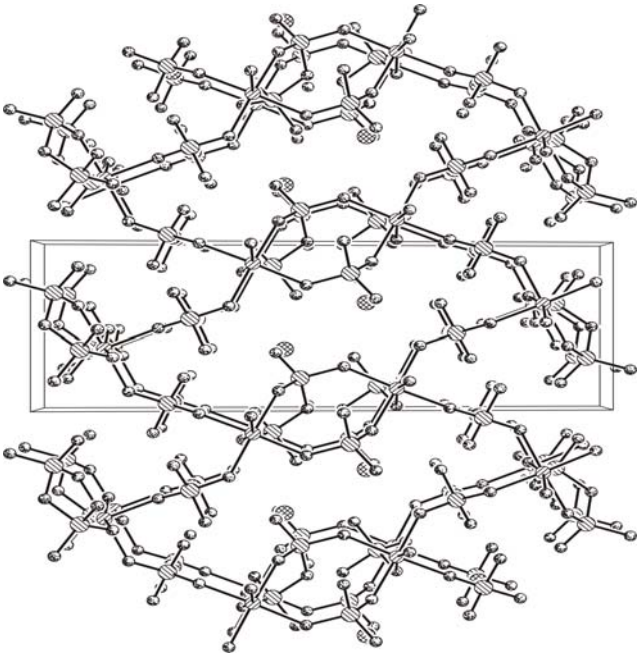

(a)

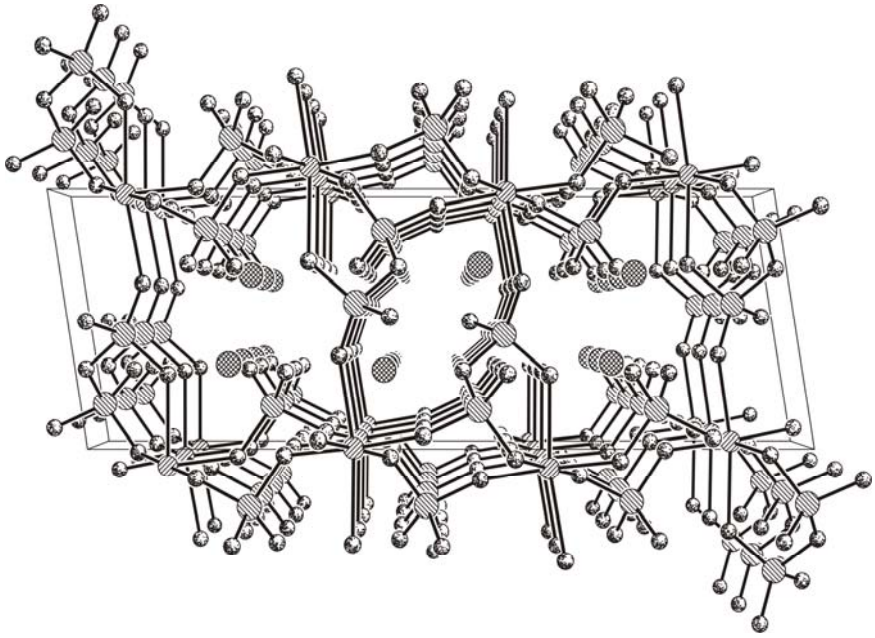

(b)

Figure 4.14. Unit cell view of $Sr_2MnP_3O_{11}$ running along a (a) and b (b) axis. The shaded circles represent the Mn atom, the crosshatched circles belong to Sr, the circles shaded bottom right to top left represent the P atoms and the dotted circles show the oxygen atoms.

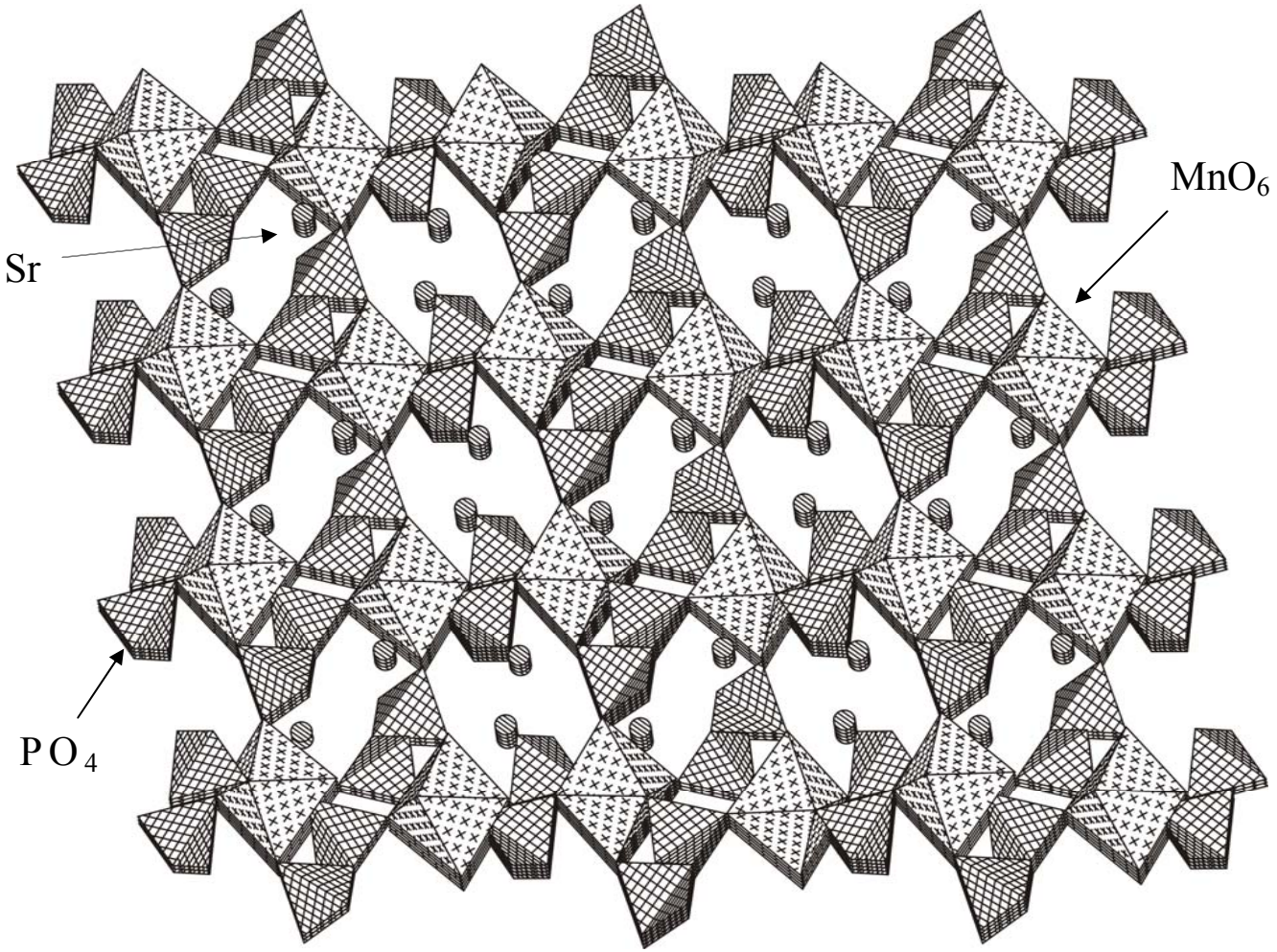

Figure 4.16. Polyhedral projection of the structure of $Sr_2MnP_3O_{11}$ along b-axis.

CHAPTER 5

HYDROTHERMAL SYNTHESIS OF METAL OXIDES INCLUDING PHOSPHATES

During this study in order to synthesize novel crystals with high quality and quantity, many different reactions were performed hydrothermally and many single crystals have been obtained from reactions mixture of different reactants including transition metal sources, phosphate sources, solvent, different mineralizers and templates by changing experimental parameters. Mostly, water was used as solvent. The mixtures were loaded into a 23-mL Teflon-lined autoclave and were heated in an oven and then slowly cooled to room temperature.

After cooling, the resulting mixtures were opened, and products were filtered, washed several times with distilled water and acetone, and finally dried in air at room temperature. The products were analyzed by powder X-ray diffractometer, single X-ray diffractometer and scanning electron microscope. Some of them have not been identified yet, however as soon as X-ray single crystal data are received, their structure will be solved. Some of the synthesized crystals are given below with their experimental conditions and analysis results.

5.1. Hydrothermal Synthesis and Structural Characterization of Hureaulite $Mn_5(H_2O)_4[PO_3(OH)]_2[PO_4]_2$

5.1.1. Experimental

Single pink hexagonal crystals of $Mn_5(H_2O)_4[PO_3(OH)]_2[PO_4]_2$ were obtained from the reaction of $SrCO_3$ (0.1475g, 0.001 mole), $MnCl_2$ (0.2516g, 0.002 mole), H_3PO_4 (0.1958g, 0.002 mole) and H_2O (9mL). The following reagents were used as obtained: $SrCO_3$ (Sigma Aldrich, 98%), $MnCl_2$ (Aldrich, 99.99%), and H_3PO_4 (Merck, 99%).

A reaction mixture was loaded into a 23mL autoclave. Nine mL (39% fill) of solvent, H_2O, was added to the starting solids. The autoclave was then sealed and heated at 180°C for 3 days; a colorless solution was obtained after cooling the reaction bomb to room temperature slowly. After filtering, the products were then washed with ultra pure water and acetone several times in order to clean the solid product from any contaminants. Single crystals of the compound (Figure 5.1) were selected for X-ray single crystal data collection. Crystals of compound $Mn_5(H_2O)_4[PO_3(OH)]_2[PO_4]_2$ were sent to *Ondokuz Mayis University* (Samsun, Turkey) for X-ray single crystal data collection. The reactants were combined in the mole ratio (1:2:2) as follows. The reaction occurred as below:

$$SrCO_3 + MnCl_2 + H_3PO_4 \xrightarrow[H_2O]{(180ºC\ /\ 3\ days)} Mn_5(H_2O)_4[PO_3(OH)]_2[PO_4]_2 \quad \text{pale pink crystals} \qquad (5\text{-}1)$$

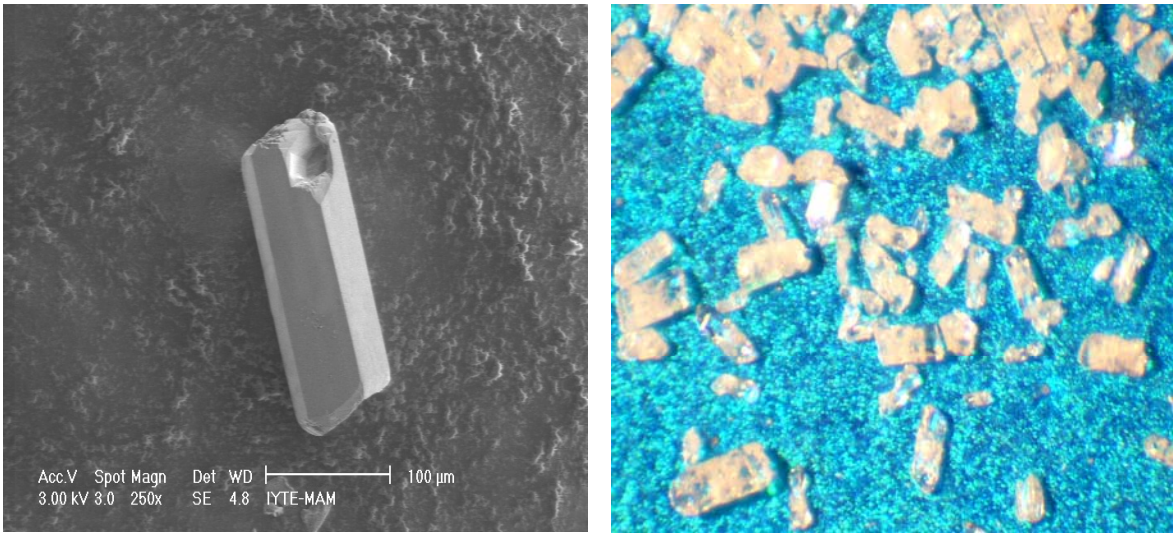

Figure 5.1. Photos of pale pink colored $Mn_5(H_2O)_4[PO_3(OH)]_2$ crystals.

In order to obtain single crystals of good quality and shape, reagents had to be changed. (e.g. 1:1:2, 1:2:2, 2:2:2). In addition, different degrees of solvent filling, different reaction times and different heat treatments were applied to increase the quantity and the quality of the products. The reaction conditions show in (5-1) yielded the best results. Pure pink crystals of the title compound were obtained with the lengths of approximately 0.1-0.2mm.

The SEM EDX results and powder X-ray diffraction pattern of the pale pink crystals are shown in Figure 5.2 and 5.3 respectively. Oxygen, phosphorous and manganese elements are in the atomic percentages of 47.08%, 13.14%, and 22.47% respectively.

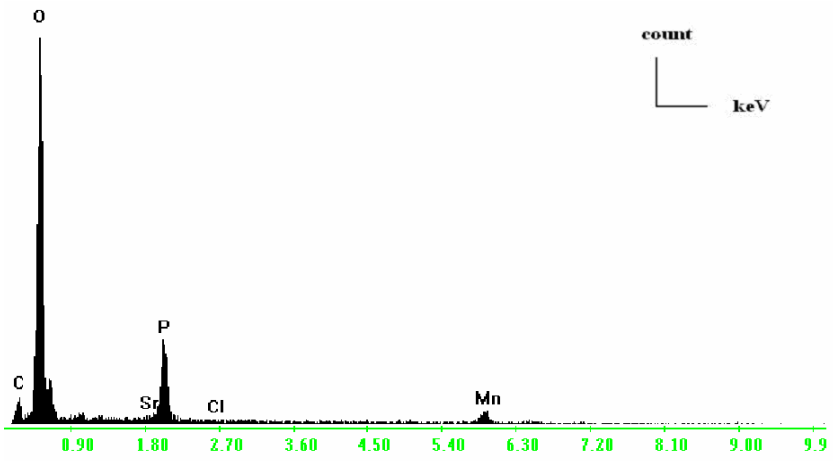

Wt %	O K	47.08	P K	13.14	MnK 22.47
At %	O K	58.06	P K	8.37	MnK 8.07

Figure 5.2. SEM EDX spectrum of the $Mn_5(H_2O)_4[PO_3(OH)]_2$

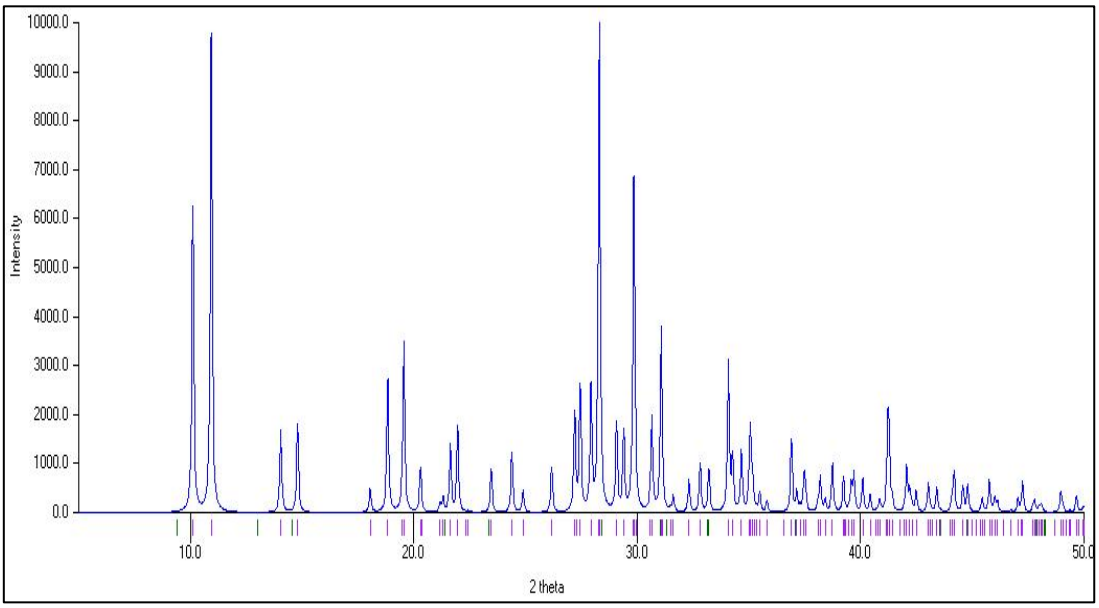

Figure 5.3**.** X-ray powder diffraction pattern of $Mn_5(H_2O)_4[PO_3(OH)]_2$

5.1.2. Single X-ray Crystallographic Analysis

The data were merged and averaged in Laue group 6 yielding an internal agreement factor of R_m=0.0261 for $Mn_5P_4O_{20}H_{10}$. A single pale pink crystal was mounted on a glass fiber with epoxy glue and centered on a STOE X-AREA diffractometer (Stoe and Cie 2002). Crystal data, details of the data collection and refinement are given in Table 5.1. The unit cell parameters and the orientation matrix were based on the centroids of 1923 reflections with $F_0 > 4sig(F_0)$.

The structure was solved by direct methods with the program SHELXS (Sheldrick) and by refined full-matrix least-squares techniques using the program SHELXL (Sheldrick) in the Crystal Structure software (Crystal Structure 2004).

Crystallographic information is given in details in Table 5.1. All atomic thermal parameters were refined anisotropically. Final values of atomic coordinates and equivalent isotropic displacement parameters are given in Table 5.2 and anisotropic displacement coefficients are given in Table 5.3. Bond distances and selected bond angles are given in Table 5.5 and 5.4 respectively.

Table 5.1. Crystal Data and Structure Refinements for $Mn_5(H_2O)_4[PO_3(OH)]_2[PO_4]_2$

Compound	$Mn_5P_4O_{20}H_{10}$
Chemical F_w	718.55
Cell F_w	1437.16
Cristal System	Monoclinic
Space Grup	C2/c
Z	2
Radiation wavelength λ (Å)	0.71073
a, Å	17.600(4)
b, Å	9.1214(18)
c, Å	9.4786(19)
α = γ degree	90
β= degree	96.52(3)
V_{cell} , $(Å)^3$	1511.8(5)
T, (K)	293(2)
ρ_c, (gcm^{-3})	2.949
2θ range, degree	2.33 – 28.73
R	0.0271
R_w	0.0261

Table 5.2. Atomic Coordinates and Equivalent Isotropic Thermal Parameters of $Mn_5(H_2O)_4[PO_3(OH)]_2[PO_4]_2$

Atom	X	Y	Z	U_{eq}
Mn1	0.0000	0.10261(4)	0.75000	0.01339(16)
Mn2	0.181825(17)	0.41099(3)	0.31526(3)	0.01383(15)
Mn3	0.174456(17)	0.02791(3)	0.36506(3)	0.01367(15)
P1	0.08276(3)	-0.17913(5)	0.91027(6)	0.01122(16)
P2	0.16066(3)	0.26040(5)	0.62822(5)	0.01056(16)
O1	-0.01176(9)	-0.28421(17)	0.91965(18)	0.0190(3).
O2	-0.07705(8)	-0.06726(18)	0.79341(17)	0.0162(3)
O3	0.20169(8)	0.40375(15)	0.67345(17)	0.0149(3)
O4	-0.08415(8)	-0.10746(16)	1.05557(18)	0.0162(3)
O5	-0.15446(8)	-0.27102(16)	0.86704(17)	0.0160(3)
O6	0.16387(8)	0.23595(16)	0.46701(16)	0.0138(3)
O7	0.07590(8)	0.26567(16)	0.65759(17)	0.0137(3)
O8	0.20180(8)	0.13328(16)	0.71123(17)	0.0148(3)
O9	0.07700(9)	0.51189(18)	0.3487(2)	0.0228(4)
O10	0.25932(9)	-0.08053(16)	0.53022(17)	0.0161(3)

Table 5.3. Anisotropic Displacement Coefficients ($Å^2$) of $Mn_5(H_2O)_4[PO_3(OH)]_2[PO_4]_2$

Atom	U11	U22	U33
Mn1	0.0125(2)	0.0134(2)	0.0141(3)
Mn2	0.0129(2)	0.0136(2)	0.0150(2)
Mn3	0.0137(2)	0.0132(2	0.0139(2)
P1	0.0104(2)	0.0119(3)	0.0111(3)
P2	0.0101(3)	0.0102(2)	0.0113(3)
O1	0.0179(7)	0.0204(8)	0.0179(8)
O2	0.0160(7)	0.0163(6)	0.0159(8)
O3	0.0150(7)	0.0135(7)	0.0163(8)
O4	0.0149(6)	0.0195(7)	0.0139(8)
O5	0.0143(7)	0.0176(7)	0.0157(8)
O6	0.0157(7)	0.0133(7)	0.0125(7)
O7	0.0098(6)	0.0143(7)	0.0172(8)
O8	0.0133(6)	0.0149(6)	0.0162(8)
O9	0.0168(7)	0.0204(8)	0.0319(10)
O10	0.0175(7)	0.0151(7	0.0157(8)

Table 5.4. Selected Bond Angles (degrees) in $Mn_5(H_2O)_4[PO_3(OH)]_2[PO_4]_2$.

Mn3	O6	Mn2	108.75(7)	O4	P1	O5	112.23(9)
O2	Mn1	O7	168.11(6)	O5	P1	O1	107.90(9)
O2	P1	O1	109.49(9)	O6	Mn3	O10	99.15(6)
O2	P1	O4	112.31(9)	O7	P2	O6	108.97(9)
O3	P2	O8	108.75(9)	O8	P2	O7	109.82(8)
O3	P2	O6	109.25(9)	O9	Mn2	O6	91.45(6)

Table 5.5. Bond Length (Å) for $Mn_5(H_2O)_4[PO_3(OH)]_2[PO_4]_2$

Environment of Mn atoms

Mn1-	O2	2.1296(16)x2	Mn2-	O9	2.1175(17)	Mn3-	O8	2.1631(15)
Mn1-	O4	2.2297(18)x2	Mn2-	O8	2.1302(14)	Mn3-	O2	2.1769(16)
Mn1-	O7	2.2427(15)x2	Mn2-	O5	2.1584(16)	Mn3-	O4	2.2110(15)
			Mn2-	O6	2.1957(15)	Mn3-	O10	2.2647(17)
			Mn2-	O3	2.2116(15)	Mn3-	O3	2.3354(15)
			Mn2-	O10	2.2946(16)	Mn3-	O6	2.1472(15)
<Mn(1) – O>		2.201(16)	<Mn(2) – O>		2.145(16)	<Mn(3) – O>		2.216(16)
∑ij sij =		*1.9966(84)*	∑ij sij =		*2.1775(82)*	∑ij sij =		*1.9237(82)*

Environment of P atoms

P1-	O2	1.5178(16)	P2-	O3	1.5312(15)
P1-	O4	1.5272(17)	P2-	O8	1.5358(15)
P1-	O5	1.5315(15)	P2-	O7	1.5489(15)
P1-	O1	1.5694(16)	P2-	O6	1.5516(16)
<P(1) – O>		1.537(16)	<P(2) – O>		1.541(15)
∑ij sij =		*4.9801 (81)*	∑ij sij =		*4.9026(78)*

Environment of O atom

O1-	P1	1.5694(16)	O2-	Mn3	2.1769(16)	O3-	Mn2	2.2116(15)
O9-	Mn2	2.1175(17)	O2-	Mn1	2.1296(16)	O3-	Mn3	2.3354(15)
			O2-	P1	1.5178(16)	O3-	P2	1.5312(15)
O4-	Mn3	2.2110(15)	O5-	Mn2	2.1584(16)	O6-	Mn3	2.1472(15)
O4-	Mn1	2.2297(18)	O5-	P1	1.5315(15)	O6-	P2	1.5516(16)
O4-	P1	1.5272(17)				O6-	Mn2	2.1957(15)
O7-	Mn1	2.2427(15)	O8-	Mn2	2.1302(14)	O10-	Mn3	2.2647(17)
O7-	P2	1.5489(15)	O8-	Mn3	2.1631(15)	O10-	Mn2	2.2945(16)

Table 5.6. Oxygen Valence in $Mn_5(H_2O)_4[PO_3(OH)]_2[PO_4]_2$

O1↔[OH]	1.1576
O2	2.0582
O3	1.8101
O4	1.9002
O5	1.6298
O6	1.9085
O7	1.5962
O8	1.527
O9↔H_2O	0.4127
O10↔H_2O	0.5329

5.1.3. Results and Discussion

The compound having a formula $Mn_5(H_2O)_4[PO_3(OH)]_2[PO_4]_2$ was prepared from the reaction of $SrCO_3$, $MnCl_2$, H_3PO_4, and H_2O as pale pink crystals. The single crystal X-ray diffraction study of the title compound $Mn_5(H_2O)_4[PO_3(OH)]_2[PO_4]_2$ showed that it possesses a three-dimensional architecture containing channels and is made up of MnO_6, $PO_3(OH)$, and PO_4, moieties. Its asymmetric unit is shown in Figure 5.4 and Figure 5.5.

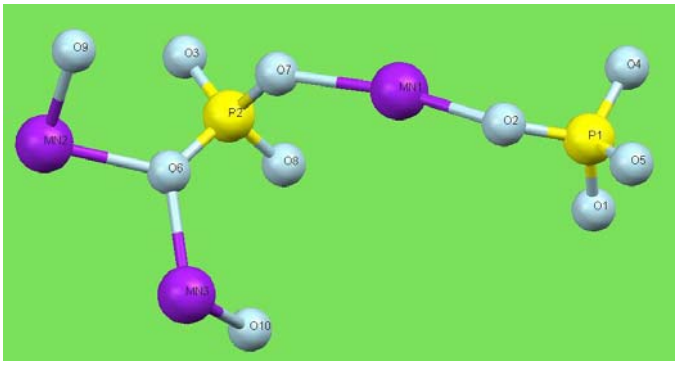

Figure 5.4. Unique atom coordination of $Mn_5(H_20)_4[PO_3(OH)]_2[PO_4]_2$ without hydrogens.

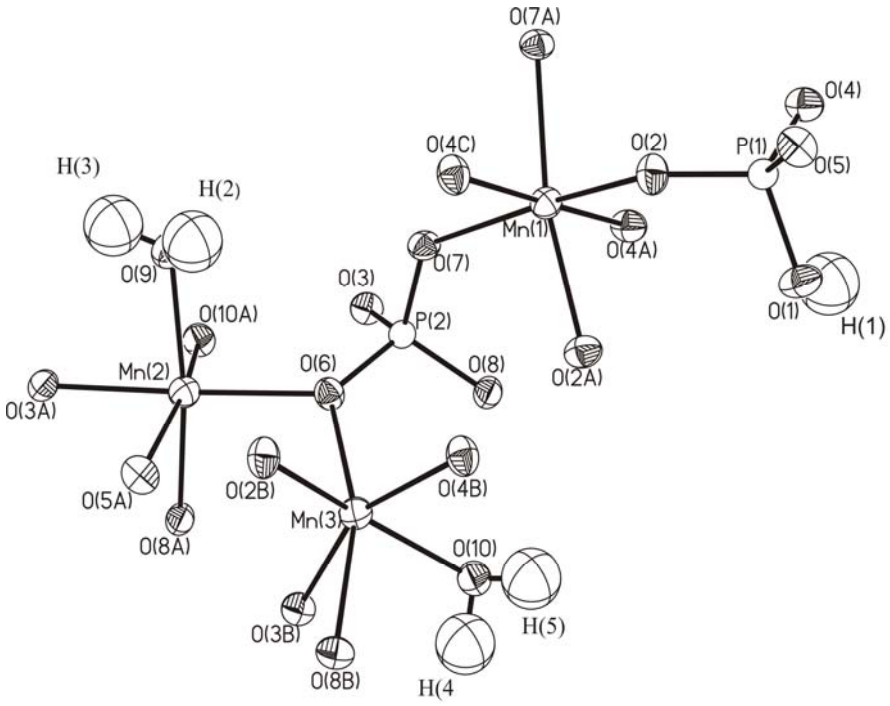

Figure 5.5. ORTEP plot of the asymmetric unit in $Mn_5(H_2O)_4[PO_3(OH)]_2[PO_4]_2$. Thermal ellipsoids are given at 70% probability.

Figure 5.6. A photograph of Hureaulite mineral
(Source: http://www.webmineral.com 2006)

The structure of this phosphate had been previously determined from natural sources by Araki and Moore (Moore and Araki 1973). A photograph of the mineral is shown in Figure 5.6. The title compound has a monoclinic crystal lattice having the unit cell parameters a=17.600(4)Å, b=9.1214(18)Å, c=9.4786(19)Å and α=γ=90º and β=96.52(3)º with space group C2/c. The unit cell shown in Figure 5.7 contains 4 of the formula units as represented in Figure 5.4.

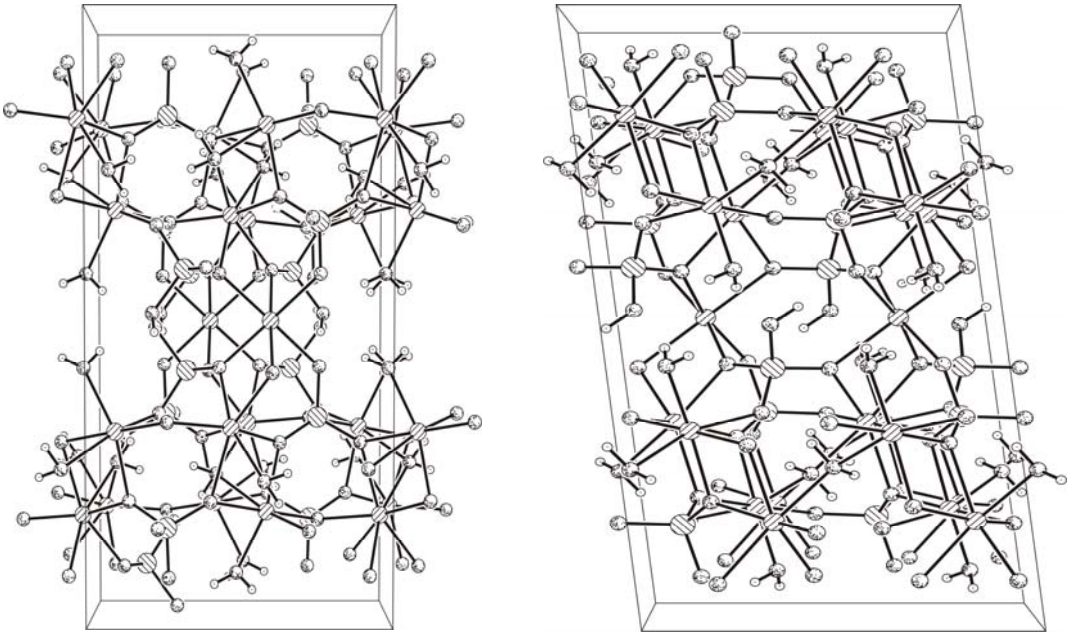

(*c* direction) (*b* direction)

Figure 5.7. The unit cell structure of title compound as viewed from both c and b direction. The shaded circle from the bottom left to the top right represents a Mn atom; the shaded circle from bottom right to the top left represents a P atom; the circles with dot patterns and highlight represent an O atom and the smallest circle with a point belongs to hydrogen.

Manganese atoms are octahedrally coordinated with oxygen. The phosphorous atoms form a tetrahedral coordination with O and OH groups. Mn(1) is 6-coordinated with oxygen atoms; Mn(2) and Mn(3) are coordinated by five oxygens and one H_2O. The average inter-atomic distances for the manganese atoms, Mn–O, lie in the range of 2.145(16)-2.216(16)Å and the O–Mn–O bond angles range from 91.45(6) to 919.15(6)º (Tables 5.4 and 5.5). The P(1) atom is tetrahedrally coordinated to three oxygen atoms

and one hydroxyl group having a P–O distances ranging from 1.5178(16) to 1.5694(16)Å [(P(1)–O)avg = 1.537(16)Å and the P(2) atom has 4 oxygens coordination with an average P(2)–O distance of 1.541(15)Å. The O–P–O angles are in the range 107.90(9) –112.23(9) ° (Tables 5.4 and 5.5).

By using the relation between bond length and bond valence as developed by Brown and Altermatt (Brown and Alternatt 1985), the formal charge of atoms in the structure was calculated (Table 5.5). According to valence calculations, Mn has a charge of +2.026(16) and P has a charge of +4.90535(16). The valence shell calculation for each oxygen atoms showed that O(1) is coordinated with one hydrogen to form an OH group, O(9) and O(10) were a coordinated by two hydrogen atoms giving H_2O. The oxygen valences in $Mn_5(H_2O)_4[PO_3(OH)]_2[PO_4]_2$ are given in Table 5.6.

The structure of title compound consists of a three dimensional compact framework formed by MnO_6 octahedra and PO_4 tetrahedra. The structure has 3 Mn^{+2} cations in three nonequivalent and 2 P^{+5} atoms in two nonequivalent crystallographic sites.

The Mn(1) atom is coordinated by three different oxygen atoms; O(2), O(7) and O(4A). The manganese atom is directly bonded to $P(1)O_3(OH)$, $P(2)O_4$ tetrahedra and other manganese octahedral groups by means of these oxygens. The Mn(2) atom is surrounded by six different oxygens one of which is the oxygen, O(9), of the water molecule, as shown in Figure 5.5. Similar to Mn(2), one of the six coordination sites of Mn(3) is made with the other water molecules, O(10). Between the Mn(2) and Mn(3) there is bridging oxygen, O(6).

In this structure five MnO_6 [1 Mn(1) and 2 Mn(2) and 2 Mn(3)] octahedra share edges to form a linked linear pentamer that extends in the a direction which is shown in Figure 5.8. The Mn(1) octahedral shares one of the its edges with the Mn(3) octahedral via O(4) and O(2). Mn(3) and Mn(2) are connected with each other through bridging via O(6) and through sharing of bond edges including the Mn-O(3) and Mn-O(8) bonds. Adjacent pentamers are linked through (PO_4) groups with which they share corners to form a thick slab parallel to c direction (Figure 5.9).

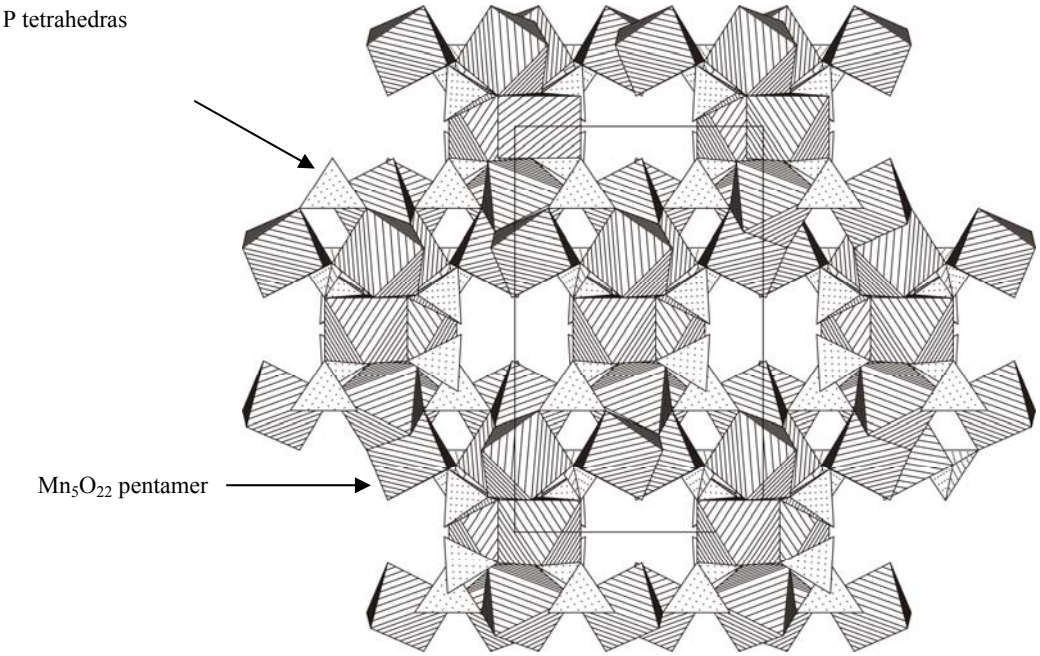

Figure 5.8. Polyhedral structure of the $Mn_5(H_2O)_4[PO_3(OH)]_2[PO_4]_2$ as view from *c* direction. Hydrogen atoms are omitted for clarity.

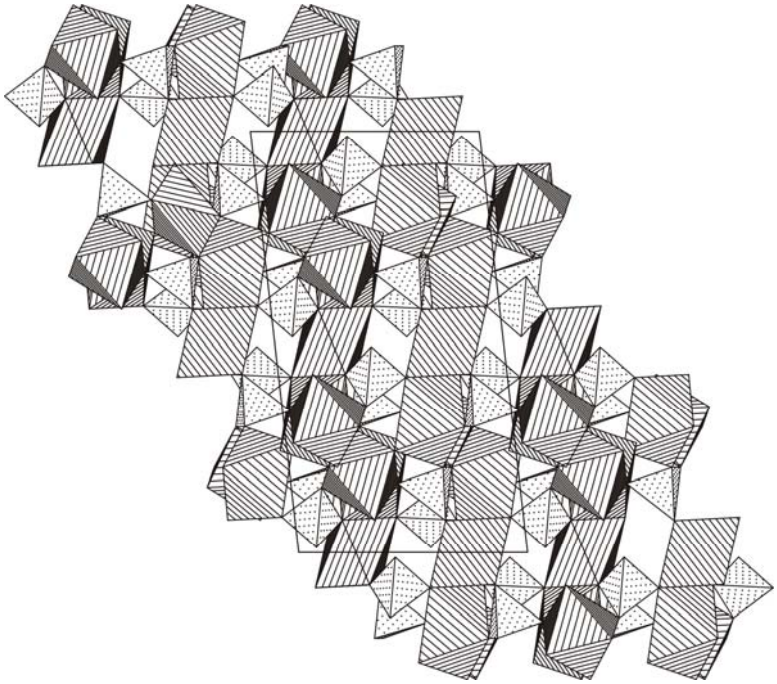

Figure 5.9. The polyhedral view of the $Mn_5(H_2O)_4[PO_3(OH)]_2[PO_4]_2$ from [100] direction showing linkanages of the slabs with phosphorous tetrahedras.

In the resulting framework there are fairly large interstices (Figure 5.9) along the c axis. These are usually unoccupied. However, Moore and Araki suggest that alkalis or alkaline earths with atomic radii of size less than 8Å could occupy this cavity with loss of the acid-phosphate groups and it was observed that occupancy of the cavities by the cations did not have an effect on basic structure (Kamf and Ross 1988).

In this study the crystals of Hureaulite mineral were obtained in two different colors as a result of two different reactions. Although the powder X-ray patterns of two crystals (Figure 5.3 and 5.12) matched with hureaulite mineral, the colors of crystals were different shown in Figure5.1 and 5.10). X-ray powder diffraction pattern of the yellow crystals has broad base line of the pattern and the base line shows that an amorphous phase present. The phase may be the carbon phase or the synthesized compound may not have completed its crystal formation.

The color differences may be resulted from different atomic arrangement with in the same unit cell. The manganese phosphate systems frequently have large interstices between polyhedras. The large interstices can accommodate a large amount of water of crystallization and the counteractions.

A bulk of attached rectangular yellow crystals of hureaulite were obtained from the reaction of KVO_3 (0.1385g, 0.001 mole), $MnMoO_4$ (0.1071g, 0.0005 mole), BPO_4 (0.1058g, 0.001 mole). The following reagents were used as obtained: KVO_3 (Fluka, >98%), $MnMoO_4$ (Aldrich), and BPO_4 (Aldrich, 99.5%) The reactants were in the (1:0.5:1) mole ratio. 8mL of water was used as solvent. The yellow rectangular shaped crystals are shown in Figure 5.10. The reaction occured as below:

$$KVO_3 + MnMoO_4 + BPO_4 + H_2O \xrightarrow[3\ \text{days}]{170^{\circ}C} \text{yellow crystals “Hureaulite”} \qquad (5\text{-}2)$$

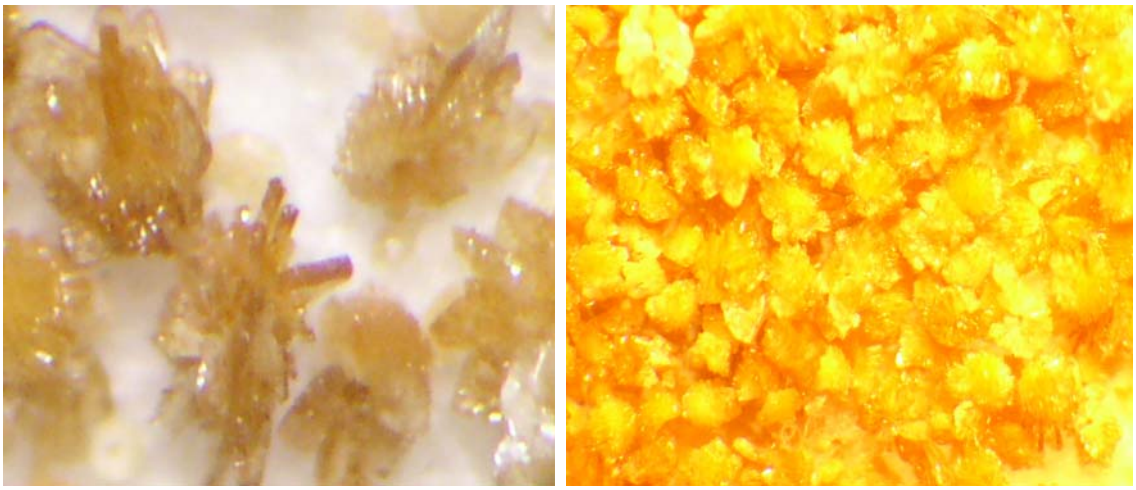

Figure 5.10. Pictures of the yellow crystals

High amount of the yellow crystals were obtained without any powder. We obtained air stable crystals in the size of approximately 0.1-0.5 mm with the yield of more than 70%. But the number of single crystal was very low. The SEM/EDX results of the yellow crystals are shown in Figure 5.11.

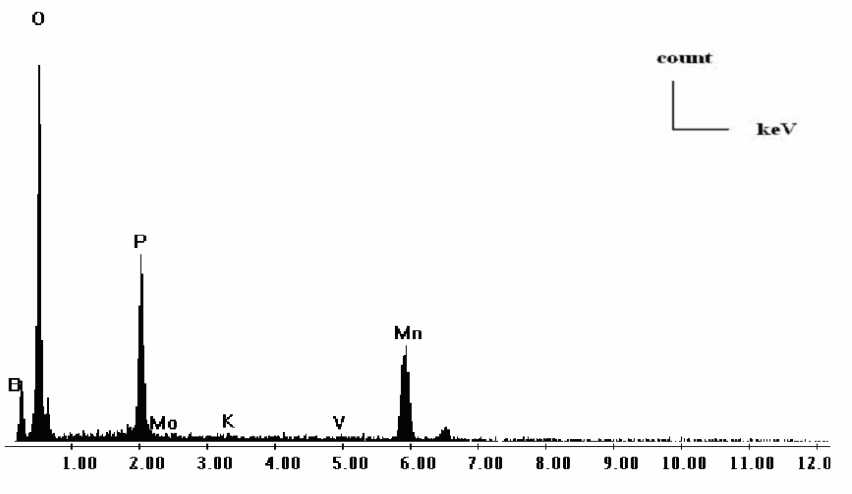

Wt % B K 18.37, O K 32.64, P K 12.26, MnK 35.02

At % B K 35.36, O K 42.47, P K 8.24, MnK 13.27

Figure 5.11. SEM /EDX spectrum of the yellow bulk crystals.

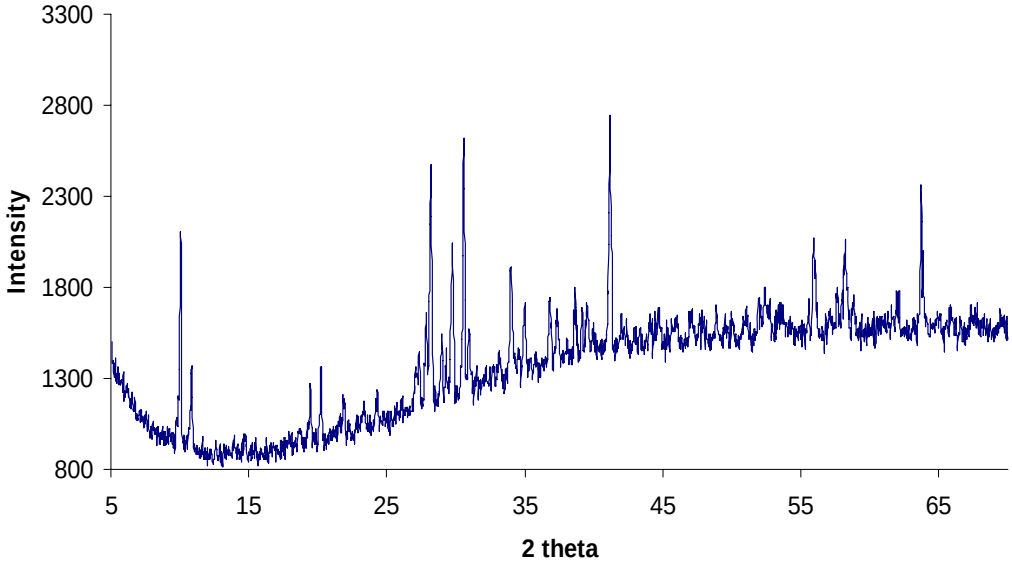

Figure 5.12. The X-ray powder peaks of the yellow crystals.

5.2. Hydrothermal Synthesis of Blue Platelike Crystals

The blue plate like crystals were obtained from the reaction of V_2O_5 (0.1818g, 0.001 mole), $SrCO_3$ (0.1451g, 0.001 mole), H_3PO_4 (0.392g, 0.003 mole), ethylenediammine ($NH_2CH_2CH_2NH_2$) (0.1mL) (Figure 5.13) in a pale green powder. The following reagents were used as obtained: V_2O_5 (Aldrich 99.5%), $SrCO_3$ (Aldrich, 98%), H_3PO_4 (Merck 99%), and ethylenediammine, (Merck, 0.9kg/L, 99%). The solid reactants were in the (1:1:3) mole ratio, 0.1mL ethylenediammine was used as organic component in the presence of 9mL water.

$$V_2O_5 + SrCO_3 + H_3PO_4 + en + H_2O \xrightarrow[3\ days]{180°C} \text{blue plate-like crystals (C, N, O, P, V)} \qquad (5\text{-}3)$$

Similar reactions were done with different ratios, such as 1:1:3, 1.5:1:3, 1:1:3, and 1:1:2 of V_2O_5, $SrCO_3$, and H_3PO_4 and with different amount of ethylenediammine. These different reaction ratios were applied for the aim of finding the clearer and better blue plate like crystals. Also the amount of solvent, the reaction

time and applied temperatures were changed. The reaction condition shown in (5-3) gave the best result. Also by small changes in these ratios it was observed that the quality, quantity, and morphology the products were changed.

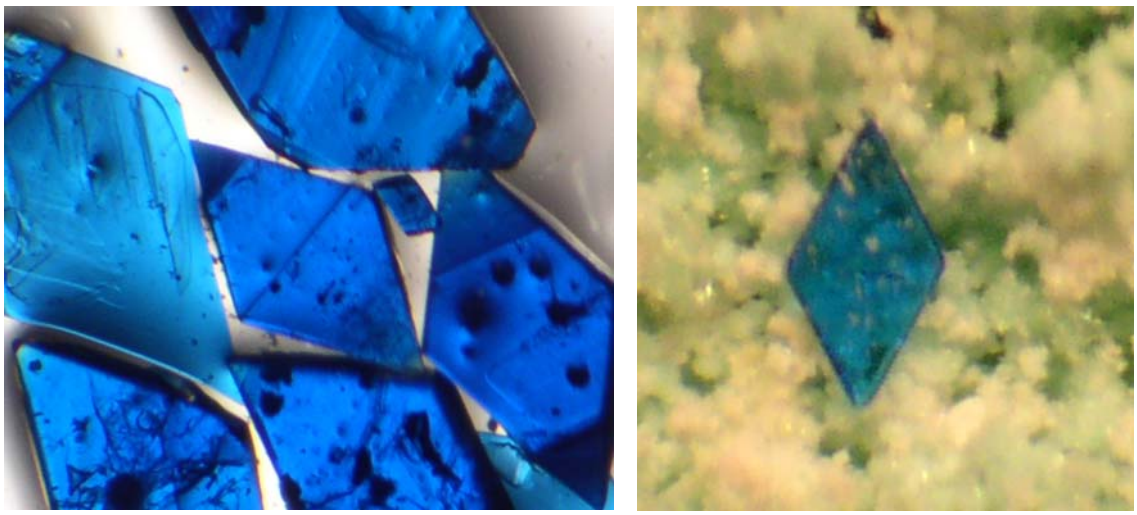

Figure 5.13. Photos of unidentified blue plate like shaped crystals including C, N, O, P, V elements.

Airstable blue crystals were obtained in the size of approximately 1-2mm with the yield of 50%. The SEM EDX results of the crystals are shown in Figure 5.14 and their X-ray powder peaks which did not match with any compound in the XRD powder data base are shown in Figure 5.15.

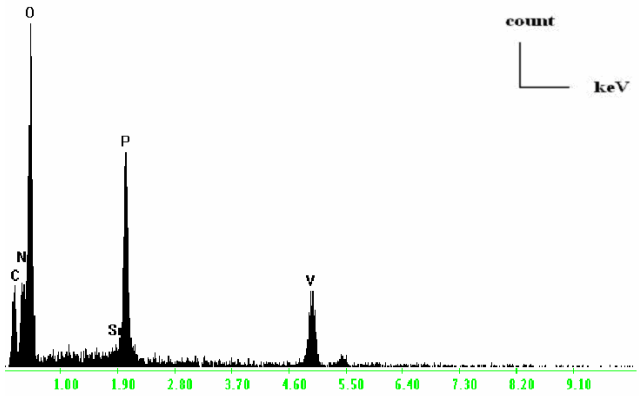

Wt % C K: 14.34, N K: 13.43, O K: 35.78, P K: 13.00, V K: 21.68.

At % C K: 22.72, N K: 18.24, O K: 42.56, P K: 7.99, V K: 8.10.

Figure 5.14. SEM / EDX specturum of unidentified blue plate like crystals.

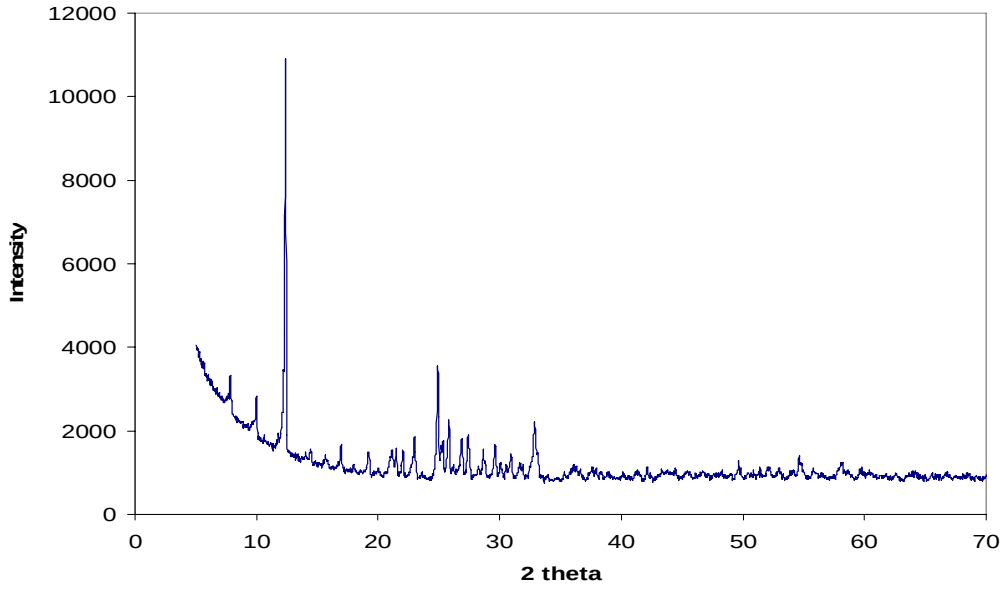

Figure 5.15. The X-ray powder peaks of unidentified blue plate like crystals.

5.3. Hydrothermal Synthesis of Green Rectangular Crystals

By reacting the compounds of $SrCO_3$ (0.1475g,), $CuCl_2.2H_2O$ (0.1705g), BPO_4 (0.1090g), $NaVO_3$ (0.0609g) and ethylenediammine ($NH_2CH_2CH_2NH_2$) in the water solvent green rectangular crystals (Figure 5.16) were obtained via the white powder. The reaction is shown below:

$$NaVO_3 + CuCl_2{\cdot}2H_2O + SrCO_3 + BPO_4 + en + H_2O \xrightarrow{170°C\ /\ 3\ days} \text{Green crystals (B, C, N, O, V)} \quad (5\text{-}4)$$

The solid reactants were in the (0.5:1:1:1) mole ratio. 9mL water was used as solvent and 0.1mL ethylenediammine was added to the mixture as an organic source. The reactions were tried several times without any organic component and the crystals could not be obtained. The trials and the SEM / EDX results show that structure of the crystals contain the organic group.

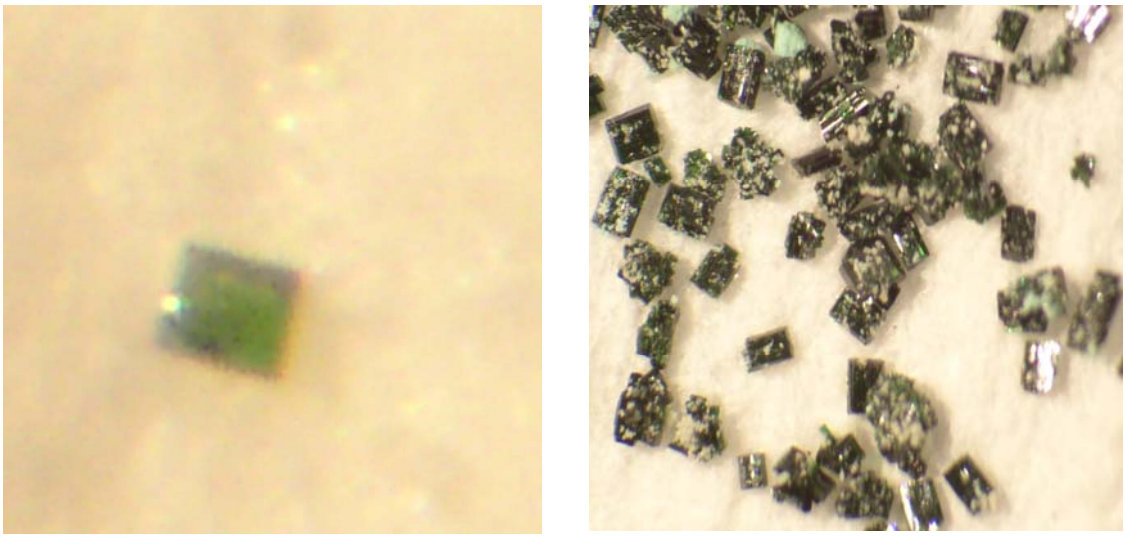

Figure 5.16. Photos of green colored unidentified crystals containing B, C, N, O, V, Cu element.

The SEM / EDX results of the green rectangular crystals are shown in Figure 5.17 and their X-ray powder peaks which did not match with any compound in the XRD powder data base are shown in Figure 5.18. The crystals are air stable.

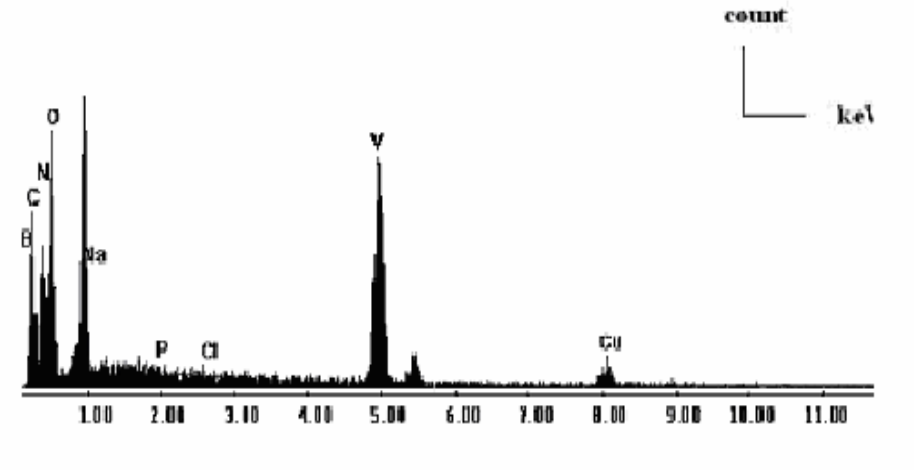

Wt % B K: 17.60, C K 20.19, N K 19.30, O K 16.57, Cu K 9.64, V K 18.6

At % B K: 26.97, C K 27.84, N K 16.32, O K 16.01, V K 6.05, Cu K 4.27

Figure 5.17. SEM /EDX spectrum of the green rectangular crystals

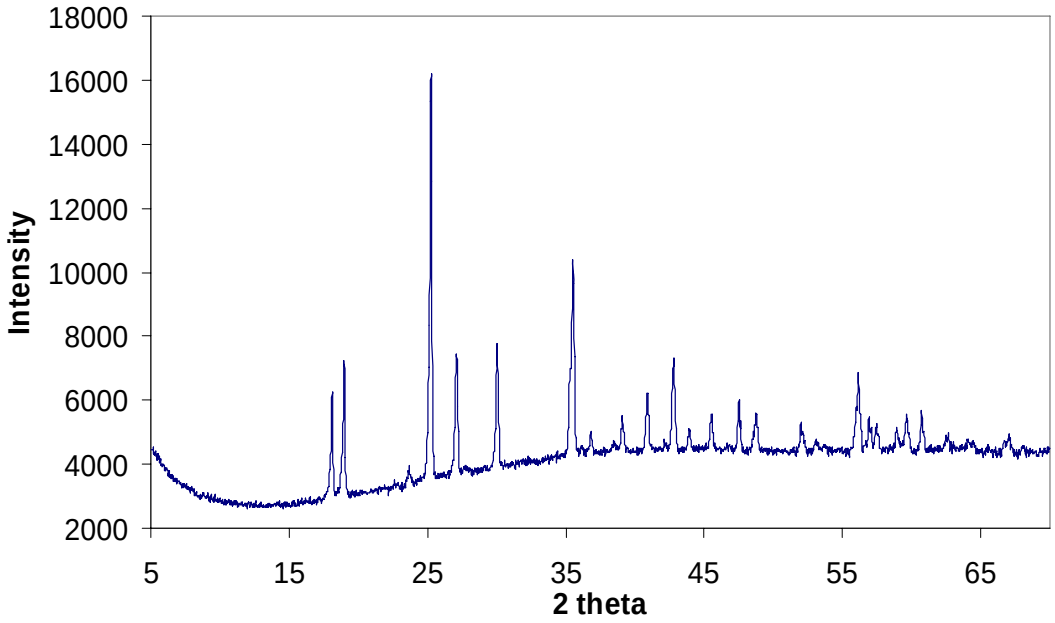

Figure 5.18. The X-ray powder pattern of the unidentified plate-like green crystals

CHAPTER 6

CONCLUSION

In this study the synthesis and crystallographic analysis of transition metal (manganese and vanadium) oxides containing phosphate oxoanionic groups were investigated. During the research, the hydrothermal method was proven to be a good method for synthesizing of metal oxide crystals. Detailed structural information of synthesized crystals was obtained by the help of commercial software programs SHELX (Sheldrick 1997) and Crystal Structure (Molecular Structure Corparation 2004).

Firstly Strontium Manganese Phosphate ($Sr_2MnP_3O_{11}$) material was synthesized in powder form and a good quality and size crystal of this compound was done in Clemson University via the reaction of 59mg $SrCO_3$, 63mg Mn_2O_3, 0.2mL H_3PO_4 (85%) and 0.5mL H_2O in a fused-silica tube under an Ar atmosphere in a glove box at 375°C for 3 days. The crystallographic analysis of the compound was done in Solid State Laboratory of İzmir Institute of Technology. The title compound crystallizes in a monoclinic system in the space group P 21/c and the lattice parameters are a=6.6410(8)Å, b=6.8341(8)Å, c=19.0554(8)Å, β=99.22(3)º, V=857.00(15)Å^3. Unit cell of the compound contains three $Sr_2MnP_3O_{11}$ formula groups. The single crystal X-ray diffraction study of the title compound, $Sr_2MnP_3O_{11}$, showed that it possesses a three-dimensional architecture. The structure is made up of MnO_6, P_2O_7, PO_4 moieties and strontium cations. The three dimensional channeled structure forms via oxygen sharing of each MnO_6 octahedra with PO_4 tetrahedra. $Sr_2MnP_3O_{11}$ has microporous structure and contains twenty-four, fourteen and twelve membered channels. The strontium cations are placed on the channels. It is the second compound with Mn, P, O, and Sr elements in literature (El-Bali 2000).

Many single crystals of known compounds were obtained in appropriate sizes during our research. Single pale pink hexagonal crystals of hureaulite mineral having formula $Mn_5(H_2O)_4[PO_3(OH)]_2[PO_4]_2$ was obtained by the hydrothermal reactions of $MnCl_2$, $SrCO_3$, H_3PO_4, and H_2O in (2:1:2:500) mole ratio at 180ºC for 3 days. Crystal of the $Mn_5(H_2O)_4[PO_3(OH)]_2[PO_4]_2$ was selected and sent to *Ondokuz Mayis University* (Samsun, Turkey) for X-ray single crystal data collection. After the data collection,

SHELX and Crystal Structure software programs were used in order to get the detailed shaped and crystal information of the material. The product crystallizes in a monoclinic system having the cell parameter a=17.600(4)Å, b=9.1214(18)Å, c=9.4786(19)Å and α=γ=90º and β=96.52(3)º. Space group of the compound is C2/c and the unit cell contains two formula groups in it. The title compound $Mn_5(H_2O)_4[PO_3(OH)]_2[PO_4]_2$ has a three-dimensional structure and it is made up of MnO_6, $PO_3(OH)$, and PO_4 polyhedras. In this structure five MnO_6 octahedra share edges to form a linked linear pentamer that extends in *a* direction and adjacent pentamers are linked through (PO_4) groups with which they share corners to form a thick slab parallel to *c* direction. The compound has channels through *c* direction and the channels are empty.

Also $Mn_5(HOPO_3)_2(PO_4)_2(H_2O)_4$ compound was obtained in different morphology and color. A bulk of attached rectangular yellow crystals was obtained from the reaction of KVO_3, $MnMoO_4$, BPO_4, and water in the mole ratio (1:0.5:1:500) at 170ºC for 3 days. The color differences between the same compounds may cause from different atomic arrangement with in the same unit cell and may cause from the accommodation of a large amount of water by the phosphate systems.

Also some other transition metal oxides were synthesized but their structures are not known yet. They are blue plate like crystals and green rectangular crystals. The blue crystals were obtained from the reaction of V_2O_5, $SrCO_3$, H_3PO_4 in (1:1:3) mole ratio and 0.1mL ethylenediamine in the presence of 9mL water at 180ºC for 3 days. According to the SEM / EDX results it is proved that this compound have carbon, nitrogen, oxygen, vanadium, phosphorous in the atomic percentages of 22.72%, 18.24%, 42.56%, 8.10%, and 7.99% respectively. The green rectangular shaped crystals were obtained via mixing the reactants of $SrCO_3$, $CuCl_2.2H_2O$, BPO_4, $NaVO_3$ and ethylenediamine ($NH_2CH_2CH_2NH_2$) in the water solvent. The reactants were in the (1:1:1:0.5) mole ratios and 0.1mL en was used. Nine mL of water was added as solvents. The reaction was done at 170ºC for 3 days. According to SEM / EDX results the green crystals include boron, carbon, nitrogen, oxygen, and vanadium elements in the atomic percentages of 26.97%, 27.84%, 16.32%, 16.01%, and 6.05% respectively. X-ray single crystal data of these compounds will be collected and their structures will be solved.

REFERENCES

Ackley, M.W.; Rege, S.U. and Saxena, H. 2003. "Application of natural zeolites in the purification and separation of gases", *Micropor. Mesopor. Mater*. Vol. 61, p. 25-42.

Baerns, M.; Schlogl, R., Delmon, B. 1996, "Oxidative dehydrogenation of *n*-pentane on magnesium vanadate catalysts", *Catalysis Today*. Vol.32, p.229.

Bahranowski, K.; Bueno, G.; Corberan, V.; Kooli, F.; Sewicka, E.; Valenzuela, R.; Wcislo, K. 1999. "Oxidative dehydrogenation of propane over calcined vanadate-exchanged Mg,Al-layered double hydroxides", *Applied Catalysis A: General*. Vol.185, p.65.

Byrappa, K. and Yoshimura, M., 2001. *Handbook of Hydrothermal Technology*, A Technology for Crystal Growth and Material Processing, (Noyes, New Jersey).

Byrappa, K., 1992. *Hydrothermal Growth of Crystals*, (Pergamon Press, Oxford, UK).
Bunsen, R.,1848. Ann., Vol.65, p. 70.

Belik, A. A.; Lazoryak,B. I.; Pokholok, K. V. ; TerekhinaI. T. P.; Leonidov, A.; Mitberg, E. B.; Karelina, V. V. and Kellerman, D. G. 2001. "Synthesis and Characterization of New Strontium Iron(II) Phosphates, $SrFe_2(PO_4)_2$ and $Sr9Fe_{1.5}(PO_4)_7$", *Journal of Solid State Chemistry* Vol.162, pp113-121.

Beuhler, E.; Walker, A.C. 1950. "Growing Large Quartz Crystals", *Ind. Eng. Chem*. Vol. 42, p. 1369.

Bierlein, J. and Geir, T. 1976 . U.S.A Patent 3,949,323, April

Boudin, S.; Guesdon, A.; Leclaire, A. and Borel, M.-M. 2000. "Review on vanadium phosphates with mono and divalent metallic cations: syntheses, structural relationships and classification, properties", *International Journal of Inorganic Materials*, Vol.2, pp.561-579 and references therein.

Brown, I.D. and Alternatt, D. 1985. "Bond-valence Parameters Obtained from a Systematic Analysis of the Inorganic Crystal Structure Database", *Acta Cryst.* Vol. B41, pp. 244-247.

Brock, S.L.; Duan, N.G.; Tian, Z.R.; Giraldo, O.; Zhou, H.; Suib, S.L. 1998. "A Review of Porous Manganese Oxide Materials", *Chem. Mater*. Vol. 10 , p. 2619-2628.

Bruker SMART Version 5.054 Data Collection and SAINT-Plus Version 6.2.2 Data Processing Software for the SMART system, Bruker Analytical X-Ray Instruments; Inc.; Madison; WI; USA; 2000.

Bunsen, R. 1848. *H. Ann.Chem. Phys*, 65, 70.

Camblor, M. A.; Villaescusa, L. A.; Diaz-Cabanas M. J. 1999. "Synthesis of all-silica and high-silica molecular sieves in fluoride media", *Top. Catal.* Vol. *9*, p.347

Centi, G. 1993. " Vanadyl Pyrophosphate", *Catalysis Today* Vol.16, pp.5-26.

Chapman, D.M. and Roe, A.L. 1990."Synthesis, characterization and crystal chemistry of microporous titanium-silicate materials" *Zeolites* Vol.10, pp.730-737

Chernaya, V.; Tsirlin, A. A.; Shpanchenko,R. ; Antipov ,E.; Gippius, A. A.; Morozova, E. N.; Dyakov,V. ; Hadermann ,J.; Kaul, E. and Geibel, C. 2004. "Crystal structure and properties of the new vanadyl(IV)phosphates $Na_2MVO(PO_4)_2$, M=Ca and Sr", *Journal of Solid State Chemistry* Vol.177, pp.2875-2880.

Cheetham, A. K.; Ferey, G., and Loiseau, T. 1999. "Open-Framework Inorganic Materials", *Angewandte Chemie International Edition* Vol.38, No.22, pp.3268-3393 and references therein.

Chen, R.; Zavalij, P. Y.; Whittingham, M. S.; Greedan, J. E.; Raju, N. P., and Bieringer, M. 1999. "The hydrothermal synthesis of the new manganese and vanadium oxides, $NiMnO_3H$, MAV_3O_7 and $MA_{0.75}V_4O_{10}.0.67H_2O$ ($MA=CH_3NH_3$)", *J. Mater. Chem.* Vol.9, pp.93-100.

Chen, Q. and Zubieta, J. 1992, "Coordination Chemistry of Soluble Metal Oxides of Molybdenum and Vanadium"; *Coord. Chem. Rev.* Vol.114, pp.107-167.

Chen, Q. ; Qian, Y.; Chen, Z.;Tang, K. ; Zhou, G. and Zhang, Y. 1994. "Preparation of a Tl-based superconductor by a hydrothermal method", *Physica C*, Vol. 224, p. 228.

Chiang, R.K.; Huang, C.-C., and Lin, C.-R. 2001. "Synthesis and Characterization of A New Open-Framework Cobalt Phosphate: $Cs_2Co_3(HPO_4)(PO_4)_2 .H_2O$", *Journal of Solid State Chemistry* Vol.156, pp.242-246 .

Chippindale, A. M.; Natarajan, S. J.; Thomas, M. and Jones, R. H. 1994. "An Example of a Reactive Template in the Synthesis of a Novel Layered Aluminum Phosphate, $(Al_3P_4O_{16})^{3-}(NH_3(CH_2)_5NH_3)^{2+}(C_5H_{10}NH_2)^{+}$", *Journal of Solid State Chemistry* Vol. 111, N: 1 , pp. 18-25.

Chunga, U-Chan; Mesab, J. L.; Pizarro, J. L.; Juberac, V.; Lezamab, L.; Arriortuaa, M. I.; Rojo, T. 2005. "Mn(HPO3): A new manganese (II) phosphite with a condensed structure", *Journal of Solid State Chemistry* Vol.178, pp.2913-2921.

Crystal Clear: Crystal Clear version 1.3, Rigaku Corp. 2001, Rigaku/Molecular Structure Corp. The Woodlands, TX.

Crystal Structure 2004. ' Single Crystal Analyses Software", Version 3.7, Molecular Structure Corparation, The Woodlands, TX 77381.

Corma A. 2003. "State of the art and future challenges of zeolites as catalysts", J. *Catal.* Vol. 216, p. 298.

Cui, Y.; Sun, J.; Meng, H.; Li, G.; Chen, C.; Liu, L.; Yuan, X. and Pang, W. 2005. "A mixed-valence vanadium phosphate with odd-number rings: Synthesis and structure of $[(C_6H_{16}N_2)_3(VO)(V_2O_4)_2(PO_4)_4 \ .2H_2O]$", Inorganic *Chemistry Communications*. Vol. 8, pp.759-762.

Cullity, B. D. 1978. Elements of X-Ray Diffraction (Addison-Wesley Publishing Co., U.S.)

Daidouh, A.; Martinez, J.L.; Pico, C. and Veiga, M.L. 1999. "Structure Characterization and Magnetic Behavior of $NaNi_4(PO_4)_3$ and $KMn_4(PO_4)_3$", *Journal of Solid State Chemistry* .Vol.144, pp.169-174 .

Davis, M. E. and Lobo, R.F. 1992. "Zeolite and Molecular Sieve Synthesis", *Chem. Mater. Vol.4, pp. 756-768.*

Dawson, W.J. and Han, M.K.,1993. *Development and scale-up of hydrothermal processes for synthesis of high performance materials*, In Hydrometallurgy fundamentals, technology and innovations, (Ed. J.B. Hiskey and G.W. Warren, SME Inc.),pp. 593-610.

DeBord, J. R. D.; Haushalter, R. C., and Zubieta, J. 1996."The First Organically Templated Layered Cobalt Phosphates:Hydrothermal Syntheses and Crystal Structures of $[H_3N(CH_2)_3NH_3]_{0.5}[Co(PO_4)]\cdot 0.5H_2O$ and $[H_3N(CH_2)_4NH_3]_{0.5}[Co(PO_4)]$", *Journal of Solid State Chemistry* Vol.125, pp.270-273.

deSenarmont, *H. Ann.Chem. Phys.,* 32, 1851, 129.

Duan, L.; Yuan, M.; Wang, E.; Li, Y.; Lu, Y.; Hu,C. 2003. "Hydrothermal synthesis and crystal structure of a new open-framework 3-D vanadium phosphate: $[C_2N_2H_{10}]\{(VO)(VO_2)\ [V(OH_2)](PO_{3.5})_4\}\cdot H_2O$", *Journal of Molecular Structure* Vol.654, pp 95-101.

Eanes, M. 2000. *Synthesis and Characterization of Alkali Silver Chalcogenides and Alkali Rare Earth Germanates by Supercritical Fluids*, (Clemson University). *Doctor of Philosophy.*

El-Bali, B. 2000. "Preparation and Structure Determination Of $SrMn_2(PO_4)_2$ and Redetermination Of β'-$Mn_3(PO_4)_2$", *Z.Anorg.Allg.Chem*. Vol.626, pp.2557-2562.

Escobal, J.; Mesa, J. L.; Pizarro, J. L.; Lezama, L.; Olazcuagac, R.; Rojo, T.. 1999. "Hydrothermal synthesis, structural, spectroscopic and magnetic studies of a lamellar phosphate: $Ba(MnPO_4)_2.H_2O$" *,J. Mater. Chem.* Vol. 9, pp.2691-2695.

Escobal, J.; Pizarro, J.´ L.; Messa, J.´ L.; Lezama, L.; Olazcuaga, R.; Arriortua, M. I., and Rojo, T. 2000. "A New Manganese (II) Phosphate Templated by

Ethylenediamine: $(C_2H_{10}N_2)[Mn_2(HPO_4)_3(H_2O)]$. Hydrothermal Synthesis, Crystal Structure, and Spectroscopic and Magnetic Properties",*Chem. Mater*.Vol.12, p.376-382.

Férey, G. 1995. "Oxyfluorinated microporous compounds ULM-*n*:chemical parameters, structures and a proposed mechanism for their molecular tectonics " *J. Fluorine Chem*. Vol. 72 , p. 187.

Ferey ,G. 2000. "Building Units Design and Scale Chemistry", *Journal of Solid State Chemistry*. Vol.152, p.37-48.

Froment, G.F. and Jacobs, P.A. 2000. ,*Top. Catal.* Vol. 13 p. 347.

Habashi, F., 1993. A Textbook of Hydrometallurgy, (Libraire Universitaire du Quebec, Canada), pp 1-50.

Hagrman, P. J.; Finn, R. C.; Zubieta, J. 2001. "Molecular Manipulation of Solid State Structure: Influences of Organic Components on Vanadium Oxide Architectures", *Solid State Sciences* Vol.3, pp.745-774.

Haushalter, R. C. and Lai, F. W. 1989. "$[Et_4N]_6[Na_{14}Mo_{24}P_{17}O_{97}(OH)_{31}]\cdot xH_2O$: A Hollow Cluster Filled with 12 Na^+ Ions and a H_3PO_4 Molecule", *Angewandte Chemie International Edition in* English Vol.28, No.6, pp. 743-746.

Haushalter, R. C. and Mundi, L. A. 1992. "Reduced Molybdenum Phosphates: Octahedral- Tetrahedral Framework Solids with Tunnels, Cages, and Microporest", *Chem. Mater.* Vol.4, pp.31-48.

Hosaka, M. 1991, in *Progress in Crystal Growth and Characterization*, (Pergamon Press, London).

Goodenough, J.B.; Kafalas, J.A. and ,Longo J.M., 1972. *Preparative Methods in Solid State Chemistry*,(P.Hagenmuller, ed.,Academic Press, New York), p 1972.

Goranson, R. W. 1931. " Solubility of Water in Granite Magmas", *Amer. J. Sci.* Vol.22, pp. 481-502.

Gier, T.E. and Stucky, G.D. 1991. "Low-temperature synthesis of hydrated zinco(beryllo)-phosphate and arsenate molecular sieves", *Nature* Vol. 349, p. 508.

Ikornikova, N.Y. and Lobchev E.A. 1971.; "*In Hydrothermal Synthesis of Crystals*"; Consultants Bureau; New York;p. 80

Inkster, I. 1991. "*Science and Technology in History: An Approach to Industrial Development"* (Rutgers University Press) 1, 2, 3.

Iwamoto, M.; Furukawa, H.; Mine, Y.; Uemura, F.; Mikuriya, S.-L.; Kagawa, S. 1986. **"**Copper(II) ion-exchanged ZSM-5 zeolites as highly active catalysts for direct

and continuous decomposition of nitrogen monoxide", *J. Chem. Soc. Chem.* Commun. Iss. 16 pp 1272.

Jessop, P.G., Leitner, W. 1998. "Chemical Synthesis Using Supercritical Fluids", (Wiley-Vch, Weinheim).

Kampf, A. R. and Ross, C. R. 1988. "End-member villyaellenite from Mapimi, Durango, Mexico: Descriptive mineralogy,crystal structure, and implications for the ordering of Mn and Ca in type villyaellenite", *American Mineralogist* Vol.73, pp. 1172-1178.

Kanatzidis, M.G. 1990. "Molten alkali-metal polychalcogenides as reagents and solvents for the synthesis of new chalcogenide materials", *Chem. Mater*. Vol 2,p. 353.

Khan, M. I.; Lee, Y.-S.; O'Connor, C. J.; Haushalter, R. C.; Zubieta, J.. 1994, Organically Templated Layered Vanadium(IV)-Oxo-Organophosphonate Exhibiting Intercalated Organic Cations and Open-Framework V/P/O Layers: $[(C_2H_5)_2NH_2][(CH_3)_2NH_2][V_4O_4(OH)_2(C_6H_5PO_3)_4]$", *J.Am. Chem.* Soc. Vol.116, pp.4525-4526.

Khan, M. I.; L. Meyer, M.; Haushalter, R. C.; Schweitzer, A. L.; Zubieta, J.; Dye, J. L. 1996. "Giant Voids in the Hydrothermally Synthesized Microporous Square Pyramidal-Tetrahedral Framework Vanadium Phosphates $[HN(CH_2CH_2)_3NH]K_{1.35}[V_5O_9(PO_4)_2]\cdot xH_2O$ and $Cs_3[V_5O_9(PO_4)_2]\cdot xH_2O$", *Chem. Mater.* Vol.8, p.43.

Khan, M.I 2000. "Novel Extended Solids Composed of Transition Metal Oxide Clusters", *J. Solid State Chem*. Vol 152, pp. 105-112.

Khan, M.I. et al 2003. "Inorganic-organic hybrid materials; synthesis and crystal structures of the layered solids $[\{M(H_2O)(2,2'\text{-bipy})\}V_2O_6]$ (M = Co, Ni) ", *Journal of Molecular Structure* Vol. 656; pp. 45-53.

Kinomura, N.; Matsui, N.; Kumada, N. and Muto, F. 1989. "Synthesis and crystal structure of $NaV_3P_3O_{12}$: A stuffed structure of α-$CrPO_4$", J. *Solid State Chem*. Vol.79, pp.232-237.

Klemperer, W.G.; Marquart, T.A.; Yaghi, O.M. 1992. "New Directions in Polyvanadate Chemistry: From Cages and Clusters to Baskets, Belts, Bowls, and Barrels"; *Angew.Chem.Int.Ed.Eng. Vol* 31, pp.49-51.

Kohn, M. J.; Rakovan, J., and Hughes, J. M. 2002. "Rewiews in Minerology and Geochemistry" in *Phosphates,Geochemical,Geobiological and Materials Importance*,edited by Pul H.Ribbe (Virginia Polytechnic Institute and State University, Virginia), pp.181-190(book)

Kongshaug, K. O.; Fjellvasg, H. and Lillerud, K.P. 2001. "The Synthesis and Characterization of a New Manganese Phosphate Templated by Piperazine", *Journal of Solid State Chemistry*. Vol.156, p.32-36.

Korzenski, Michael B.; Schimek, George L., and Joseph W. Kolis 1998. "Hydrothermal Synthesis, Structure, and Characterization of a Mixed-Valent Iron(II/III) Phosphate, NaFe3.67(PO4)3: A New Variation of the Alluaudite Structure Type",*Journal of Solid State Chemistry* Vol.139, pp.152-160.

Krishnan, V.V. and Suib, S. L. 1999. "Oxidative Dehydrogenation of 1-Butene over Manganese Oxide Octahedral Molecular Sieves", *Journal of Catalysis* Vol.184, pp.305-315.

Laudise, R.A.; Ballman A.A.; Kirk-Othmer, 1969. *Encyclopedia of Chemical Technology* 2nd Ed., (John Wiley and Sons; New York), p. 105.

Laudise, R.A.,1970. *The Growth of Single Crystals*, (Prentice-Hall, Englewood Cliffs, NJ).

Murchison, Sir R., 1840s. (cited by S. Somiya).

Laudise A. 1987."Hydrothermal Synthesis of Crystals",*Chem. Eng. News*. Vol.30, pp.30-43

Lethbridge, Z. A. D.; Smith, M. J.; Tiwary, S. K.; Harrison, A.; Lightfoot, P. 2004. "Synthesis of Hybrid Framework Materials under "Dry" Hydrothermal Conditions:Crystal Structure and Magnetic Properties of Mn_2 $(H_2PO_4)_2(C_2O_4)$", *Inorg. Chem*. Vol.*43*, pp.11-13.

Li, M.; Wong, K.K.W. and Mann S. 1999. "Organization of Inorganic Nanoparticles Using Biotin - Streptavidin Connectors", *Chem. Mater. Vol. 11, pp 23-26.*

Liao, J.–H.; Kanatzidis, M.G.1992. "Platinum (IV) complexes of a tetraaza macrocycle with pendent dichloroamine or ammonium groups"; *Inorg. Chem*. Vol.31, pp. 631-634.

Lii, K.-H.; Huang, Y.-F.; Zima, V.; Huang, C.-Y.; Lin, H.-M.; Jiang, Y.-C.; Liao, F.-L.; Wang, S.-L. 1998. "Syntheses and Structures of Organically Templated Iron Phosphates",*Chem. Mater.* Vol.10 ,pp. 2599-2609.

Lobachev, A.N. 1973. Crystallization *Processes under Hydrothermal Conditions*, (Consultants Bureau, New York).

Loy, D.A. 1997. "Direct Formation of Aerogels by Sol-Gel Polymerizations of Alkoxysilanes in Supercritical Carbon Dioxide", *Chem. Mater.*Vol. 9, p. 2264.

Luo, J.; Zhang, Q.; Huang, A.; Suib, S. L. 2000. "Total oxidation of volatile organic compounds with hydrophobic cryptomelane-type octahedral molecular sieves", *Microporous and Mesoporous Materials* Vol.35–36, pp.209–217.

Maiman, T. H. 1960."Stimulated Optical Radiation in Ruby", *Nature* Vol. 187, no. 4736, pp. 493-494.

Mambote , R.C.M.; Reuter , M.A. ; Krijgsmank, P. and Schuiling R. 2000. "D. Hydrothermal Metallurgy :An Overview of Basic Concepts and Applications", *Minerals Engineering* Vol. 13, No. 8-9, pp. 803-822.

Massa, W.; Yakubovich, O. V.; Dimitrova, O. V. 2005. "A novel modification of manganese orthophosphate $Mn_3(PO_4)_2$", *Solid State Sciences* Vol.7, pp.950-956.

Meier, M.; Olsen, D. H.; Baerlocher, C. *Atlas of Zeolite Structure Types*, Elsevier, London, 1996.

Moore,P.B. and Araki, T. 1973. "Hureaulite, its atomic arrangement", *Amer. Mineral*. Vol.58, p.302-307.

Morozov, V.A.; Pokholok, K.V.; Lazoryak,B.I.; Malakho, A.P.; Lachgar, A.; Lebedev, O.I. and Tendeloob G.V. 2003. "A new iron oxophosphate $SrFe_3(PO_4)_3O$ with chain-like structure", *Journal of Solid State Chemistry* Vol. 170, pp. 411-417.

Müller, A.; Reuter, H., and Dillinger, S. 1995. "Supramolecular Inorganic Chemistry: Small Guests in Small and Large Hosts", *Angew. Chem. Int. Ed.Engl.* Vol. 34, p.2328.

Müller, A.; Peters, F.; Pope, M.T.; Gatteschi, D. 1998. "Polyoxometalates: Very Large Clusters-Nanoscale Magnets", *Chem*. *Rev*.Vol.98, p. 239

Nacken, R., 1946.Artificial Quartz Crystals, etc., U.S. Office of Technical Services Report, PB-18–748 and 28–897.

Natarajan, S.; Neeraj, S.; Choudhury, A.; Rao, C.N.R. 2000. "Three-Dimensional Open-Framework Cobalt(II) Phosphates by Novel Routes", *Inorg. Chem.* Vol.39, p.1426.

Neeraj, S.; Noy, M. L. and Cheetham, A. K. 2002. "Structure and magnetic properties of a three-dimensional framework manganese (II) phosphate, $[NH_4][Mn_4(PO_4)_3]$", *Solid State Sciences* Vol.4, pp. 397-404.

Neeraj, S. and Natarajan, S. 2000. "Three-Dimensional Zinc Phosphates with Open Architectures", *Chem. Mater.* Vol. 12, pp. 2753-2762.

Occelli, M.L. and Robson, H.C. 1989. "Zeolite Syntheses", *American Chemical Society*. Washington, DC.

O'Mahony L.; Henry, J.; Curtin, D. T.; Hodnett, B.K. 2003. "Crystallisation of $VOHPO_4{\cdot}0.5H_2O$", *Applied Catalysis* A .Vol.253, pp. 409-416.

Parise, J.B. 1985. "Preparation and structural characterization of two metallophosphate frameworks clathrating diprotonated ethylenediamine: AlPO4-12(en) and GaPO4-12(en)", *Inorg. Chem.* Vol. 24, p .4312.

Parr Instrument Company, 211 53rd Street, Moline, Illinois 61265.

Pope, M.T. ,1983 “Heteropoly and Isopoly Oxometalates”: Springer-Verlag, Berlin.

Pope, M.T. and Müller, A. 1991. “Polyoxometalate Chemistry: An Old Field with New Dimensions in Several Disciplines”; *Angew. Chem. Int. Ed. Engl*. Vol.30, p.34

Post, J. E.; Von Dreele, R. B.; Buseck, P. R. 1982. “Symmetry and cation displacements in hollandites: structure refinements of hollandite, cryptomelane and priderite”,*Acta Crystallogr.* Vol. *B38*. , pp.1056-1065.

Rabenau, A. 1985. “The Role Hydrothermal Synthesis in Preparative Chemistry”, *Angew. Chem., Int. Eng. Ed.* Vol. 24, pp. 1026-1040.

Rajic, N.; Stojakovi, D.; Hanzel, D.; Kaucic, V. 2004, “The structure directing role of 1,3-diaminopropane in the hydrothermal synthesis of iron(III) phosphate”, *J.Serb.Chem.Soc.* Vol.69, pp.179-185.

Rajic, N. 2005, “Open-framework aluminophosphates: synthesis, characterization and transition metal modifications”, *J. Serb. Chem. Soc. Vol.70*, pp.371-391 and references therein.

Roy, R. and Tuttle, O.F., 1956. *Investigations under hydrothermal conditions, Physics and Chemistry of the Earth*, Vol. 1, Ahrens, L.H.; Rankama, K. and Runcorn ,S. K. (Eds.), (Pergamon, New York), p.138.

Rao, C.N.R., 1994. Chemical *Approaches to the synthesis of Inorganic Materials*, (John Wiley and Sons, New York), pp.78-99

Rao, C.N.R. and Merkanzov, A.G. 1992. *“Chemistry of Advanced Materials”* Blacwell, Oxford.

Rao, C.N.R. and Raveau, B. 1998. “*Transition Metal Oxides,Structures,Properties,and Synthesis of Ceramic Oxides*”, John Wiley and Sons, New York.

REQAB 1998. Emperical Absorption Correction, Version 1.1, Jacobson, R.A. Molecular Structure Corp. The Woodlands, TX.

Rowsel, J. L.C. and Yoghi, O. M. 2004. “Metal–organic frameworks: a new class of porous materials”, *Microporous and Mesoporous Materials* Vol.73, pp 3-14 and references therein.

Schafthaul, K. F. E.,1845. Gelehrte Anzeigen Bayer. Akad., pp.20, 557, 569, 575, 592 .

Schubert, U. and Hüsing, N. 2000. *Synthesis of Inorganic Materials* pp. 170-190

Sheldrick, G.M. 1997 “SHELXTL-PLUS,” Version 6.10, Bruker AXS, Siemens Analytical X-Ray Instruments, Inc., Madison, WI.

Sheldrick, G.M. 2000, SHELXTL Dos / Windows / NT Version 6.12, Bruker Analytical X-Ray instruments; Inc.; Madison; WI; USA.

Soghomoniam, V.; Chen, Q.; Haushalter, R.C.; Zubieta, J. 1995. "Investigations into the Targeted Design of Solids: Hydrothermal Synthesis and Structures of One-, Two-, and Three-Dimensional Phases of the Oxovanadium Organodiphosphonate System", *Angew. Chem. Int. Ed. Engl*.Vol.34, p.223.

Song, Y.; Zavalij, P. Y.; Chernova, N. A.; Whittingham, M. S. 2003. "Synthesis and Characterization of a New Layered Ethylene-Diammonium Manganese(II) Phosphate, $(C_2N_2H_{10})Mn_2(PO_4)_2.2H_2O$)", *Chem. Mater.* Vol.15, pp.4968-4973.

Stoe&Cie (2002). X-AREA (Version 1.18) and X-RED32 (Version 1.04). Stoe&Cie, Darmstadt, Germany

Suib, S.L. 1996. "A Review of Open Framework Structures", Annual Review of Material Science. Vol.26, pp.135-151.

Sugita, M.; Tsuji, M. and Abe, M. 1990. "Synthetic Inorganic Ion-Exchange Materials. LVIII. Hydrothermal Synthesis of a New Layered Lithium Titanate and Its Alkali Ion Exchange"*Bull. Chem. Soc. Jpn.*,Vol. 63, pp.1978-1984.

Thoma, S. G.; Bonhomme, F. and Cygan, R. T. 2004. "Synthesis, Crystal Structure, and Molecular Modeling of a Layered Manganese(II) Phosphate $Mn_3(PO_4)_4.2(H_3NCH_2CH2)_3N.6(H_2O)$", *Chem. Mater.* Vol.*16 , pp.*2068-2075.

Tian, Z.R; Tong, W. Wang, J.Y.; Duan, N.G.; Krishnan, V.V. and Suib, S. L. 1992. "Manganese Oxide Mesoporous Structures: Mixed-Valent Semiconducting", *Catalysts* . Vol. 276. No.5314, pp.926-930.

Tong, W.; Xia, G.G.; Tian, Z. R. ; Liu, J.; Cai, J.; Suib, Steven L.; Hanson, J. C. 2002. "Hydrothermal Synthesis and Characterization of Sodium Manganese Oxo-Phosphate $Na_2Mn_2O(PO_4)_2.H_2O$" ,*Chem. Mater.* Vol.14, pp.615-620.

Xia, G. G.; Yin, Y. G.; Willis, W. S.; Wang, J. Y.; Suib, S. L. 1999. "Efficient Stable Catalysts for Low Temperature Carbon Monoxide Oxidation", *Journal of Catalysis* Vol.185, pp.91-105.

WEB_1,2006.Webmineral.com,05/06/2006.http://www.webmineral.com/specimens .shtml/specimens/help/specimens/picshow.php?id=2955

West, A. R.1996. *Solid State Chemistry and Its Applications,* (John Wiley and Sons, New York), pp.4-115

Wilson, S. T.; Lok, Brent M.; Messina C. A.; Cannan, T. R. and Flanigen, E. M. 1982. "Aluminophosphate molecular sieves: a new class of microporous crystalline inorganic solids", *J. Am. Chem. Soc.* Vol *104* (4), pp. 1146-1147.

Whittingham, M.; Chen, R.; Chirayil, T., and Zavalij, P. 1996, *Electrochem Soc Proc. Vol.* 96, p.76.

Yoshimura, M. and Suda, H., 1994. *Hydrothermal Processing of Hydroxyapatite Past, Present, and Future*, in: "Hydroxyapatite and Related Materials (P. W. Brown and B. Constanz, eds., CRC Press),pp 45-72.

Yu , R.; Xing , X.; Saito , T. ; Azuma , M.; Takano M. ; Wang, D. ; Chen , Y.; Kumada, N.; Kinomura, N. 2005. "A novel organically templated hybrid open-framework manganese phosphate-oxalate", *Solid State Sciences.* Vol.7, pp.221-226.

Zapf, P. J.; Rose, David J.; Haushalter, R. C.; Zubieta, J. 1996, "Synthesis and Structural Characterization of Solid Phases of the Sn(II)– Organophosphonate System: The 1-Dimensional $[Sn(HO_3PCH_2PO_3H)].H_2O$ and the 3-Dimensional $[Sn_2\{O_3PC(OH)(CH_3)PO_3\}]$", *Journal of Solid State Chemistry* Vol.125, pp.182-185.

Zhang, Y.; O'Connor, C. J.; Clearfield, A.; Haushalter, R. C. 1996. "An Organically Templated Layered Vanadium Oxide:Hydrothermal Synthesis, Single-Crystal Structure, and Magnetic Properties of $(H_3N(CH_2)_3NH_3)[V_4O_{10}]$", *Chem. Mater.* Vol.8, pp.595-597.

Zhang, Y.; C. Haushaiter, R.; Zubieta, J. 1998. "A new form of decavanadate: hydrothermal synthesis and structural characterization of $Ba_{5.33}(H_30)_{0.33}V_{10}0_{30}$", *Inorganica Chimica Acta* . Vol.277 ,pp 263-267.

Zhao, X.; Roy, R.; Cherian, K. and Badzian, A. 1997., *Science*, Vol. 385, p. 513

Zhou, H.; Shen, Y.F.; Wang, J.Y.; Chen, X.; O'Young, Chi-Lin, and Suib, S. L. 1998. "Studies of Decomposition of H_2O_2 over Manganese Oxide Octahedral Molecular Sieve Materials", *Journal of Catalysis* Vol.176, pp.321-328.